Equilibrium and Transport Properties of Gas Mixtures at Low Density: Eleven Polyatomic Gases and Five Noble Gases

J. Bzowski, J. Kestin, E. A. Mason, and F. J. Uribe

View Online   Export Citation

AIP Publishing

Equilibrium and Transport Properties of Gas Mixtures at Low Density: Eleven Polyatomic Gases and Five Noble Gases

J. Bzowski,[a] J. Kestin, E. A. Mason, and F. J. Uribe[b]

Division of Engineering, Brown University, Providence, Rhode Island 02912

This paper uses results from statistical-mechanical theory, applied through a combination of an extended principle of corresponding states with some knowledge of intermolecular potentials, to the calculation of the transport and equilibrium properties of gas mixtures at low density. The gases involved are: N_2, O_2, NO, CO, CO_2, N_2O, CH_4, CF_4, SF_6, C_2H_4, C_2H_6, and He, Ar, Ne, Kr, Xe. The properties included are: second virial coefficient, viscosity, diffusion, and thermal diffusion, but not thermal conductivity.

The calculations are internally, thermodynamically consistent and the resulting algorithms, which are fully programmable, operate in an entirely predictive mode by means of validated combination rules.

This paper is a sequel to one on the five noble gases and all their possible mixtures and a second on the above eleven polyatomic gases.

The paper contains ten tables (mainly intended for the checking of computer codes) and 201 graphs of deviation and comparison plots. An additional 98 tables have been deposited with the Physics Auxiliary Publication Service (PAPS) of the AIP.

The algorithms presented in this paper, together with those mentioned above, make it possible to program calculations for a wide range of low-density equilibrium and transport properties of 16 gases and of all possible multicomponent mixtures formed with them, for a total of 65,535 systems. For each system, the program would cover the full range of compositions.

Key words: Polyatomic gases, Noble gases, Mixtures of gases, Combination rules for mixtures of gases, Equilibrium properties of gases, Transport properties of gases

Contents

[a] Permanent address: Institute of Heat Engineering, Warsaw Technical University, Warsaw, Poland.
[b] Permanent address: Department of Physics, Universidad Autonoma Metropolitana, Iztapalapa, Mexico, D.F.

List of Tables for Properties of an Equimolar Mixture

List of Figures

List of Symbols

A^*	ratio of collision integrals, Eq. (B3b)
a	rigid-core diameter, Eq. (1)
B	second virial coefficient
B^*	reduced second virial coefficient, Eqs. (B4) and (C7a); ratio of collision integrals, Eq. (B3c)
B_{ns}^*	reduced nonspherical contribution to B^*, Eq. (B4)
B_0^*	reduced spherical contribution to B^*, Eq. (B4)
C^*	ratio of collision integrals, Eq. (B3d)
$C^{(6)}$	long-range dispersion coefficient
C_6^*	reduced dispersion coefficient, Table A6
D_{ij}	binary diffusion coefficient, Eq. (C4)
E^*	ratio of collision integrals, Eq. (B3e)
F^*	ratio of collision integrals, Eq. (B3f)
f_η	higher-order correction factor for viscosity, Eq. (C1a)
H^*	ratio of collision integrals, Eq. (B3g)
k	Boltzmann constant
M	molecular weight
m	mass of a molecule
N_A	Avogadro constant
P	pressure
R	universal gas constant
r	molecule separation in pair-potential

T	temperature	κ	polarizability anisotropy, Table A6
T^*	reduced temperature, kT/ϵ	κ_T	higher-order correction for thermal diffusion factor, Eq. (C6)
V	intermolecular force potential		
V_0	short-range energy parameter, Eq. (8)	μ_0	dipole moment
V_0^*	high-temperature scaling parameter, Eq. (11)	μ^*	reduced dipole moment, Table A6
x	mole fraction	ρ	short-range length parameter, Eq. (8)
α^*	reduced dipole polarizability, Table A6	ρ^*	high-temperature scaling parameter, Eq. (11)
α_T	thermal diffusion factor, Eq. (C6)	θ	quadrupole moment
Δ_{ij}	higher-order correction term for binary diffusion coefficient, Eq. (C5)	θ^*	reduced quadrupole moment, Table A6
		σ	length scaling parameter
ϵ	energy scaling parameter	$\Omega^{(l,s)*}$	reduced collision integral
η	viscosity		

1. Introduction

There exists a voracious need in industry for reliable data on the thermophysical properties of a very large set of pure substances and an even larger set of mixtures of all kinds. The number of systems is so large that direct experimental measurements on all of them is out of the question, and a maximum input from theory is required. Considerable success has been achieved by use of statistical-mechanical theory, applied through a combination of an extended principle of corresponding states with some knowledge of intermolecular potentials.

Previous work was concerned with the five noble gases and all their possible mixtures,[1,2] and with eleven polyatomic gases.[3] We now consider mixtures involving these polyatomic gases, both with themselves and with the noble gases. It is necessary to follow a different route than was the case for the noble gases, for which the parameters for the unlike interactions in the mixtures could be determined directly from a large body of accurate experimental data. A comparable body of data does not exist for all the mixtures now under consideration, and recourse is necessary to combination rules that predict the parameters for unlike interactions from the known parameters for the corresponding like interactions. Since no combination rules yet devised are completely accurate in all cases, there will naturally be some loss of accuracy in the prediction of mixture properties. This loss of accuracy turns out to be fairly small for most of the systems considered here. In compensation, we now operate in an entirely predictive mode, and do not depend on the existence of any accurate measurements on mixtures.

As in the previous work on single polyatomic gases,[3] we do not include the explicit effects of the internal degrees of freedom on the properties, and thus do not treat the thermal conductivity. We do include thermal diffusion, however, even though it depends on the contributions of individual species to the thermal conductivity of the mixture.[4] The reason is that the thermal diffusion factor is usually dominated by the effects of molecular mass and size, and the effects of inelastic collisions and nonspherical interactions become apparent only for a few systems in which the mass and size effects happen to be very small (e.g., $Ar + CO_2$, $Ar + HCl$, $Ne + CH_4$, and $D_2 + HT$ mixtures[5,6]).

Although we do not consider quantum effects explicitly, there is no difficulty here in treating mixtures containing helium. The largest quantum effects appear in those quanti-

ties concerned with He–He interactions, and these have been taken into account in the published noble-gas calculations,[2] which can be used directly in those parts of the mixture formulas where they occur. The remaining quantum effects of interest appear in the quantities concerned with the interaction of a He atom with one of the eleven molecules, and these effects are small for two reasons. First, we are concerned only with temperatures for which $T^* > 1$, where quantum effects are less important than at lower temperatures. Second, the much larger mass and size of the molecular collision partner make the quantum effects much smaller than for He–He collisions. Thus all the present mixture calculations can safely ignore quantum effects, except possibly for a few interaction second virial coefficients involving He, where a small perturbation correction can be directly supplied.[1,2]

The algorithms presented in this paper make it possible to program calculations for a wide range of low–density equilibrium and transport properties of 16 gases and of all possible multicomponent mixtures formed with them, for a total of 65,535 systems. For each system, the program would cover the full range of compositions.

2. Principle of Corresponding States for Mixtures

At the low densities considered here, only pairwise interactions between molecules in a mixture are significant. The properties of even multicomponent mixtures can therefore be expressed in terms of the properties of its single pure components, plus functionals corresponding only to the possible binary interactions in the mixture. No functionals corresponding to three-body or higher interactions occur. The principle of corresponding states for single gases expresses their equilibrium and transport properties in terms of functionals that are (nearly) universal when written in terms of scale factors representing pairwise molecular energy and size. These scale factors are conveniently chosen to be the depth of the potential-energy well ϵ and the separation σ at which the potential energy is zero. (Secondary parameters describe deviations from complete universality of the functionals at very low and very high temperatures.) Earlier work[7] on the viscosities of binary gas mixtures strongly indicated that a similar principle could be applied in terms of the mixed-interaction parameters ϵ_{12} and σ_{12}, and this was later confirmed in detail for mixtures of noble gases.[1,2] The pres-

ent paper is essentially the confirmation of this result for molecular gases.

More specifically, we list in Table a the various functionals needed for single gases and for binary mixtures. Similar results hold for the various pairs in multicomponent mixtures. The functionals listed as "secondary" occur in small correction terms. It can be seen that no new functionals are required for mixtures, only new scale factors ϵ_{12} and σ_{12} (plus corresponding secondary parameters).

Some minor complications arise, however, because the principle of corresponding states applies in a more limited form to molecular gases than to noble gases. First, as already mentioned, the temperature range is more restricted ($T^* = kT/\epsilon > 1$). Second, the diffusion functional $\Omega^{(1,1)*}$ is somewhat different for molecular gases than for noble gases, raising the question of the proper functional to use for the mixed interaction $\Omega_{12}^{(1,1)*}$ involving a noble gas and a molecular gas. Since the differences are small, we have simply used the arithmetic mean of the two functionals in such cases. Third, the functional B_0^*, representing the effective spherical-interaction contribution to the second virial coefficient, is also not quite universal. Although the same B_0^* functional can be used for all the noble gases,[1,2] somewhat different functionals must be used for the various molecular gases.[3] For the mixed-interaction functional $(B_0^*)_{12}$ we have therefore used the arithmetic mean of the functionals for gases 1 and 2. The differences are sufficiently small that almost any sensible averaging procedure will be satisfactory. It should be mentioned that no similar problem arises with the functionals B_{ns}^*, corresponding to the contribution of the nonspherical part of the intermolecular potential to the second virial coefficient. The B_{ns}^* are calculated explicitly for each specific pair according to theoretical formulas for the various orientation-dependent interactions (e.g., dipole-dipole, dipole-quadrupole, etc.).

The main problem for mixtures is thus only to predict the new scale factors and secondary parameters for the interaction terms; this is done via the combination rules discussed next.

TABLE a. List of functionals required for single gases and for mixtures.

Property	Functionals	
	Primary	Secondary
Single gas		
B	B_0^*, B_{ns}^*	---
η	$\Omega^{(2,2)*}$	E^*
D	$\Omega^{(1,1)*}$	A^*, C^*
α_0	A^*, B^*, C^*	κ_0
Mixtures		
B	$(B_0^*)_{12}, (B_{ns}^*)_{12}$	---
η	$\Omega_{12}^{(2,2)*}, A_{12}^*$	---
D_{12}	$\Omega_{12}^{(1,1)*}$	$\Omega_{22}^{(2,2)*}, C_{12}^*$
α_T	$\Omega_{11}^{(2,2)*}, \Omega_{22}^{(2,2)*}, \Omega_{12}^{(1,1)*}$ $A_{12}^*, B_{12}^*, C_{12}^*$	κ_T

3. Combination Rules for Mixtures

Very accurate combination rules for the noble-gas potentials have been devised by Tang and Toennies,[8] and extended to molecular systems by Bzowski, Mason, and Kestin.[9] The molecular rules do not attempt to predict the entire anisotropic potential-energy function, but only the effective spherical parameters ϵ_{12} and σ_{12} corresponding to the potential-well region, which is all that is needed for use with the principle of corresponding states. Four pieces of input information are needed for each of the single gases involved, namely the parameters ϵ and σ, the dipole polarizabilities α, and the $C^{(6)}$ dispersion coefficients that describe the long-range attraction. Accurate values of α and $C^{(6)}$ are known from independent experiments and calculations.

The combination rules for ϵ_{12} and σ_{12} are applied as follows. First, effective rigid-core diameters a_1 and a_2 are calculated for each of the single systems,

$$a_1 = \sigma_1 [1 - (C_1^*/2.2)^{1/6}], \tag{1}$$

where

$$C_1^* \equiv C_1^{(6)}/\epsilon_1\sigma_1^6. \tag{2}$$

If C_1^* happens to be greater than 2.2, then a_1 is taken to be zero. A similar expression holds for a_2. The interaction core diameter a_{12} is then calculated by the simple arithmetic-mean combination rule

$$a_{12} = \frac{1}{2}(a_1 + a_2). \tag{3}$$

It is this rigid-core diameter that is the characteristic parameter for molecular systems. The noble-gas combination rules are recovered by setting a_1 and a_2 equal to zero.

Next, the value of σ_{12} is calculated from the expression

$$\sigma_{12} - a_{12} = \frac{1}{2}[(\sigma_1 - a_1) + (\sigma_2 - a_2)]$$
$$\times \left\{1 + \frac{1}{2}\left[\ln(\sigma_{12} - a_{12}) - \frac{1}{7}\ln E\right]\right\}, \tag{4}$$

where

$$\ln E = \frac{1}{2}\ln(\epsilon_1\epsilon_2) + 3\ln(\sigma_1 - a_1)(\sigma_2 - a_2)$$
$$- \frac{\sigma_1 - a_1}{(\sigma_1 - a_1) + (\sigma_2 - a_2)}\ln\left(\frac{\epsilon_1}{\sigma_1 - a_1}\right) \tag{5}$$
$$- \frac{\sigma_2 - a_2}{(\sigma_1 - a_1) + (\sigma_2 - a_2)}\ln\left(\frac{\epsilon_2}{\sigma_2 - a_2}\right).$$

Although Eq. (4) appears complicated, it is actually quite simple to use because the factor in braces is very close to unity. Thus the iteration of Eq. (4) to find σ_{12} converges rapidly. To a first approximation, in which the factor in braces is taken as unity, we recover the conventional arithmetic-mean rule, $\sigma_{12} = \frac{1}{2}(\sigma_1 + \sigma_2)$. The introduction of the rigid-core parameters changes the value of σ_{12} by less than 1% for all the systems considered here. It should be mentioned that Eq. (4) is based on a representation of the potential in the immediate vicinity of the well by an (exp, 6) model in which the dimensionless repulsion parameter is given the value 14.

Finally, the combination rule for ϵ_{12} requires knowledge of $C_{12}^{(6)}$, the interaction dispersion coefficient. Although experimental values of $C_{12}^{(6)}$ are often known directly, it is easier to use the following well-tested combination rule; this rule is accurate on the 1% level:

$$\frac{\alpha_1\alpha_2}{C_{12}^{(6)}} = \frac{1}{2}\left[\frac{\alpha_1^2}{C_1^{(6)}} + \frac{\alpha_2^2}{C_2^{(6)}}\right], \tag{6}$$

in which α_1 and α_2 are the dipole polarizabilities. Once $C_{12}^{(6)}$ is known, the value of ϵ_{12} is readily calculated from the expression

$$\epsilon_{12} = (\epsilon_1\epsilon_2)^{1/2}\left[\frac{(\sigma_1 - a_1)^3\,(\sigma_2 - a_2)^3}{(\sigma_{12} - a_{12})^6}\right]$$

$$\times \frac{C_{12}^{(6)}}{(C_1^{(6)}\,C_2^{(6)})^{1/2}}. \tag{7}$$

The first factor on the right represents the conventional geometric-mean rule, $\epsilon_{12} = (\epsilon_1\epsilon_2)^{1/2}$, and the other factors give corrections. The introduction of the rigid-core parameters has a greater effect on ϵ_{12} than on σ_{12}; changes up to 10% occur in ϵ_{12} for the systems considered here.

Notice that only mean-spherical values of the α's and $C^{(6)}$'s are to be used in Eqs. (2) and (6), since we are seeking merely the effective spherical values of ϵ_{12} and σ_{12}.

At high temperatures the role of the potential well diminishes in importance, and the properties are dominated by an effective spherical repulsive potential, which can be represented by the form,

$$V(r) = V_0\exp(-r/\rho), \tag{8}$$

where V_0 and ρ are parameters deduced from high-energy beam scattering experiments. In other words, the scale factors ϵ and σ are replaced at high temperatures by V_0 and ρ, and the functionals for the two temperature ranges are joined smoothly through their second derivatives. We therefore need combination rules to predict the mixed-interaction parameters $(V_0)_{12}$ and ρ_{12} for use at high temperatures $(T^* > 10)$. The best combination rules available at present are based on an atomic-distortion model proposed by Gilbert[10,11] and elaborated somewhat by Smith;[12] they are as follows:

$$\rho_{12} = \frac{1}{2}(\rho_1 + \rho_2), \tag{9}$$

$$[(V_0)_{12}/\rho_{12}]^{2\rho_{12}} = [(V_0)_1/\rho_1]^{\rho_1}\,[(V_0)_2/\rho_2]^{\rho_2}. \tag{10}$$

The foregoing combination rules enable us to operate in a completely predictive mode for the properties of mixtures.

4. Parameters and Functionals

Parameters and physical constants are given in Appendix A, the functionals for the collision integrals and second virial coefficients in Appendix B, and the general formulas for their use in Appendix C.

Table A1 contains values of the universal physical constants that are needed,[13] and Table A2 lists the values of the atomic and molecular weights of the gases.[14] Table A3 lists the values of the scaling parameters σ and ϵ/k for all the interactions involved, and Table A4 lists the core parameters

a for the single gases involved in the combination rules. The latter are not directly needed in using the present results because we tabulate all the mixed interaction parameters σ_{12} and ϵ_{12}/k as calculated from the combination rules. We do not list the mixed core parameters a_{12} because they are easily obtained from Eq. (3). The values of σ and ϵ/k for single gases are the same as those used previously.[2,3] All values have been normalized with respect to argon, for which we assume

$$\sigma = 0.3350\text{ nm}, \quad \epsilon/k = 141.5\text{ K}.$$

Table A5 lists the values of the high-temperature scaling parameters ρ and V_0; the values for the single gases are the same as used previously,[2,3] and those for the mixed interactions have been calculated from the combination rules of Eqs. (9) and (10). They are given in dimensionless form,

$$\rho^* = \rho/\sigma, \quad V_0^* = V_0/\epsilon. \tag{11}$$

No values involving C_2H_4 and C_2H_6 are given, owing to the lack of suitable molecular-beam measurements.[5]

Table A6 lists the material parameters needed for the calculation of the nonspherical contributions to the second virial coefficients. The quantities α and $C^{(6)}$ also appear in the combination rules for σ_{12} and ϵ_{12}, but are not directly needed in this connection because we list σ_{12} and ϵ_{12}/k in Table A3. We have not included the mixed dispersion coefficients $C_{12}^{(6)}$ because they are easily calculated from Eq. (6).

The equations for the functionals in Appendix B are given only for $T^* > 1$ for the molecular gases, because a suitable correlation for them does not yet exist at lower temperatures. However, the noble gases functionals are given for $T^* < 1$, because they are needed for mixture calculations in some cases. For instance, consider the mixture $N_2 + Xe$ at 200 K. For N_2, $T^* = 200/98.4 = 2.033$, which is well above the lower limit of the correlation, but at the same temperature the value of T^* for Xe is $200/274.0 = 0.730$, for which the low-temperature functionals are needed. Moreover, for the N_2–Xe interaction the reduced temperature is $T_{12}^* = 200/159.3 = 1.255$, which is close to the lower limit. For this mixture, the lowest temperature for accurate application of the correlation would correspond to $T_{12}^* = 1$, or 159.3 K.

These constraints on the range of T^*, plus the fact that no beam data are available for C_2H_4 and C_2H_6, produce a uselessly small temperature range for C_2H_4–He and C_2H_6–He mixtures.

5. Experimental Data

The experimental data considered in this work were contained in about 800 references. These were based on three computer outputs supplied to us by the Purdue University Center for Information and Numerical Data Analysis (CINDAS), and on a fourth computer output provided by Project MIDAS[15] of the University of Stuttgart operated under the direction of Professor K. Stephan with the cooperation of Dr. A. Laesecke. These computer outputs were supplemented with citations from our own resources. All references were scrutinized and reduced to about 135 upon which our comparisons with experiment are ultimately

based. The latter were read, critically evaluated, and divided into two classes called primary data (PD) and secondary data (SD).

The division into two classes was based on several objective and subjective criteria. These were: (a) an evaluation of the capability of the method used and of the theory of the instrument; (b) a subjective assessment of the reliability of the data, guided by an examination of internal consistency of error analysis and reproducibility; (c) the authors' statement of precision and accuracy; and (d) a direct intercomparison of results from different laboratories and of results obtained by different methods.

The primary data were used for the most part as guides to the original formulation of the combination rules for σ_{12} and ϵ_{12}.[9] Secondary data served for validation. The references listed in the bibliography of Appendix E contain both primary and secondary data.

6. Validation, Deviation Plots, and Accuracy

Validation of our computational procedures is represented by 201 comparison plots in Appendix D. The class of the data (PD or SD) is indicated in the captions.

Figures 1–62 are deviation plots for the mixture viscosities. The viscosities of the pure components that were used in these calculations were also calculated from the correlation scheme rather than taken directly from experiment, so that the deviations shown are indicative of what can be expected from a calculation based entirely on a principle of corresponding states and combination rules. Comparison of these deviation plots with the corresponding ones for the single polyatomic gases in Ref. 3 shows that the agreement between calculated and experimental results is about as good for the mixtures as for the single gases. This good agreement can be at least partly attributed to the fact that mixture viscosities are not very sensitive to combination rules, for two reasons. The first reason is that the like interactions in a mixture contribute to the viscosity on an equal footing with the unlike interactions. The second reason is that there is usually a compensation effect in the values of σ_{12} and ϵ_{12} as obtained from the combination rules: the errors in σ_{12} and ϵ_{12} are usually in opposite directions, and tend to compensate each other in the calculation of the interaction term η_{12} in the mixture viscosity.[9]

Based on the above considerations, our estimate of the accuracy of calculated mixture viscosities is about 1%. The reader who wishes a more precise estimate in a particular case must examine in detail the relevant deviation plots and the reliability of the data.

Deviation plots for binary diffusion coefficients are shown in Figs. 63–122. Diffusion coefficients depend almost entirely on the unlike interactions in the mixture, and are influenced by the like interactions to the extent of a few percent at most. They therefore supply a more direct test of the combination rules than do mixture viscosities, but unfortunately the experimental accuracy of the measurements is distinctly lower than in the case of the viscosity. Scatter in the data as high as $\pm$ 10% can be seen to be not uncommon. The measurements that we believe to be the most reliable are

the comparatively recent ones by P. J. Dunlop and his collaborators reported in Appendix E, Refs. 8, 14, 32, 33, 90, 109, and 111–113. In the 34 mixtures for which comparisons with the measurements of Dunlop et al. are possible, only two points (for O_2–CO_2 and SF_6–Ar) deviate by more than 5%, and in most cases the agreement is much closer. For other systems for which measurements are available from more than one laboratory, the agreement is almost always within the experimental scatter.

We therefore feel justified in giving an estimated accuracy of about 5% for our calculated binary diffusion coefficients. This is consistent with the estimated accuracies of calculated self-diffusion coefficients for the eleven molecular gases reported in Ref. 3. For some systems the accuracy is probably greater, as validated by the agreement with the measurements of Dunlop et al., and as can be determined by reference to the deviation plots.

Deviation plots for the second virial coefficients of mixtures are shown in Figs. 123–173. Here it seems best to show the interaction coefficient B_{12} rather than B_{mix} for the whole mixture. The coefficient B_{12} contributes to B_{mix} with a weight factor of at most 1/2, for an equimolar binary mixture. The interaction coefficients B_{12} depend entirely on the unlike interactions in the mixture, and thus supply a direct test of the combination rules, being similar to the diffusion coefficients in this respect. However, B_{12} and D_{12} have quite different sensitivities to the scaling parameters σ_{12} and ϵ_{12}, and in particular there is less of a compensation effect in B_{12} for errors in σ_{12} and ϵ_{12} than is the case for D_{12} (and η_{12}). It is consequently rather difficult to give a brief overall summary of the estimated accuracy of the present correlation scheme for B_{12}, and hence for B_{mix}. Examination of the deviation plots shows that for most of the pairs the deviations in B_{12} are comparable to, but somewhat greater than, the deviations in the corresponding B_{11} and B_{22} for the single components reported in Ref. 3. Thus the overall accuracy in B_{mix} would be about the same as that for the single components. However, in some cases the deviations in B_{12} appear to be shockingly large in comparison with B_{12} itself --for example, in a number of the mixtures involving SF_6. But in most such cases it happens that the large deviations can be explained by a strong temperature dependence of B_{12} that causes the results to be extremely sensitive to the value of ϵ_{12}. For example, the calculated value of B_{12} for N_2–SF_6 at 300 K is too small in magnitude by nearly a factor of 2, but this corresponds to an error in ϵ_{12} of only about 12%. In other words, it is not the value of B_{12} that should be considered to be in error, but rather the temperature at which that value occurs.

A rough general estimate of the reliability of calculated values of B_{mix} can thus be formulated as follows. The uncertainty in B_{12} is either about 5×10^{-3} m^3/kmol, or else corresponds to an uncertainty of 10–15% in ϵ_{12}, whichever is worse. This uncertainty is reduced by about a factor of 2 in B_{mix}. For a more precise estimate in any particular case, it is necessary to examine deviation plots.

Calculated and experimental thermal diffusion factors α_T are compared in Figures 174–201. Because of the complicated dependence of α_T on composition, as well as on molecular masses and collision integrals, it is convenient to make

the comparison in terms of reduced thermal diffusion factors, defined as

$$\text{Reduced } \alpha_T \equiv \alpha_T \left(\frac{x_1^2 Q_1 + x_2^2 Q_2 + x_1 x_2 Q_{12}}{x_1 S_1 - x_2 S_2} \right), \quad (12)$$

where the S's and Q's are defined in Eqs. (C6a)–(C6c) of Appendix C. Multiplication of α_T by the factor containing the S's and Q's removes the major dependence of α_T on composition, molecular masses, and those collision integrals that represent the interactions between pairs of like molecules in the mixture, leaving a temperature-dependent quantity that is dominated by only the unlike interactions. In particular, from Eq. (C6) we have

$$\text{Reduced } \alpha_T \approx (6 C_{12}^* - 5)(1 + \kappa_T), \quad (13)$$

where C_{12}^* is the functional defined by Eq. (B3d) of Appendix B, which is independent of the parameter σ_{12} and depends only on $T_{12}^* = kT/\epsilon_{12}$ (plus any dimensionless parameters needed to specify the shape of the interaction potential for unlike pairs). The quantity κ_T is a small but complicated correction term that we have neglected in our calculations.

Although Eq. (13) is only approximate, because it derives from a theory that neglects inelastic collisions and nonspherical interactions, it demonstrates the extreme sensitivity of the reduced α_T to the unlike interactions. That is, from Eq. (B3d) we see that C_{12}^* depends on the temperature derivative of the functional $\Omega_{12}^{(1,1)*}$ that determines D_{12}, so that errors in $\Omega_{12}^{(1,1)*}$ are magnified. These errors are further magnified because the quantity $(6 C_{12}^* - 5)$ involves the difference between two numbers of comparable magnitude. These features mean that calculated values of α_T may well involve uncertainties that are about one order of magnitude (about a factor of 10) larger than the corresponding uncertainties in η_{mix} and D_{12}. The saving grace is that measured values of α_T also involve uncertainties of similar magnitude.

The comparisons in Figs. 174–201 document the above-mentioned uncertainties in the calculated and experimental values of α_T. These comparisons are fairly selective in that many early measurements, believed to be of lower accuracy, are omitted. Also omitted are the results for the systems CH_4–Ne and CO_2–Ar, for which α_T is very small because the molecular masses of the components are close to each other, and the calculations are unreliable. Even so, disagreements of as much as a factor of two occur for a few systems. But if we consider only those measurements that we believe

to be the most reliable [Appendix E, Refs. 32, 53, 106, 109–114], an estimate of accuracy of roughly 25% appears to be justified. (The systems N_2–Ne and CO–Ne seem to be exceptions.)

To summarize, our estimated accuracies are about 1% for η_{mix}, 5% for D_{12}, 25% for α_T, and either 5×10^{-3} m^3/kmol or 10–15% in ϵ_{12} for B_{12}, whichever is worse. These accuracies are comparable to, but somewhat poorer than, the corresponding estimated accuracies for the pure components reported in Ref. 3. They are poorer than the corresponding accuracies for noble-gas mixtures reported in Ref. 2, but enjoy the advantage of operation in an entirely predictive mode. For more precise estimates of accuracy for particular mixtures, it is necessary to examine Figs. 1–201 in detail.

7. Description of the Tables

The tables of numerical data are not meant to be exhaustive and have not been designed for linear interpolation. They are convenient extracts only, because the entire algorithm for each property of every mixture can be programmed on a computer without difficulty on the basis of the information supplied here. They can be used for numerical checks of such programs. A more extensive tabulation would be prohibitively large.

The tables are identical in their structure and give values of B, η, D_{12}, and α_T in SI units. Below 0°C, the temperatures are listed in kelvins, and above that in degrees Celsius in comformity with prevailing common practice. The number of significant figures given was partly determined by aesthetic considerations, and exceeds that which would be justified by the analysis of Sec. 6. There are 108 tables, one for each mixture, except C_2H_4-He and C_2H_6-He, which have uselessly small temperature ranges for the reasons discussed in Sec. 4. As noted in Sec. 6, the tables list B_{mix} for the mixture itself, whereas the deviation plots refer to the interaction coefficient B_{12}. The calculations for D_{12} refer to a pressure of 1 atm = 101325 N/m^2. Because of space limitations, only the first 10 tables are presented here. The remaining 98 tables have been deposited with the Physics Auxilliary Publication Service (PAPS) of the American Institute of Physics.[a]

The algorithms presented in this paper make it possible to program calculations for a wide range of low-density equilibrium and transport properties of 16 gases and of all possible multicomponent mixtures formed with them. For each system, the program would cover the full range of compositions.

8. Tables

TABLE 1. Properties of an equimolar mixture of nitrogen and oxygen (N_2–O_2).

T K or °C	B 10^{-3} m³/kmol	η $\mu Pa\,s$	D(1.013 bar) 10^{-4} m²/s	α_T
150 K	− 79.87	10.62	0.0611	0.0094
200	− 41.92	13.83	0.1046	0.0164
250	− 21.27	16.71	0.1565	0.0206
300	− 8.31	19.34	0.2161	0.0232
0 °C	− 14.60	17.95	0.1832	0.0219
20	− 9.79	18.99	0.2075	0.0229
40	− 5.68	20.00	0.2329	0.0238
60	− 2.14	20.98	0.2595	0.0245
80	0.94	21.93	0.2871	0.0251
100	3.63	22.86	0.3158	0.0257
150	9.01	25.08	0.3920	0.0268
200	12.99	27.19	0.4744	0.0275
250	15.97	29.20	0.5626	0.0281
300	18.23	31.12	0.6565	0.0285
350	19.94	32.97	0.7560	0.0288
400	21.26	34.76	0.8609	0.0290
450	22.28	36.50	0.9711	0.0291
500	23.07	38.18	1.0864	0.0292
600	24.19	41.42	1.3321	0.0293
700	24.96	44.51	1.5975	0.0293
800	25.59	47.48	1.8818	0.0292
900	26.15	50.35	2.1846	0.0289
1000	26.67	53.14	2.5064	0.0281
1500	28.19	66.29	4.4076	0.0251
2000	28.48	78.54	6.7683	0.0242
2500	28.26	90.18	9.5545	0.0240
3000	27.83	101.37	12.7435	0.0241

TABLE 2. Properties of an equimolar mixture of nitrogen and nitric oxide (N_2–NO).

T K or °C	B 10^{-3} m³/kmol	η $\mu Pa\,s$	D(1.013 bar) 10^{-4} m²/s	α_T
150 K	− 87.73	10.16	0.0605	0.0051
200	− 46.45	13.24	0.1036	0.0089
250	− 24.23	16.01	0.1551	0.0110
300	− 10.34	18.55	0.2143	0.0123
0 °C	− 17.07	17.21	0.1816	0.0117
20	− 11.92	18.21	0.2058	0.0122
40	− 7.52	19.18	0.2310	0.0126
60	− 3.73	20.13	0.2574	0.0129
80	− 0.44	21.04	0.2849	0.0132
100	2.43	21.94	0.3134	0.0134
150	8.20	24.08	0.3890	0.0139
200	12.46	26.11	0.4708	0.0142
250	15.67	28.04	0.5585	0.0144
300	18.10	29.90	0.6518	0.0146
350	19.96	31.68	0.7506	0.0147
400	21.40	33.40	0.8548	0.0148
450	22.51	35.07	0.9642	0.0148
500	23.38	36.69	1.0787	0.0148
600	24.62	39.81	1.3228	0.0148
700	25.46	42.78	1.5862	0.0148
800	26.12	45.64	1.8686	0.0148
900	26.71	48.40	2.1692	0.0147
1000	27.24	51.09	2.4886	0.0142
1500	28.85	63.75	4.3820	0.0124
2000	29.16	75.65	6.7474	0.0118
2500	28.91	87.02	9.5519	0.0116
3000	28.43	98.01	12.7738	0.0116

TABLE 3. Properties of an equimolar mixture of nitrogen and carbon monoxide (N_2–CO).

T K or °C	B 10^{-3} m³/kmol	η $\mu Pa\,s$	D(1.013 bar) 10^{-4} m²/s	α_T
100 K	− 173.00	6.71	0.0279	0.000
150	− 76.90	10.02	0.0613	0.000
200	− 38.16	12.94	0.1041	0.000
250	− 17.09	15.55	0.1551	0.000
300	− 3.94	17.93	0.2135	0.000
0 °C	− 10.30	16.67	0.1812	0.000
20	− 5.44	17.61	0.2051	0.000
40	− 1.29	18.53	0.2300	0.000
60	2.26	19.41	0.2560	0.000
80	5.33	20.27	0.2831	0.000
100	8.00	21.11	0.3111	0.000
150	13.29	23.12	0.3857	0.000
200	17.13	25.03	0.4662	0.000
250	19.95	26.85	0.5526	0.000
300	22.04	28.59	0.6445	0.000
350	23.60	30.27	0.7419	0.000
400	24.77	31.89	0.8446	0.000
450	25.66	33.47	0.9524	0.000
500	26.34	35.00	1.0654	0.000
600	27.34	37.94	1.3062	0.000
700	28.12	40.76	1.5663	0.000
800	28.82	43.47	1.8451	0.000
900	29.49	46.10	2.1425	0.000
1000	30.04	48.67	2.4583	0.000
1500	31.39	60.91	4.3105	0.000
2000	31.42	72.50	6.6074	0.000
2500	30.96	83.64	9.3333	0.000
3000	30.31	94.43	12.4747	0.000

TABLE 4. Properties of an equimolar mixture of nitrogen and carbon dioxide (N_2–CO_2).

T K or °C	B 10^{-3} m³/kmol	η $\mu Pa\,s$	D(1.013 bar) 10^{-4} m²/s	α_T
250 K	− 79.59	14.06	0.1180	0.0583
300	− 49.28	16.58	0.1652	0.0754
0 °C	− 63.61	15.25	0.1391	0.0670
20	− 52.60	16.25	0.1583	0.0734
40	− 43.47	17.22	0.1785	0.0790
60	− 35.78	18.16	0.1997	0.0838
80	− 29.24	19.09	0.2217	0.0881
100	− 23.61	19.98	0.2446	0.0918
150	− 12.48	22.14	0.3055	0.0995
200	− 4.31	24.19	0.3714	0.1053
250	1.88	26.14	0.4422	0.1099
300	6.69	28.01	0.5175	0.1134
350	10.50	29.81	0.5973	0.1162
400	13.55	31.55	0.6814	0.1185
450	16.03	33.22	0.7697	0.1203
500	18.07	34.85	0.8621	0.1217
600	21.18	37.97	1.0588	0.1238
700	23.40	40.93	1.2709	0.1251
800	25.06	43.77	1.4979	0.1259
900	26.33	46.51	1.7394	0.1263
1000	27.31	49.15	1.9950	0.1265
1500	30.18	61.37	3.4746	0.1248
2000	31.54	72.51	5.2816	0.1188
2500	32.19	82.96	7.4049	0.1151
3000	32.45	92.93	9.8285	0.1130

TABLE 5. Properties of an equimolar mixture of nitrogen and nitrous oxide (N_2–N_2O).

T K or °C	B 10^{-3} m³/kmol	η $\mu Pa\,s$	D(1.013 bar) 10^{-4} m²/s	α_T
300 K	− 53.95	16.58	0.1662	0.0717
0 °C	− 67.90	15.23	0.1398	0.0630
20	− 57.19	16.24	0.1593	0.0696
40	− 48.25	17.23	0.1797	0.0753
60	− 40.68	18.19	0.2011	0.0803
80	− 34.18	19.12	0.2233	0.0847
100	− 28.54	20.04	0.2465	0.0886
150	− 17.27	22.24	0.3082	0.0966
200	− 8.86	24.32	0.3749	0.1026
250	− 2.39	26.31	0.4466	0.1074
300	2.71	28.21	0.5229	0.1111
350	6.81	30.04	0.6037	0.1140
400	10.14	31.81	0.6889	0.1164
450	12.88	33.52	0.7784	0.1183
500	15.16	35.17	0.8720	0.1198
600	18.69	38.35	1.0712	0.1220
700	21.27	41.37	1.2861	0.1235
800	23.21	44.26	1.5160	0.1244
900	24.70	47.04	1.7605	0.1249
1000	25.86	49.73	2.0193	0.1252
1500	29.09	62.14	3.5170	0.1246
2000	30.54	73.43	5.3396	0.1204
2500	31.19	84.01	7.4753	0.1170
3000	31.48	94.08	9.9101	0.1147

TABLE 6. Properties of an equimolar mixture of nitrogen and methane (N_2–CH_4).

T K or °C	B 10^{-3} m³/kmol	η $\mu Pa\,s$	D(1.013 bar) 10^{-4} m²/s	α_T
200 K	− 66.75	10.36	0.1105	0.0516
250	− 38.45	12.60	0.1666	0.0728
300	− 20.90	14.66	0.2312	0.0876
0 °C	− 29.40	13.57	0.1955	0.0803
20	− 22.90	14.38	0.2219	0.0858
40	− 17.34	15.17	0.2495	0.0907
60	− 12.54	15.94	0.2784	0.0950
80	− 8.35	16.68	0.3084	0.0988
100	− 4.69	17.41	0.3396	0.1022
150	2.73	19.14	0.4225	0.1092
200	8.31	20.79	0.5122	0.1146
250	12.59	22.36	0.6083	0.1187
300	15.92	23.87	0.7106	0.1219
350	18.54	25.31	0.8189	0.1244
400	20.61	26.71	0.9331	0.1264
450	22.27	28.06	1.0530	0.1279
500	23.60	29.38	1.1785	0.1291
600	25.56	31.90	1.4458	0.1307
700	26.90	34.31	1.7341	0.1316
800	27.87	36.62	2.0430	0.1319
900	28.64	38.85	2.3717	0.1319
1000	29.26	41.01	2.7199	0.1319
1500	31.33	51.13	4.7533	0.1188
2000	32.17	60.53	7.2727	0.1112
2500	32.30	69.43	0.2435	0.1077
3000	32.09	77.97	3.6386	0.1056

TABLE 7. Properties of an equimolar mixture of nitrogen and carbon tetra-fluoride (N_2–CF_4).

T K or °C	B 10^{-3} m³/kmol	η $\mu Pa\,s$	D(1.013 bar) 10^{-4} m²/s	α_T
200 K	− 105.91	12.72	0.0623	0.1293
250	− 61.71	15.51	0.0938	0.1712
300	− 34.48	18.08	0.1300	0.1992
0 °C	− 47.65	16.72	0.1100	0.1855
20	− 37.58	17.74	0.1248	0.1959
40	− 28.99	18.72	0.1403	0.2050
60	− 21.59	19.67	0.1565	0.2128
80	− 15.16	20.60	0.1733	0.2197
100	− 9.52	21.51	0.1908	0.2258
150	1.84	23.68	0.2373	0.2381
200	10.35	25.73	0.2875	0.2472
250	16.85	27.69	0.3414	0.2542
300	21.89	29.57	0.3988	0.2595
350	25.84	31.37	0.4595	0.2635
400	28.96	33.12	0.5235	0.2666
450	31.44	34.80	0.5907	0.2689
500	33.43	36.44	0.6610	0.2707
600	36.33	39.58	0.8108	0.2729
700	38.30	42.58	0.9725	0.2739
800	39.72	45.46	1.1456	0.2741
900	40.83	48.23	1.3299	0.2738
1000	41.75	50.92	1.5244	0.2733
1500	44.72	63.42	2.6749	0.2290
2000	46.07	74.77	4.1132	0.2249
2500	46.49	85.25	5.7999	0.2330
3000	46.46	95.06	7.7096	0.2420

TABLE 8. Properties of an equimolar mixture of nitrogen and sulfur hexa-fluoride (N_2–SF_6).

T K or °C	B 10^{-3} m³/kmol	η $\mu Pa\,s$	D(1.013 bar) 10^{-4} m²/s	α_T
250 K	− 139.80	14.38	0.0741	0.2109
300	− 86.37	16.90	0.1028	0.2470
0° C	− 111.84	15.57	0.0869	0.2293
20	− 92.29	16.56	0.0987	0.2428
40	− 75.94	17.53	0.1110	0.2545
60	− 62.08	18.47	0.1239	0.2646
80	− 50.20	19.39	0.1373	0.2736
100	− 39.93	20.28	0.1512	0.2814
150	− 19.52	22.43	0.1881	0.2974
200	− 4.46	24.46	0.2281	0.3094
250	6.96	26.40	0.2710	0.3185
300	15.81	28.26	0.3166	0.3255
350	22.77	30.05	0.3650	0.3310
400	28.33	31.77	0.4159	0.3352
450	32.80	33.44	0.4694	0.3384
500	36.45	35.06	0.5254	0.3409
600	41.92	38.16	0.6446	0.3443
700	45.76	41.12	0.7731	0.3460
800	48.57	43.95	0.9108	0.3466
900	50.74	46.68	1.0573	0.3466
1000	52.49	49.32	1.2124	0.3472
1500	57.44	61.53	2.1147	0.3285
2000	59.50	72.62	3.2216	0.3233
2500	60.55	82.93	4.5146	0.3240
3000	60.90	92.65	5.9806	0.3257

TABLE 9. Properties of an equimolar mixture of nitrogen and ethylene (N_2–C_2H_4).

T K or °C	B 10^{-3} m³/kmol	η $\mu Pa\,s$	D(1.013 bar) 10^{-4} m²/s	α_T
250 K	− 85.95	11.70	0.1212	0.0152
300	− 54.42	13.77	0.1692	0.0180
0 °C	− 69.45	12.68	0.1426	0.0167
20	− 57.92	13.50	0.1622	0.0177
40	− 48.26	14.29	0.1828	0.0185
60	− 40.05	15.06	0.2043	0.0191
80	− 33.00	15.81	0.2267	0.0196
100	− 26.88	16.54	0.2499	0.0200
150	− 14.65	18.31	0.3118	0.0207
200	− 5.53	19.97	0.3787	0.0211
250	1.47	21.57	0.4505	0.0213
300	6.97	23.09	0.5269	0.0214
350	11.36	24.56	0.6079	0.0214
400	14.91	25.97	0.6932	0.0214
450	17.82	27.34	0.7828	0.0214
500	20.22	28.66	0.8765	0.0213
600	23.90	31.21	1.0761	0.0211
700	26.54	33.63	1.2913	0.0210
800	28.51	35.95	1.5217	0.0208
900	30.02	38.18	1.7668	0.0206
1000	31.18	40.35	2.0263	0.0205

TABLE 10. Properties of an equimolar mixture of nitrogen and ethane (N_2–C_2H_6).

T K or °C	B 10^{-3} m³/kmol	η $\mu Pa\,s$	D(1.013 bar) 10^{-4} m²/s	α_T
250 K	− 106.44	11.03	0.1107	0.0273
300	− 68.71	12.97	0.1544	0.0332
0 °C	− 86.71	11.95	0.1302	0.0304
20	− 72.90	12.71	0.1481	0.0326
40	− 61.32	13.46	0.1669	0.0344
60	− 51.47	14.19	0.1865	0.0366
80	− 43.00	14.89	0.2069	0.0373
100	− 35.64	15.58	0.2281	0.0385
150	− 20.90	17.24	0.2845	0.0407
200	− 9.88	18.81	0.3455	0.0423
250	− 1.40	20.31	0.4109	0.0435
300	5.28	21.75	0.4806	0.0443
350	10.63	23.13	0.5544	0.0450
400	14.96	24.46	0.6322	0.0454
450	18.52	25.75	0.7139	0.0458
500	21.46	27.00	0.7993	0.0460
600	25.99	29.39	0.9812	0.0464
700	29.25	31.67	1.1774	0.0465
800	31.67	33.86	1.3875	0.0465
900	33.51	35.96	1.6110	0.0464
1000	34.93	37.99	1.8476	0.0464

9. Acknowledgments

10. References to Introductory Text

[a] See AIP document no. PAPS JPCRD-19-1179-98 for 98 pages comprising Tables 11–108. Order by PAPS number and journal reference from American Institute of Physics, Physics Auxiliary Publication Service, 335 East 45th Street, New York, NY 10017. The price is $1.50 for each microfiche (98 pages) or $5.00 for photocopies of up to 30 pages, and $0.15 for each additional page over 30 pages. Airmail additional. Make checks payable to the American Institute of Physics.

[1] B. Najafi, E. A. Mason, and J. Kestin, Physica **119A**, 387 (1983).

[2] J. Kestin, K. Knierim, E. A. Mason, B. Najafi, S. T. Ro, and M. Waldman, J. Phys. Chem. Ref. Data **13**, 229 (1984).

[3] A. Boushehri, J. Bzowski, J. Kestin, and E. A. Mason, J. Phys. Chem. Ref. Data **16**, 445 (1987).

[4] L. Monchick, S. I. Sandler, and E. A. Mason, J. Chem. Phys. **49**, 1178 (1968).

[5] E. A. Mason, R. J. Munn, and F. J. Smith, Adv. At. Mol. Phys. **2**, 33 (1966).

[6] S. I. Sandler and J. S. Dahler, J. Chem. Phys. **47**, 2621 (1967).

[7] J. Kestin, H. E. Khalifa, S. T. Ro, and W. A. Wakeham, Physica **88A**, 242 (1977).

[8] K. T. Tang and J. P. Toennies, Z. Phys. **D1**, 91 (1986).

[9] J. Bzowski, E. A. Mason, and J. Kestin, Int. J. Thermophys. **9**, 131 (1988).

[10] T. L. Gilbert, J. Chem. Phys. **49**, 2640 (1968).

[11] T. L. Gilbert, O. C. Simpson, and M. A. Williamson, J. Chem. Phys. **63**, 4061 (1975).

[12] F. T. Smith, Phys. Rev. **A5**, 1708 (1972).

[13] E. R. Cohen and B. N. Taylor, J. Phys. Chem. Ref. Data **17**, 1795 (1988).

[14] J. R. DeLaeter, J. Phys. Chem. Ref. Data **17**, 1791 (1988).

[15] A. Laesecke, K. Stephan, and R. Krauss, Int. J. Thermophys **7**, 973 (1986).

Appendix A: Material and physical constants including scaling factors

TABLE A1. Universal constants.[a]

Boltzmann constant	$k = 1.380\,658 \times 10^{-23}$ JK^{-1}
Avogadro constant	$N_A = 6.022\,1367 \times 10^{23}$ mol^{-1}
Universal gas constant	$R = 8.314\,510$ J mol^{-1} K^{-1}

[a] Ref. 13.

TABLE A2. Atomic and molecular weights[a] (average isotopic composition, kg/kmol).

N_2	28.0135
O_2	31.9988
NO	30.0061
CO	28.010
CO_2	44.010
N_2O	44.0129
CH_4	16.043
CF_4	88.005
SF_6	146.056
C_2H_4	28.054
C_2H_6	30.070
^{3}He	3.0160
^{4}He	4.0026
Ne	20.1797
Ar	39.948
Kr	83.80
Xe	131.29

[a] Ref. 14.

TABLE A3. Effective spherical scaling parameters σ_{ij} and ϵ_{ij}.

σ(nm)

	N_2	O_2	NO	CO	CO_2	N_2O	CH_4	CF_4	SF_6	C_2H_4	C_2H_6	He	Ne	Ar	Kr	Xe
N_2	0.3652	0.3529	0.3562	0.3652	0.3711	0.3676	0.3687	0.4132	0.4521	0.3878	0.4032	0.3243	0.3253	0.3499	0.3610	0.3778
O_2		0.3407	0.3441	0.3529	0.3596	0.3561	0.3569	0.4016	0.4409	0.3765	0.3919	0.3096	0.3118	0.3378	0.3492	0.3665
NO			0.3474	0.3562	0.3627	0.3592	0.3601	0.4045	0.4435	0.3794	0.3948	0.3139	0.3157	0.3412	0.3524	0.3695
CO				0.3652	0.3711	0.3676	0.3687	0.4132	0.4520	0.3878	0.4032	0.3244	0.3253	0.3499	0.3610	0.3778
CO_2					0.3769	0.3736	0.3745	0.4172	0.4536	0.3923	0.4074	0.3339	0.3343	0.3568	0.3671	0.3829
N_2O						0.3703	0.3710	0.4138	0.4503	0.3890	0.4042	0.3297	0.3304	0.3534	0.3637	0.3796
CH_4							0.3721	0.4156	0.4530	0.3904	0.4057	0.3302	0.3307	0.3540	0.3645	0.3808
CF_4								0.4579	0.4932	0.4323	0.4474	0.3814	0.3790	0.3986	0.4079	0.4228
SF_6									0.5252	0.4672	0.4820	0.4298	0.4236	0.4377	0.4453	0.4580
C_2H_4										0.4071	0.4221	0.3553	0.3537	0.3736	0.3830	0.3978
C_2H_6											0.4371	0.3717	0.3697	0.3890	0.3982	0.4128

ϵ/k (K)

	N_2	O_2	NO	CO	CO_2	N_2O	CH_4	CF_4	SF_6	C_2H_4	C_2H_6	He	Ne	Ar	Kr	Xe
N_2	98.4	108.8	110.8	98.4	155.0	161.4	125.0	118.0	121.2	148.6	146.8	23.42	52.97	117.7	139.4	159.3
O_2		121.1	122.9	108.7	168.8	175.9	136.8	127.0	127.6	159.7	157.4	27.94	61.77	130.9	152.8	171.7
NO			125.0	110.8	172.9	180.3	140.1	131.1	132.7	164.8	162.5	27.56	61.24	132.9	156.2	177.0
CO				98.4	155.2	161.9	125.4	118.5	121.5	149.2	147.3	23.23	52.41	117.6	139.7	160.0
CO_2					245.3	255.2	198.5	193.0	204.1	241.0	238.9	34.14	70.70	182.2	219.6	256.3
N_2O						266.8	207.9	201.4	210.4	251.4	248.7	35.82	80.37	190.2	229.5	268.0
CH_4							161.4	155.4	161.6	194.8	192.5	27.78	62.64	148.1	178.6	208.2
CF_4								156.5	172.6	195.9	194.8	22.31	52.69	137.4	171.0	207.2
SF_6									207.7	215.0	216.1	19.24	48.18	137.4	176.7	223.6
C_2H_4										244.3	242.9	28.72	67.05	172.6	214.0	258.3
C_2H_6											241.9	27.81	65.49	170.0	211.4	256.4

TABLE A4. Core parameters for combination rules.

	a(nm)
N_2	0.0006
O_2	0.0000
NO	0.0000
CO	0.0000
CO_2	0.0094
N_2O	0.0102
CH_4	0.0029
CF_4	0.0358
SF_6	0.0319
C_2H_4	0.0022
C_2H_6	0.0239
He	0
Ne	0
Ar	0
Kr	0
Xe	0

TABLE A5. High-temperature dimensionless scaling parameters, $\rho^* = \rho/\sigma$ and $V_0^* = V_0/\epsilon$.

	N₂	O₂	NO	CO	CO₂	N₂O	CH₄	CF₄	SF₆	He	Ne	Ar	Kr	Xe
N₂	0.1080	0.0918	0.0984	0.1080	0.0897	0.0904	0.0887	0.0588	0.0727	0.0929	0.0938	0.0964	0.0957	0.0961
O₂		0.0745	0.0815	0.0918	0.0730	0.0736	0.0719	0.0430	0.0586	0.0746	0.0753	0.0790	0.0788	0.0799
NO			0.0883	0.0984	0.0797	0.0803	0.0786	0.0492	0.0642	0.0820	0.0828	0.0860	0.0856	0.0864
CO				0.1080	0.0897	0.0904	0.0887	0.0588	0.0727	0.0929	0.0938	0.0964	0.0957	0.0961
CO₂					0.0720	0.0725	0.0709	0.0435	0.0589	0.0718	0.0729	0.0773	0.0774	0.0788
N₂O						0.0730	0.0714	0.0437	0.0592	0.0725	0.0736	0.0779	0.0780	0.0793
CH₄							0.0698	0.0423	0.0576	0.0708	0.0719	0.0762	0.0763	0.0777
CF₄								0.0200	0.0359	0.0393	0.0406	0.0466	0.0476	0.0501
SF₆									0.0500	0.0548	0.0565	0.0620	0.0628	0.0649

$$V_0^{*\,a}$$

	N₂	O₂	NO	CO	CO₂	N₂O	CH₄	CF₄	SF₆	He	Ne	Ar	Kr	Xe
N₂	5.308(4)	1.790(5)	9.563(4)	5.311(4)	2.420(5)	2.322(5)	2.490(5)	2.060(7)	2.031(6)	2.547(5)	2.048(5)	1.303(5)	1.252(5)	1.297(5)
O₂		1.322(6)	4.877(5)	1.792(5)	2.011(6)	1.937(6)	2.070(6)	3.455(9)	3.039(7)	1.546(6)	1.464(6)	8.057(5)	7.602(5)	7.346(5)
NO			2.145(5)	9.566(4)	7.094(5)	6.812(5)	7.256(5)	2.797(8)	8.273(6)	6.099(5)	5.418(5)	3.238(5)	3.092(5)	3.105(5)
CO				5.308(4)	2.418(5)	2.314(5)	2.482(5)	2.052(7)	2.026(6)	2.568(5)	2.070(5)	1.304(5)	1.250(5)	1.291(5)
CO₂					2.800(6)	2.705(6)	2.946(6)	4.520(9)	3.586(7)	3.016(6)	2.929(6)	1.202(6)	1.074(6)	9.577(5)
N₂O						2.600(6)	2.827(6)	4.460(9)	3.513(7)	2.880(6)	2.584(6)	1.155(6)	1.030(6)	9.182(5)
CH₄							3.066(6)	5.669(9)	4.060(7)	2.954(6)	2.689(6)	1.231(6)	1.106(6)	9.978(5)
CF₄								1.460(19)	2.160(11)	9.329(9)	9.689(9)	9.765(8)	6.522(8)	3.322(8)
SF₆									4.067(8)	7.590(7)	5.904(7)	1.606(7)	1.255(7)	9.047(6)

[a] Values in parentheses are the powers of 10 by which the entries are multiplied.

TABLE A6. Dimensionless material parameters for the calculation of the nonspherical contributions to second virial coefficients.

	μ^*	θ^*	α^*	κ	C_6^*
N₂	0	0.47	0.0357	0.131	2.18
O₂	0	0.141	0.0397	0.229	2.27
NO	0.180	0.61	0.0408	0.162	2.20
CO	0.138	0.84	0.0404	0.090	2.63
CO₂	0	0.85	0.0547	0.268	1.86
N₂O	0.122	0.59	0.0607	0.329	1.89
CH₄	0	0	0.0503	0	2.10
CF₄	0	0	0.0402	0	1.35
SF₆	0	0	0.0452	0	1.51
C₂H₄	0	0.33	0.0631	0.143	2.13
C₂H₆	0	0.11	0.0529	0.058	1.57
He	0	0	0.0115	0	3.09
Ne	0	0	0.0189	0	2.594
Ar	0	0	0.0437	0	2.210
Kr	0	0	0.0547	0	2.164
Xe	0	0	0.0690	0	2.162

Dipole moment	$\mu^* = \mu_0/(\epsilon\sigma^3)^{1/2}$
Quadrupole moment	$\theta^* = \theta/(\epsilon\sigma^5)^{1/2}$
Dipole polarizability	$\alpha^* = \overline{\alpha}/\sigma^3$
	$\overline{\alpha} = (1/3)(\alpha^{\parallel} + 2\alpha^{\perp})$
Polarizability anisotropy	$\kappa = (1/3)(\alpha^{\parallel} - \alpha^{\perp})/\overline{\alpha}$
Dispersion coefficient	$C_6^* = \overline{C}^{(6)}/\epsilon\sigma^6$

Data from Refs. 1–3 and the sources listed therein.

Appendix B. Correlation equations for functionals

Collision Integrals

$\Omega^{(2,2)*}$, molecular gases

$1 \leqslant T^* \leqslant 10$

$$\Omega^{(2,2)*} = \exp\,[0.46641 - 0.56991(\ln T^*)$$
$$+ 0.19591\,(\ln T^*)^2 - 0.03879\,(\ln T^*)^3$$
$$+ 0.00259\,(\ln T^*)^4]. \tag{B1a}$$

$T^* \geqslant 10$

$$\Omega^{(2,2)*} = (\rho^*)^2 \alpha^2 [1.04 + a_1(\ln T^*)^{-1} + a_2(\ln T^*)^{-2}$$
$$+ a_3(\ln T^*)^{-3} + a_4(\ln T^*)^{-4}], \tag{B1b}$$

where

$a_1 = 0,$

$a_2 = -33.0838 + (\alpha_{10}\rho^*)^{-2}[20.0862$
$\quad + (72.1059/\alpha_{10}) + (8.27648/\alpha_{10})^2],$

$a_3 = 101.571 - (\alpha_{10}\rho^*)^{-2}[56.4472$
$\quad + (286.393/\alpha_{10}) + (17.7610/\alpha_{10})^2],$

$a_4 = -87.7036 + (\alpha_{10}\rho^*)^{-2}[46.3130$
$\quad + (277.146/\alpha_{10}) + (19.0573/\alpha_{10})^2],$

in which $\alpha_{10} = \ln\,(V_0^*/10)$ is the value of $\alpha = \ln V_0' - \ln T^*$ at the matching point of $T^* = 10$.

$\Omega^{(2,2)*}$, noble gases

$T^* \leqslant 1.2$

$$\Omega^{(2,2)*} = 1.1943(C_6^*/T^*)^{1/3}[1 + a_1(T^*)^{1/3}$$
$$+ a_2(T^*)^{2/3} + a_3(T^*) + a_4(T^*)^{4/3}$$
$$+ a_5(T^*)^{5/3} + a_6(T^*)^2], \tag{B1c}$$

where

$a_1 = 0.18,$

$a_2 = 0,$

$a_3 = -1.20407 - 0.195866(C_6^*)^{-1/3},$

$a_4 = -9.86374 + 20.2221(C_6^*)^{-1/3},$

$a_5 = 16.6295 - 31.3613\,(C_6^*)^{-1/3},$

$a_6 = -6.73805 + 12.6611\,(C_6^*)^{-1/3}.$

$1.2 \leqslant T^* \leqslant 10$

$\Omega^{(2,2)*} =$ same as Eq. (B1a).

$T^* \geqslant 10$

$\Omega^{(2,2)*} =$ same as Eq. (B1b).

$\Omega^{(1,1)*}$, molecular gases

$1 \leqslant T^* \leqslant 10$

$$\Omega^{(1,1)*} = \exp[0.295402 - 0.510069\,(\ln T^*)$$
$$+ 0.189395\,(\ln T^*)^2$$
$$- 0.045427\,(\ln T^*)^3$$
$$+ 0.0037928\,(\ln T^*)^4]. \tag{B2a}$$

$T^* \geqslant 10$

$$\Omega^{(1,1)*} = (\rho^*)^2 \alpha^2 [0.89 + b_2(T^*)^{-2}$$
$$+ b_4(T^*)^{-4} + b_6(T^*)^{-6}], \tag{B2b}$$

where

$b_2 = -267.00 + (\alpha_{10}\rho^*)^{-2}[201.570$
$\quad + (174.672/\alpha_{10}) + (7.36916/\alpha_{10})^2],$

$b_4 = 26700 - (\alpha_{10}\rho^*)^{-2}[19.2265$
$\quad + (27.6938/\alpha_{10}) + (3.29559/\alpha_{10})^2] \times 10^3,$

$b_6 = -8.90 \times 10^5 + (\alpha_{10}\rho^*)^{-2}[6.31013$
$\quad + (10.2266/\alpha_{10}) + (2.33033/\alpha_{10})^2] \times 10^5,$

in which $\alpha_{10} = \ln\,(V_0^*/10)$ is the value of $\alpha = \ln V_0^* - \ln T^*$ at the matching point of $T^* = 10$.

$\Omega^{(1,1)*}$, noble gases

$T^* \leqslant 1.2$

$$\Omega^{(1,1)*} = 1.1874(C_6^*/T^*)^{1/3}[1 + b_1(T^*)^{1/3}$$
$$+ b_2(T^*)^{2/3} + b_3(T^*) + b_4(T^*)^{4/3}$$
$$+ b_5(T^*)^{5/3} + b_6(T^*)^2], \tag{B2c}$$

where

$b_1 = 0,$

$b_2 = 0,$

$b_3 = 10.0161 - 10.5395(C_6^*)^{-1/3},$

$b_4 = -40.0394 + 46.0048\,(C_6^*)^{-1/3},$

$b_5 = 44.3202 - 53.0817\,(C_6^*)^{-1/3},$

$b_6 = -15.2912 + 18.8125\,(C_6^*)^{-1/3}.$

$1.2 \leqslant T^* \leqslant 10$

$$\Omega^{(1,1)*} = \exp\,[0.357588 - 0.472513\,(\ln T^*)$$
$$+ 0.0700902\,(\ln T^*)^2 + 0.0165741\,(\ln T^*)^3$$
$$- 0.00592022\,(\ln T^*)^4]. \tag{B2d}$$

$T^* \geqslant 10$

$\Omega^{(1,1)*} =$ same as Eq. (B2b).

TABLE B1. Coefficients of Eq. (B4a) for the computation of the functional B_0^*.

	c_0	c_1	c_2	c_3	c_4
Noble gases	0.74685	−1.03840	0.31634	0.02096	−0.01498
N_2, CO, O_2, NO	0.96843	−1.34424	0.46405	−0.00689	−0.01358
CO_2	0.82601	−1.39073	0.68581	−0.12653	0.00543
N_2O	0.86875	−1.28642	0.50153	−0.03949	−0.00767
CH_4	0.89921	−1.25084	0.42071	0.00059	−0.01384
CF_4	1.06288	−1.49408	0.55240	−0.02979	−0.01138
SF_6	1.21852	−1.91794	0.92850	−0.16763	0.00673
C_2H_4	0.09434	−1.39738	0.60582	−0.07896	−0.00238
C_2H_6	0.98755	−1.47580	0.61382	−0.06880	−0.00484

Collision-integral ratios

$$\frac{\Omega^{(l,s+1)*}}{\Omega^{(l,s)*}} = 1 + \frac{T^*}{s+2}\frac{d\ln\Omega^{(l,s)*}}{dT^*}, \tag{B3a}$$

$$A^* = \Omega^{(2,2)*}/\Omega^{(1,1)*}, \tag{B3b}$$

$$B^* = [5\Omega^{(1,2)*} - 4\Omega^{(1,3)*}]/\Omega^{(1,1)*}$$

$$= 1 + 3C^* - 3(C^*)^2 - \frac{(T^*)^2}{3}\frac{d^2\ln\Omega^{(1,1)*}}{d(T^*)^2}$$

$$= 4C^* - 3(C^*)^2 - \frac{1}{3}\frac{d^2\ln\Omega^{(1,1)*}}{d(\ln T^*)^2}, \tag{B3c}$$

$$C^* = \Omega^{(1,2)*}/\Omega^{(1,1)*} = 1 + \frac{T^*}{3}\frac{d\ln\Omega^{(1,1)*}}{dT^*}, \tag{B3d}$$

$$E^* = \Omega^{(2,3)*}/\Omega^{(2,2)*} = 1 + \frac{T^*}{4}\frac{d\ln\Omega^{(2,2)*}}{dT^*}, \tag{B3e}$$

$$F^* = \Omega^{(3,3)*}/\Omega^{(1,1)*} \approx 0.9543 + 0.00124T^*, \tag{B3f}$$

$$H^* = (3B^* + 6C^* - 35/4)(6C^* - 5)^{-1}. \tag{B3g}$$

The numerical expression for F^* is an approximate correlation from Ref. 1 (Sec. 10); the other expressions are definitions and exact recursion relations.

Second Virial Coefficients

$$B^* = B_0^* + B_{ns}^*$$

B_0^*, molecular gases

$1 \leqslant T^* \leqslant 10$

$$B_0^* = - (T^*)^{1/2}\exp(1/T^*)[c_0 + c_1(\ln T^*)$$

$$+ c_2(\ln T^*)^2 + c_3(\ln T^*)^3 + c_4(\ln T^*)^4], \tag{B4a}$$

where the coefficients c_i are given in Table B1.

$T^* \geqslant 10$

$$B_0^* = \beta [1 + d_2(\ln T^*)^{-2}$$

$$+ d_4(\ln T^*)^{-4} + d_6(\ln T^*)^{-6}], \tag{B4b}$$

where

$$\beta = (\rho^*)^3 [(\alpha + \gamma)^3 + (\pi^2/2)(\alpha + \gamma) + 2.40411],$$

$$\alpha = \ln V_0^* - \ln T^*$$

$\gamma = 0.577215...$ is Euler's constant,

and

$$d_2 = - 15.9057 + (9.85958/\beta_{10})$$

$$+ [(\rho^*)^3/\beta_{10}^2][25.6607(\alpha_{10} + \gamma)^2$$

$$- 9.73766(\alpha_{10} + \gamma) + 42.2102]$$

$$+ 3.24589[(\rho^*)^2/\beta_{10}]^3[3(\alpha_{10} + \gamma)^2 + \pi^2/2]^2,$$

$$d_4 = 84.3304 - (61.9124/\beta_{10})$$

$$+ [(\rho^*)^3/\beta_{10}^2][- 227.258(\alpha_{10} + \gamma)^2$$

$$+ 103.256(\alpha_{10} + \gamma) - 373.824]$$

$$- 34.4187[(\rho^*)^2/\beta_{10}]^3[3(\alpha_{10} + \gamma)^2 + \pi^2/2]^2,$$

$$d_6 = - 149.037 + (119.937/\beta_{10})$$

$$+ [(\rho^*)^3/\beta_{10}^2][483.571(\alpha_{10} + \gamma^2)$$

$$- 273.727(\alpha_{10} + \gamma) + 795.442]$$

$$+ 91.2423[(\rho^*)^2/\beta_{10}]^3[3(\alpha_{10} + \gamma)^2 + \pi^2/2]^2,$$

in which β_{10} is the value of β and α_{10} is the value of α at the matching point of $T^* = 10$.

B_0^*, noble gases

$T^* \leqslant 1.1$

$$B_0^* = - (T^*)^{1/2}\exp(1/T^*)[1.18623 + 1.00824T^*$$

$$+ 4.25571(T^*)^2 - 18.6033(T^*)^3 + 20.4734(T^*)^4$$

$$- 8.71903(T^*)^5 + 1.14829(T^*)^6]. \tag{B4c}$$

$1.1 \leqslant T^* \leqslant 10$

$B_0^* = $ same as Eq. (B4a).

$T^* \geqslant 10$

$B_0^* = $ same as Eq. (B4b).

B_{ns}^*, molecular gases

These nonspherical contributions are zero for the interaction of two noble-gas atoms, but not for the interaction of a noble-gas atom with a molecule.

$T^* \geqslant 1$

$$B_{ns}^* = B_{ns}^*(\mu\mu) + B_{ns}^*(\mu\theta) + B_{ns}^*(\theta\theta) + ...$$

$$+ B_{ns}^*(\mu, \text{ind}\mu) + B_{ns}^*(\mu\theta, \text{ind}\mu)$$

$$+ B_{ns}^*(\theta, \text{ind}\mu) + ...B_{ns}^*(C_6 \text{ anis})$$

$$+ ... + \text{cross terms.} \tag{B5}$$

Explicit formulas for the various contributions of B_{ns}^* are given in Appendix C as power series in $(T^*)^{-1}$.

Appendix C: General formulas

Single Substances

Only the viscosity and second virial coefficient are needed for use in mixture calculations.

Viscosity η

$$\eta = \frac{5}{16}\left(\frac{mkT}{\pi}\right)^{1/2}\frac{f_\eta}{\sigma^2\Omega^{(2,2)*}}, \tag{C1}$$

$$f_\eta = 1 + \frac{3}{196}(8E^* - 7)^2. \tag{C1a}$$

Second Virial Coefficient B

$$B = \frac{2\pi}{3}N_A\sigma^3B^*. \tag{C2}$$

Mixtures

Viscosity

$$\eta_{mix} = - \frac{\begin{vmatrix} H_{11} & H_{12} & \cdots & H_{1v} & x_1 \\ H_{21} & H_{22} & \cdots & H_{2v} & x_2 \\ \vdots & & & \vdots & \vdots \\ H_{v1} & H_{v2} & \cdots & H_{vv} & x_v \\ x_1 & x_2 & \cdots & x_v & 0 \end{vmatrix}}{\begin{vmatrix} H_{11} & H_{12} & \cdots & H_{1v} \\ H_{21} & H_{22} & \cdots & H_{2v} \\ \vdots & & & \vdots \\ H_{v1} & H_{v2} & \cdots & H_{vv} \end{vmatrix}} \qquad (C3)$$

where

$$H_{ii} = \frac{x_i^2}{\eta_i} + \sum_{\substack{k=1 \\ k \neq i}}^{v} \frac{2 x_i x_k}{\eta_{ik}} \frac{m_i m_k}{(m_i + m_k)^2} \left(\frac{5}{3 A_{ik}^*} + \frac{m_k}{m_i} \right), \qquad (C3a)$$

$$H_{ij}(i \neq j) = - \frac{2 x_i x_j}{\eta_{ij}} \frac{m_i m_j}{(m_i + m_j)^2} \left(\frac{5}{3 A_{ij}^*} - 1 \right), \qquad (C3b)$$

$$\eta_{ij} = \frac{5}{16} \left[\left(\frac{2 m_i m_j}{m_i + m_j} \right) \frac{kT}{\pi} \right]^{1/2} \frac{1}{\sigma_{ij}^2 \Omega_{ij}^{(2,2)*}(T_{ij}^*)}. \qquad (C3c)$$

The expression (C3) is only a first approximation, but accurate results can be obtained if the single-component viscosities η_i are calculated according to Eqs. (C1) and (C1a).[1] The formula holds for binary as well as multicomponent mixtures.

Diffusion

Diffusion in multicomponent mixtures is described entirely in terms of binary diffusion coefficients, D_{ij},

$$D_{ij} = \frac{3}{8} \left[\left(\frac{m_i + m_j}{2 m_i m_j} \right) \frac{kT}{\pi} \right]^{1/2} \frac{kT}{P} \frac{(1 + \Delta_{ij})}{\sigma_{ij}^2 \Omega_{ij}^{1,1)*}(T_{ij}^*)}. \qquad (C4)$$

The higher-order correction term Δ_{ij} is a complicated function of composition, but since it is small the following approximate formula should be adequate:[1,2]

$$\Delta_{ij} \approx 1.3 (C_{ij}^* - 5)^2 \frac{a_{ij} x_{ij}}{1 + b_{ij} x_{ij}}, \qquad (C5)$$

where

$$a_{ij} = \frac{2^{1/2}}{8 [1 + 1.8 (m_j/m_i)]^2} \frac{\Omega_{ij}^{1,1*}(T_{ij}^*)}{\Omega_{jj}^{(2,2)*}(T_j^*)}, \qquad (C5a)$$

$$b_{ij} = 10 a_{ij} [1 + 1.8 (m_j/m_i) + 3 (m_j/m_i)^2] - 1, \qquad (C5b)$$

$$x_{ij} = \frac{x_i}{x_i + x_j}, \qquad (C5c)$$

in which the subscript i denotes the heavier component and subscript j denotes the ligher component of the i-j pair.

Thermal Diffusion Factor

Thermal diffusion in multicomponent mixtures is complicated,[5] and we give here only the expression for a binary mixture,

$$\alpha_T = (6 C_{ij}^* - 5) \left(\frac{x_1 S_1 - x_2 S_2}{x_1^2 Q_1 + x_2^2 Q_2 + x_1 x_2 Q_{12}} \right) (1 + \kappa_T), \qquad (C6)$$

where κ_T is a correction term arising from the higher approximations of kinetic theory, and is usually negligibly small in comparison with experimental uncertainties in α_T. We have ignored κ_T in the tabulations reported in this paper. The other quantities in Eq. (C6) are

$$S_1 = \frac{m_1}{m_2} \left(\frac{2 m_2}{m_1 + m_2} \right)^{1/2} \frac{\sigma_{11}^2 \Omega_{11}^{(2,2)*}(T_1^*)}{\sigma_{12}^2 \Omega_{12}^{(1,1)*}(T_{12}^*)}$$
$$- \frac{4 m_1 m_2 A_{12}^*}{(m_1 + m_2)^2} + \frac{15 m_2 (m_1 - m_2)}{2 (m_1 + m_2)^2}, \qquad (C6a)$$

$$Q_1 = \frac{2}{m_2 (m_1 + m_2)} \left(\frac{2 m_2}{m_1 + m_2} \right)^{1/2} \frac{\sigma_{11}^2 \Omega_{11}^{(2,2)*}(T_1^*)}{\sigma_{12}^2 \Omega_{12}^{(1,1)*}(T_{12}^*)}$$
$$\times \left[\left(\frac{5}{2} - \frac{6}{5} B_{12}^* \right) m_1^2 + 3 m_2^2 + \frac{8}{5} m_1 m_2 A_{12}^* \right], \qquad (C6b)$$

$$Q_{12} = 15 \left(\frac{m_1 - m_2}{m_1 + m_2} \right)^2 \left(\frac{5}{2} - \frac{6}{5} B_{12}^* \right)$$
$$+ \frac{4 m_1 m_2 A_{12}^*}{(m_1 + m_2)^2} \left(11 - \frac{12}{5} B_{12}^* \right)$$
$$+ \frac{8 (m_1 + m_2)}{5 (m_1 m_2)^{1/2}} \frac{\sigma_{11}^2 \Omega_{11}^{(2,2)*}(T_1^*)}{\sigma_{12}^2 \Omega_{12}^{(1,1)*}(T_{12}^*)}$$
$$\times \frac{\sigma_{22}^2 \Omega_{22}^{(2,2)*}(T_2^*)}{\sigma_{12}^2 \Omega_{12}^{(1,1)*}(T_{12}^*)}, \qquad (C6c)$$

and the expressions for S_2 and Q_2 are obtained from those for S_1 and Q_1 by interchange of the subscripts 1 and 2. The sign convention for α_T requires that subscript 1 denote the heavier component $(m_1 > m_2)$.

Second Virial Coefficient

$$B_{mix} = \sum_{i=1}^{v} \sum_{j=1}^{v} x_i x_j B_{ij}, \qquad (C7)$$

$$B_{ij} = \frac{2\pi}{3} N_A \sigma_{ij}^3 B_{ij}^*(T_{ij}^*), \qquad (C7a)$$

$$B_{ij}^* = (B_0^*)_{ij} + (B_{ns}^*)_{ij}. \qquad (C7b)$$

The equations for the spherical functionals $(B_0^*)_{ij}$ are those given in Appendix B. The equations for the nonspherical contributions $(B_{ns}^*)_{ij}$ are as follows:

$$B_{ns}^*(\mu\mu)_{ij} = - \frac{2}{3} \left(\frac{\mu_i^* \mu_j^*}{T_{ij}^*} \right)^2$$
$$\times \left[J_6 + \frac{1}{25} \left(\frac{\mu_i^* \mu_j^*}{T_{ij}^*} \right)^2 J_{12} + \cdots \right], \qquad (C8)$$

$$B_{ns}^*(\theta\theta)_{ij} = - \frac{6}{5} \left(\frac{\theta_i^* \theta_j^*}{T_{ij}^*} \right)^2$$
$$\times \left[J_{10} - \frac{6}{49} \left(\frac{\theta_i^* \theta_j^*}{T_{ij}^*} \right) J_{15} + \cdots \right], \qquad (C9)$$

$B_{ns}*(\mu\theta)_{ij}$

$$= -\frac{3}{5}\left(\frac{\mu_i*\theta_j*}{T_{ij}*}\right)^2 \left\{J_8 + \frac{J_{16}}{1820}\left[141\left(\frac{\mu_i*\theta_j*}{T_{ij}*}\right)^2\right.\right.$$

$$\left.\left.+ \frac{1917}{7}\left(\frac{\mu_j*\theta_i*}{T_{ij}*}\right)^2\right] + \cdots\right\} - \frac{3}{5}\left(\frac{\mu_j*\theta_i*}{T_{ij}*}\right)^2\left\{J_8 + \frac{J_{16}}{1820}\right.$$

$$\left.\times\left[141\left(\frac{\mu_j*\theta_i*}{T_{ij}*}\right)^2 + \frac{1917}{7}\left(\frac{\mu_i*\theta_j*}{T_{ij}*}\right)^2\right] + \cdots\right\}, \quad (C10)$$

$B_{ns}*(\mu,\text{ind}\,\mu)_{ij}$

$$= -\frac{1}{15}\left(\frac{\mu_i*\alpha_j*}{T_{ij}*}\right)^2 [(\mu_i*)^2 J_{12} + 11(\mu_j*\alpha_i*)^2$$

$$\times J_{18} + \cdots] - \frac{1}{15}\left(\frac{\mu_j*\alpha_i*}{T_{ij}*}\right)^2$$

$$\times [(\mu_j*)^2 J_{12} + 11(\mu_i*\alpha_j*)^2 J_{18} + \cdots], \quad (C11)$$

$$B_{ns}*(\theta,\text{ind}\,\mu)_{ij} = -\frac{81}{455}\left[\left(\frac{\theta_i*^2\alpha_j*}{T_{ij}*}\right)^2\right.$$

$$\left. + \left(\frac{\theta_j*^2\alpha_i*}{T_{ij}*}\right)^2\right]J_{16} + \cdots, \quad (C12)$$

$$B_{ns}*(\mu\theta,\text{ind}\,\mu)_{ij} = -\frac{432}{77}\left[\left(\frac{\mu_i*\theta_i*\alpha_j*}{T_{ij}*}\right)^2\right.$$

$$\left. + \left(\frac{\mu_j*\theta_j*\alpha_i*}{T_{ij}*}\right)^2\right]J_{14} + \cdots, \quad (C13)$$

$$B_{ns}*(C_6\text{anis})_{ij} = -\frac{1}{15}\left(\frac{(C_6*)_{ij}}{T_{ij}*}\right)^2$$

$$\times\left(\kappa_i^2 + \kappa_j^2 + \frac{19}{5}\kappa_i^2\kappa_j^2\right)J_{12} + \cdots, \quad (C14)$$

$$B_{ns}*(\mu\times\theta)_{ij} = \frac{3}{5}\left(\frac{\mu_i*\mu_j*\theta_i*\theta_j*}{T_{ij}*^2}\right)$$

$$\times\left[\left(\frac{\mu_i*\mu_j*}{T_{ij}*}\right)J_{11} + \frac{24}{35}\left(\frac{\theta_i*\theta_j*}{T_{ij}*}\right)J_{13} + \cdots\right], \quad (C15)$$

$$B_{ns}*(\mu,\text{ind}\,\mu\times\theta,\text{ind}\,\mu)_{ij} = -\frac{72}{385}\left[\left(\frac{\mu_i*\theta_i*\alpha_j*}{T_{ij}*}\right)^2\right.$$

$$\left. + \left(\frac{\mu_j*\theta_j*\alpha_i*}{T_{ij}*}\right)^2\right]J_{14} + \cdots, \quad (C16)$$

$$B_{ns}*(\mu\mu\times\mu,\text{ind}\,\mu)_{ij} = -\frac{4}{3}\left(\frac{\mu_i*\mu_j*}{T_{ij}*}\right)^2$$

$$\times\left[\alpha_i*\alpha_j* + \frac{1}{30}\left(\frac{\mu_i*^2\alpha_j* + \mu_j*^2\alpha_i*}{T_{ij}*}\right) + \cdots\right]J_{12} + \cdots, \quad (C17)$$

$$B_{ns}*(\mu\mu\times\theta,\text{ind}\,\mu)_{ij} = -\frac{24}{385}\left(\frac{\mu_i*\mu_j*}{T_{ij}*}\right)^2$$

$$\times\left(\frac{\theta_i*^2\alpha_j* + \theta_j*^2\alpha_i*}{T_{ij}*}\right)J_{14} + \cdots, \quad (C18)$$

$$B_{ns}*(\theta\theta\times C_6\text{anis})_{ij} = \frac{27}{25}\frac{\theta_i*\theta_j*(C_6*)_{ij}}{T_{ij}*^2}\kappa_i\kappa_j J_{11} + \cdots, \quad (C19)$$

$$B_{ns}*(\mu,\text{ind}\,\mu\times C_6\text{anis})_{ij} = -\frac{2}{15}\left[\left(\frac{\mu_i*}{T_{ij}*}\right)^2\alpha_j*\kappa_i\right.$$

$$\left. + \left(\frac{\mu_j*}{T_{ij}*}\right)^2\alpha_i*\kappa_j\right](C_6*)_{ij}J_{12} + \cdots, \quad (C20)$$

$$B_{ns}*(\theta,\text{ind}\,\mu\times C_6\text{anis})_{ij} = -\frac{72}{385}\left[\left(\frac{\theta_i*}{T_{ij}*}\right)^2\alpha_j*\kappa_i\right.$$

$$\left. + \left(\frac{\theta_j*}{T_{ij}*}\right)^2\alpha_i*\kappa_j\right](C_6*)_{ij}J_{14} + \cdots. \quad (C21)$$

Equations (C17)–(C21) represent the leading cross terms that are indicated in Eq. (B5). The terms $(B_{ns}*)_{ij}$ for like molecular interactions are obtained from the above formulas by equating i and j. The auxiliary functions $J_n(T_{ij}*)$ are tabulated for

$$0.5 \leqslant T* \leqslant 10 \text{ and } 6 \leqslant n \leqslant 30,$$

by A. Boushehri, E. A. Mason, and J. Kestin [Int. J. Thermophys. 7, 1115 (1986)]. These functions are slowly varying, so that interpolation in the tables is easy. For $T* > 10$ the nonspherical contribution $B_{ns}*$ is usually negligible compared to the corresponding spherical contribution B_0*.

Appendix D: Deviation Plots

In the deviation plots, the ordinate refers to the difference between the measured and calculated quantity, i.e., the percentage quantity 100 $(X_{\text{meas}} - X_{\text{calc}})/X_{\text{calc}}$ or the difference $(X_{\text{meas}} - X_{\text{calc}})$.

As discussed in Sec. 6, the deviation plots for the second virial coefficient refer to the interaction coefficient B_{12}, whereas the tables list B_{mix} for the whole mixture.

The reduced thermal diffusion factor is defined as,

$$\alpha_T = \left(\frac{x_1^2 Q_1 + x_2^2 Q_2 + x_1 x_2 Q_{12}}{x_1 S_1 - x_2 S_2}\right).$$

The calculated curve for this quantity equals $(6C_{12}* - 5)$.

Several points at a given temperature refer to different mixture compositions.

O Ref. 52, PD
□ Ref. 108, SD
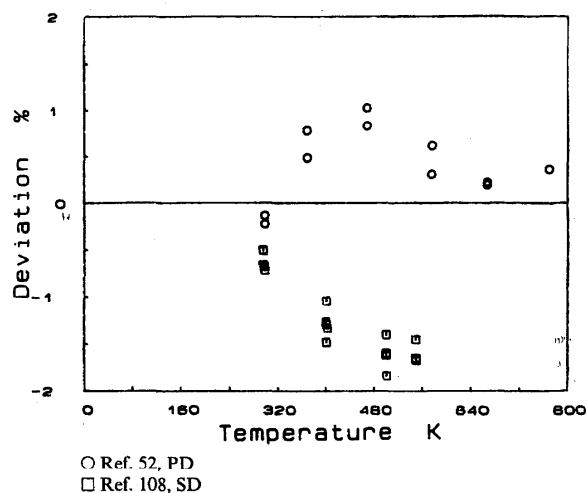
D1. Deviation plot for the viscosity of N_2-O_2 mixtures.

O Ref. 68, PD
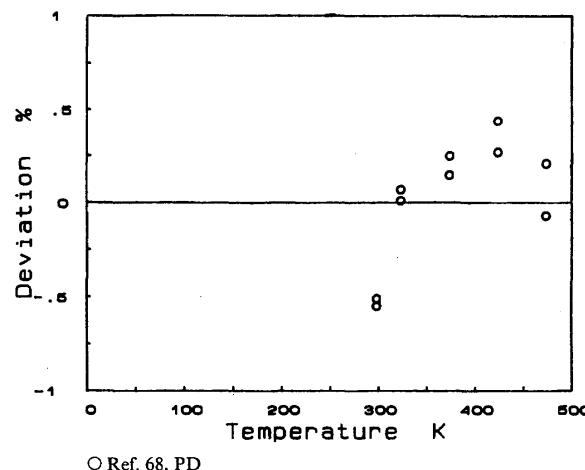
D4. Deviation plot for the viscosity of N_2-N_2O mixtures.

O Ref. 72, PD
□ Ref. 108, SD
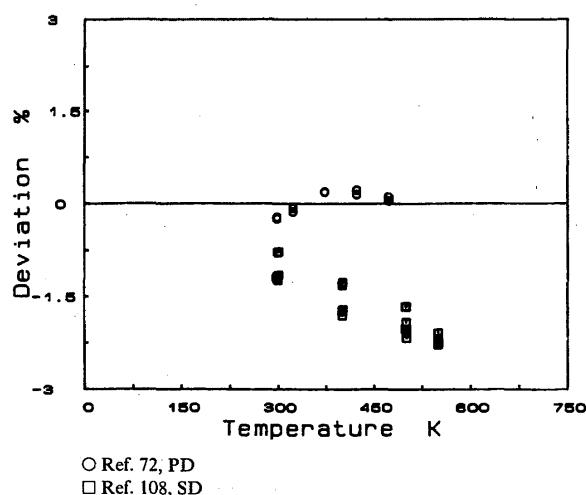
D2. Deviation plot for the viscosity of N_2-CO mixtures.

O Ref. 67, PD
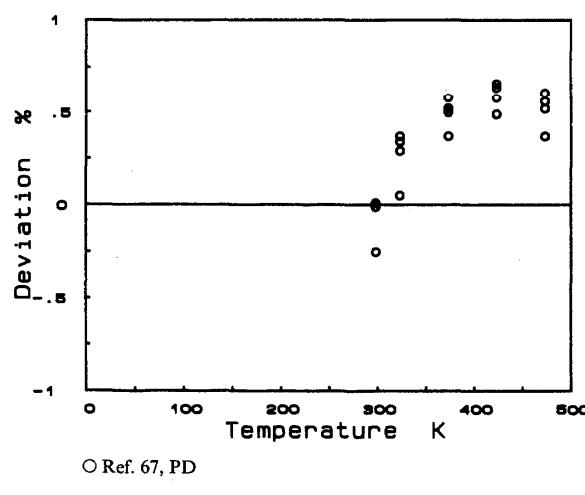
D5. Deviation plot for the viscosity of N_2-CH_4 mixtures.

O Ref. 66, PD
□ Ref. 67, SD
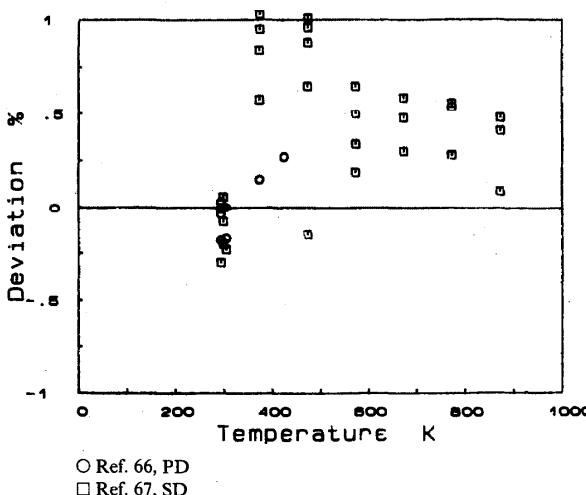
D3. Deviation plot for the viscosity of N_2-CO_2 mixtures.

O Ref. 64, PD
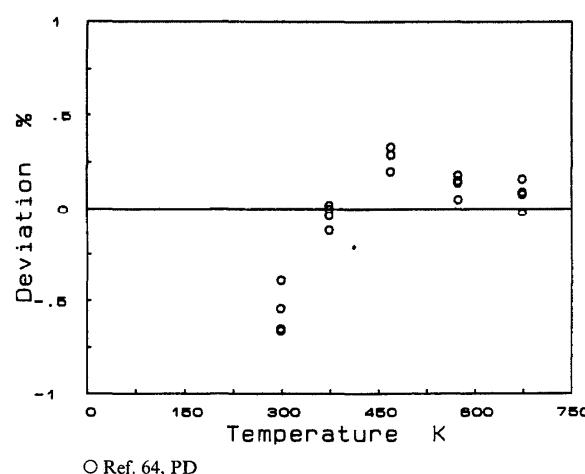
D6. Deviation plot for the viscosity of N_2-CF_4 mixtures.

O Ref. 64, PD
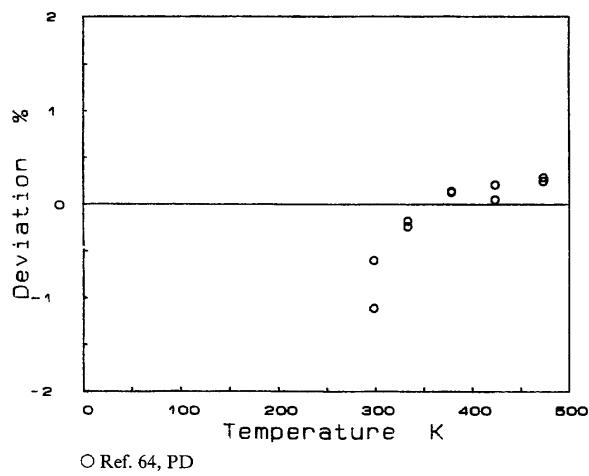
D7. Deviation plot for the viscosity of N_2-SF_6 mixtures.

O Ref. 66, PD
□ Ref. 70, PD
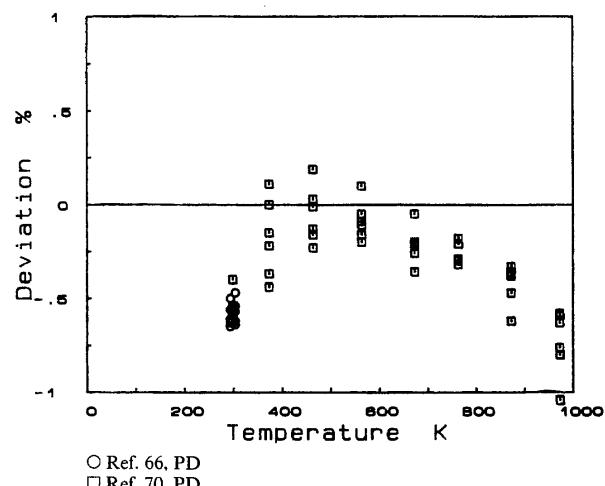
D10. Deviation plot for the viscosity of N_2-He mixtures.

O Ref. 108, SD
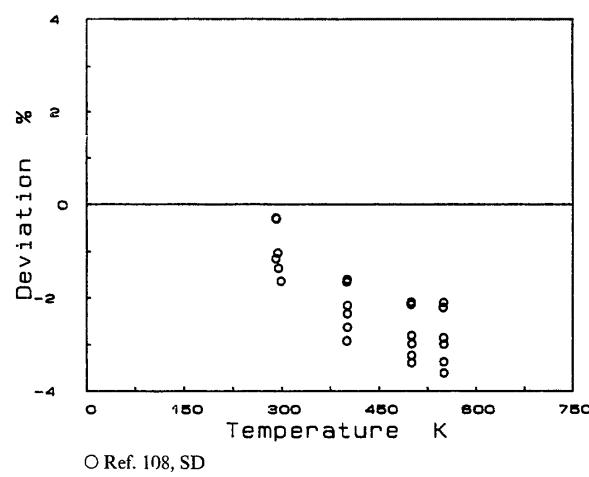
D8. Deviation plot for the viscosity of N_2-C_2H_4 mixtures.

O Ref. 29, PD
□ Ref. 71, PD
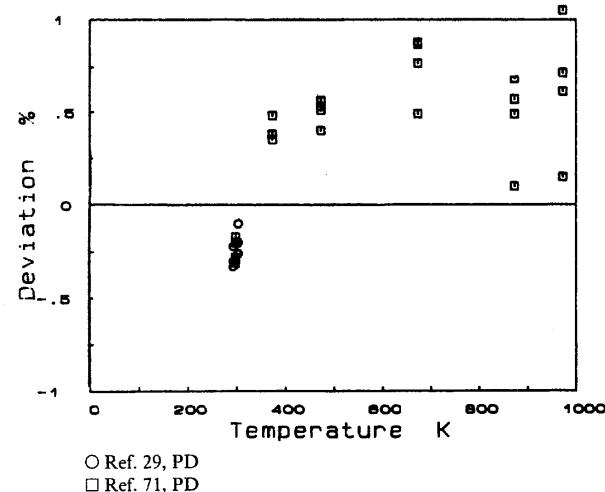
D11. Deviation plot for the viscosity of N_2-Ne mixtures.

O Ref. 2, PD
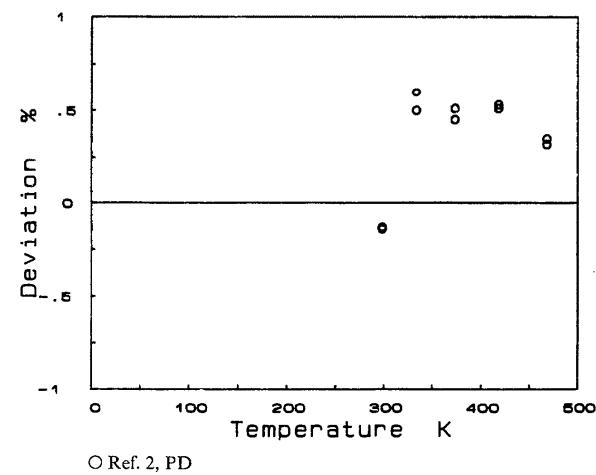
D9. Deviation plot for the viscosity of N_2-C_2H_6 mixtures.

O Ref. 29, PD
□ Ref. 51, PD
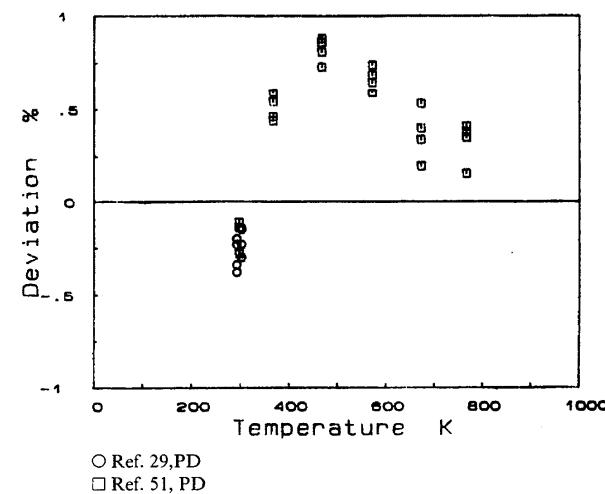
D12. Deviation plot for the viscosity of N_2-Ar mixtures.

O Ref. 51, PD

D13. Deviation plot for the viscosity of N_2-Kr mixtures.

O Ref. 64, PD

D16. Deviation plot for the viscosity of O_2-CF_4 mixtures.

O Ref. 108, SD

D14. Deviation plot for the viscosity of O_2-CO mixtures.

O Ref. 64, PD

D17. Deviation plot for the viscosity of O_2-SF_6 mixtures.

O Ref. 64, PD

D15. Deviation plot for the viscosity of O_2-CO_2 mixtures.

O Ref. 108, SD

D18. Deviation plot for the viscosity of O_2-C_2H_4 mixtures.
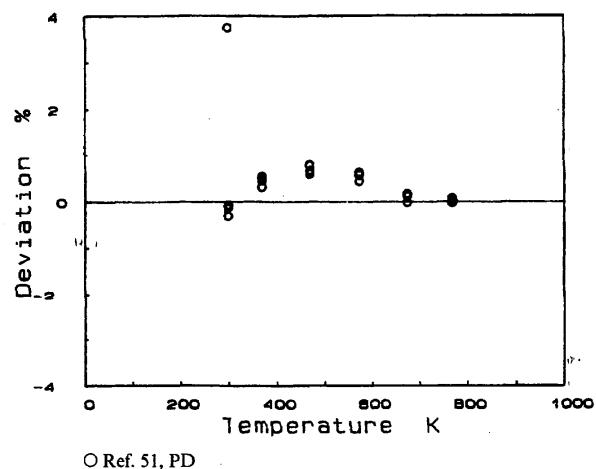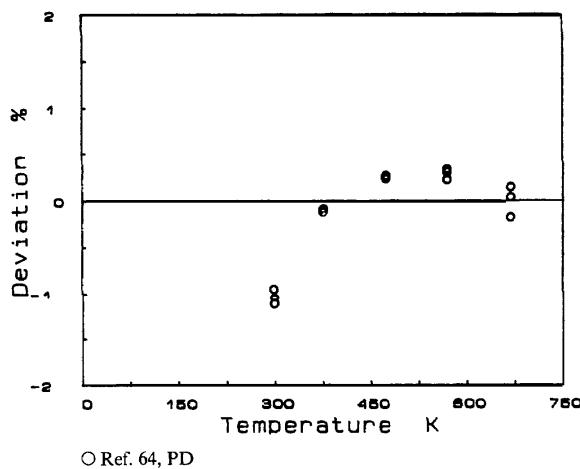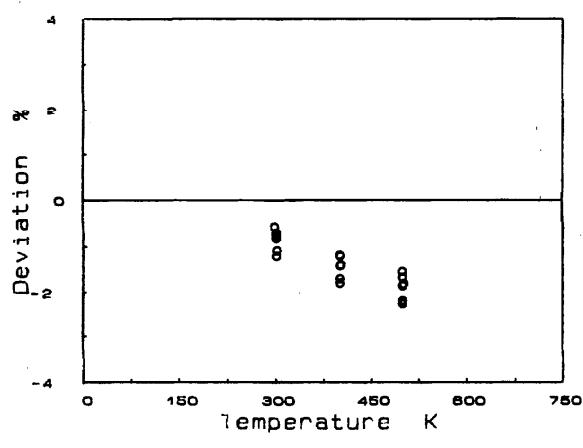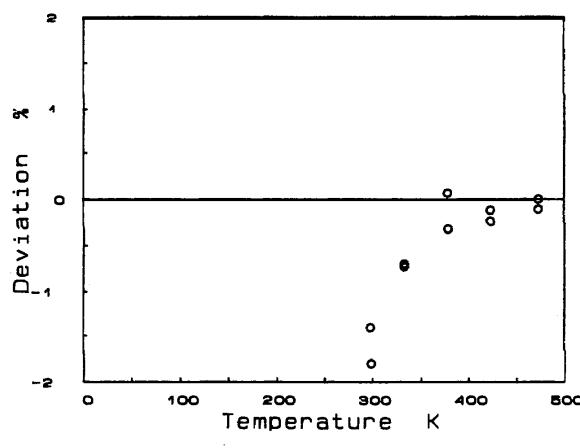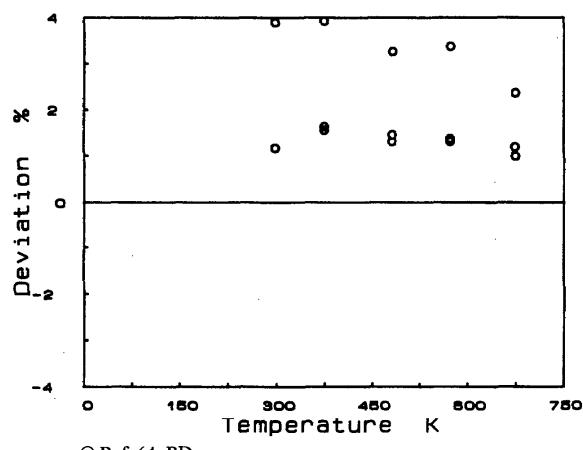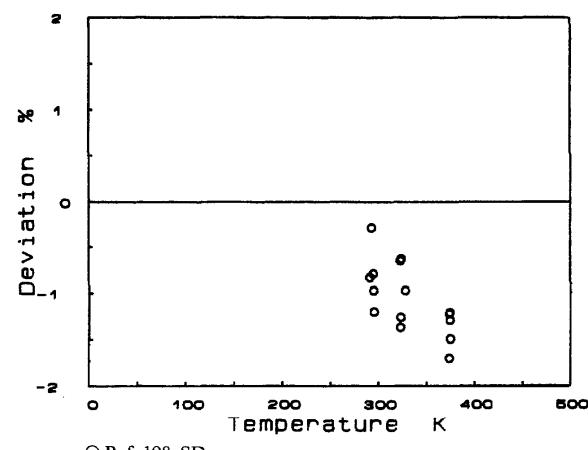
O Ref. 74,PD
□ Ref. 64, PD
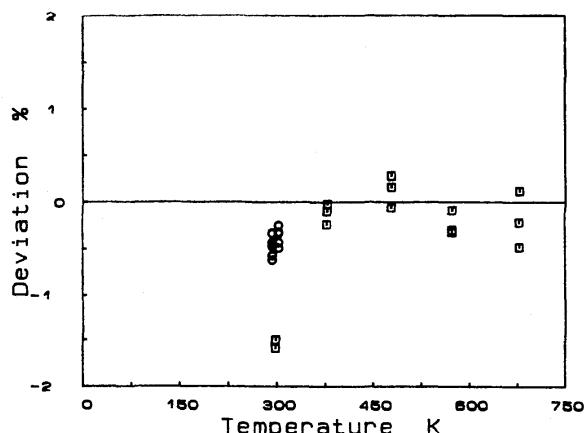
D19. Deviation plot for the viscosity of O_2-He mixtures.

O Ref. 52, PD
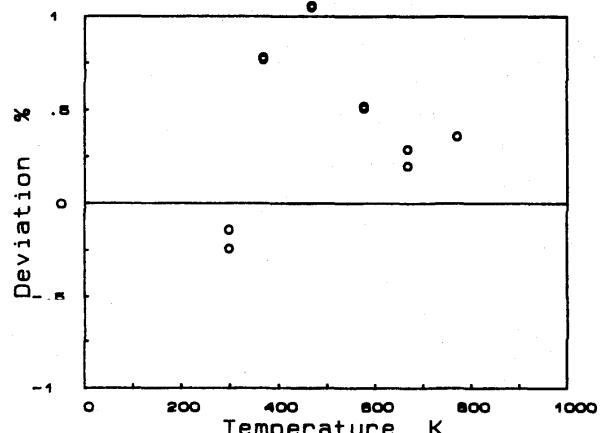
D22. Deviation plot for the viscosity of O_2-Kr mixtures.

O Ref. 64, PD
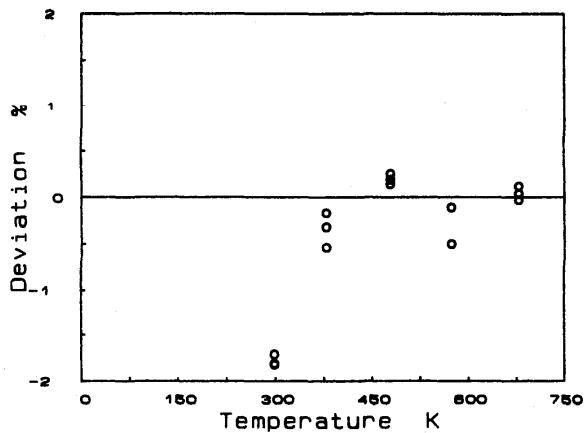
D20. Deviation plot for the viscosity of O_2-Ne mixtures.
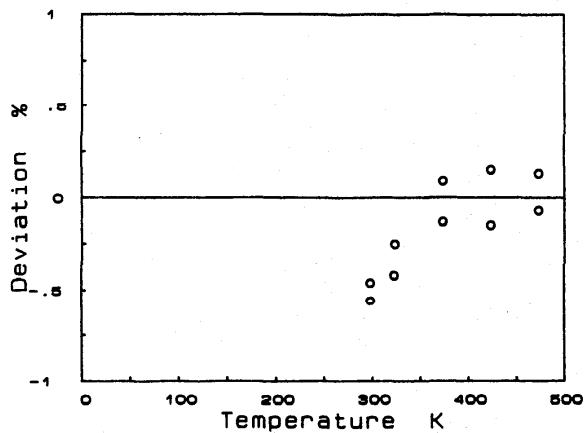
O Ref. 69, PD

D23. Deviation plot for the viscosity of CO CO$_2$ mixtures.

O Ref. 52, PD
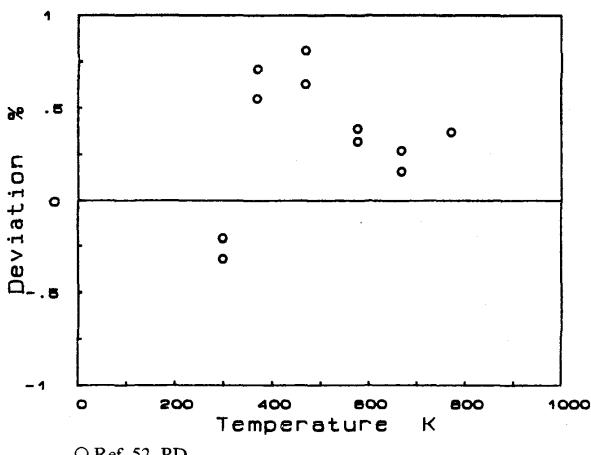
D21. Deviation plot for the viscosity of O_2-Ar mixtures.

O Ref. 73, PD
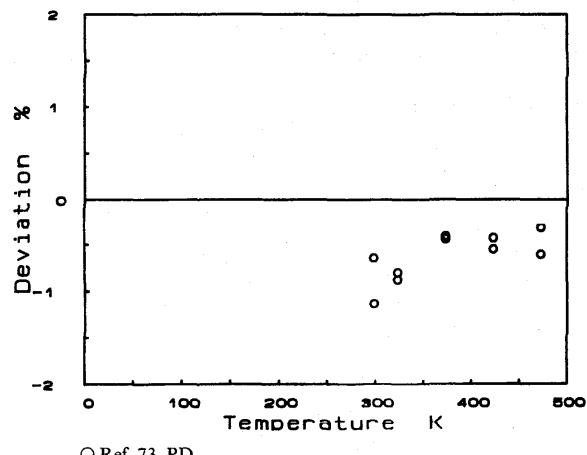
D24. Deviation plot for the viscosity of CO-N$_2$O mixtures.
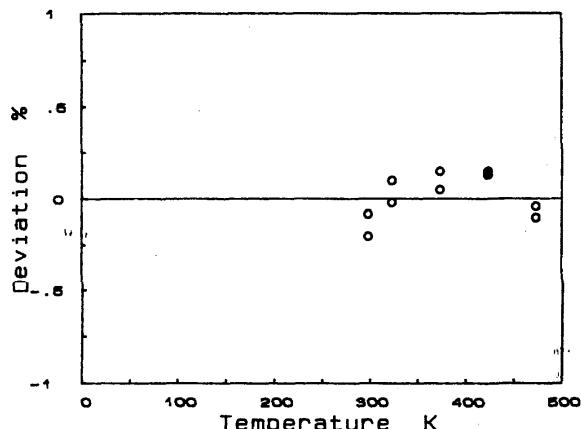
O Ref. 69, PD

D25. Deviation plot for the viscosity of CO-CH$_4$ mixtures.
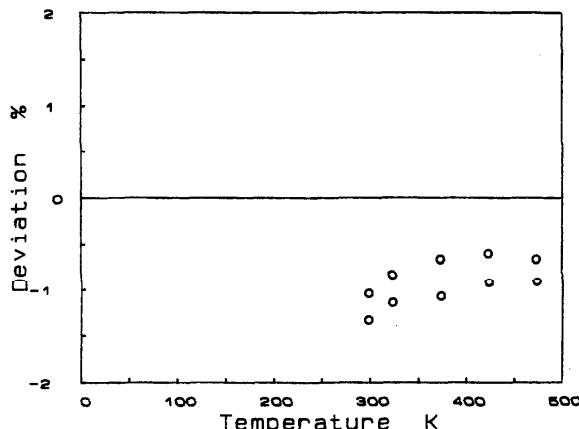
O Ref. 72, PD

D28. Deviation plot for the viscosity of CO-He mixtures.
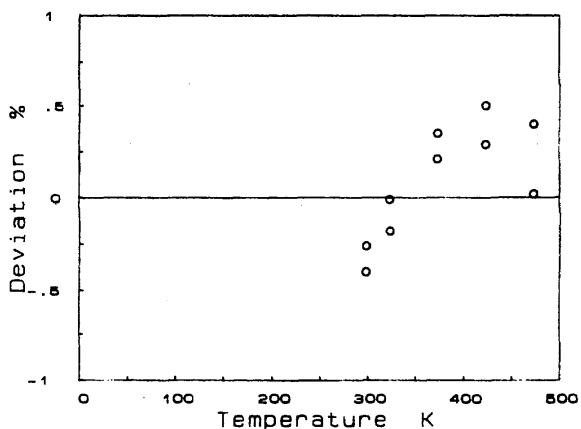
O Ref. 69, PD

D26. Deviation plot for the viscosity of CO-CF$_4$ mixtures.
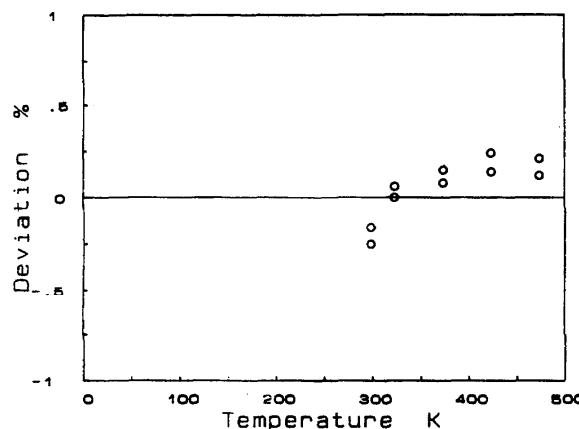
O Ref. 72, PD

D29. Deviation plot for the viscosity of CO-Ne mixtures.
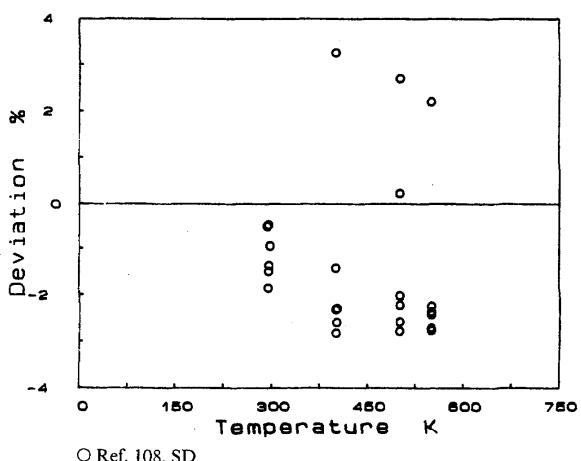
O Ref. 108, SD

D27. Deviation plot for the viscosity of CO-C$_2$H$_4$ mixtures.
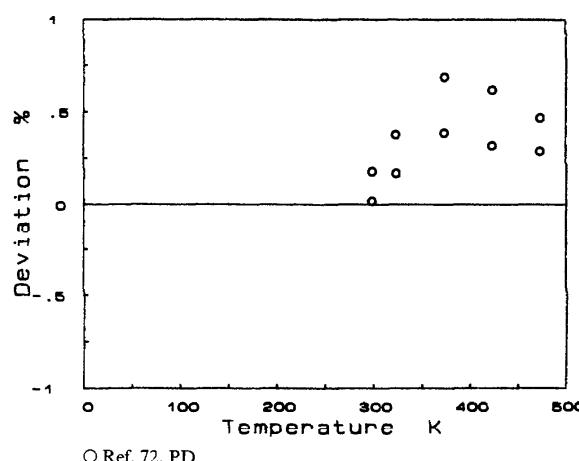
O Ref. 72, PD

D30. Deviation plot for the viscosity of CO-Ar mixtures.

O Ref. 69, PD

D31. Deviation plot for the viscosity of CO-Kr mixtures.

O Ref. 64, PD

D34. Deviation plot for the viscosity of CO_2-CF_4 mixtures.

O Ref. 68, PD

D32. Deviation plot for the viscosity of CO_2-N_2O mixtures.

O Ref. 64, PD

D35. Deviation plot for the viscosity of CO_2-SF_6 mixtures.

O Ref. 61, SD
□ Ref. 74, PD
◊ Ref. 67, PD

D33. Deviation plot for the viscosity of CO_2-CH_4 mixtures.

O Ref. 2, PD

D36. Deviation plot for the viscosity of CO_2-C_7H_6 mixtures.

○ Ref. 29, PD
□ Ref. 67, PD

D37. Deviation plot for the viscosity of CO₂-He mixtures.

○ Ref. 74,PD
□ Ref. 65, PD
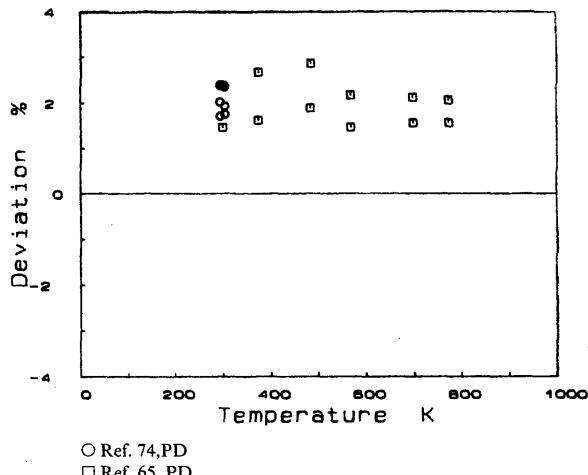
D40. Deviation plot for the viscosity of CO₂-Kr mixtures.

○ Ref. 17, SD
□ Ref. 67, PD
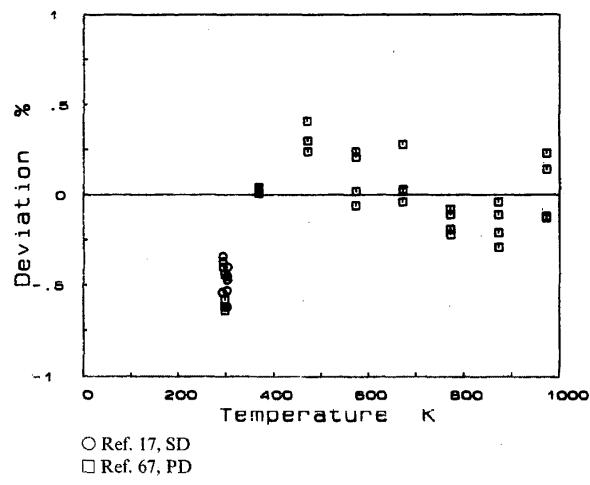
D38. Deviation plot for the viscosity of CO₂-Ne mixtures.

○ Ref. 73, PD
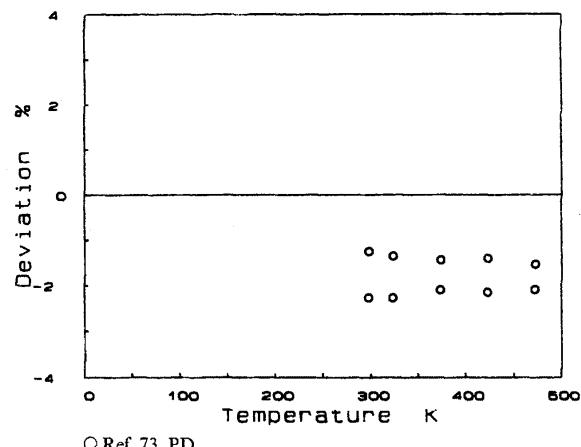
D41. Deviation plot for the viscosity of N₂O-He mixtures.

○ Ref. 66, PD
□ Ref. 67, PD
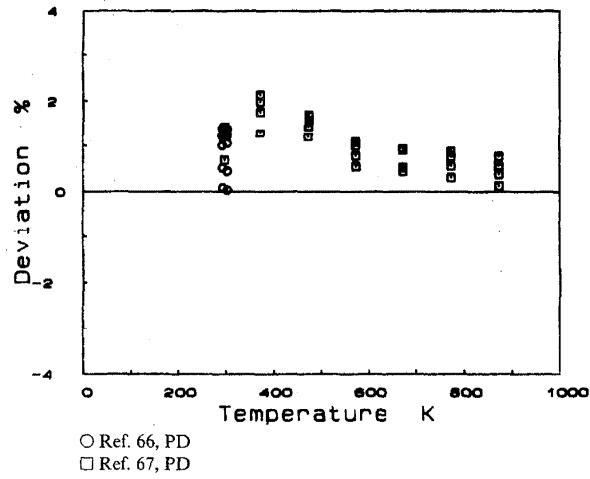
D39. Deviation plot for the viscosity of CO₂-Ar mixtures.

○ Ref. 73, PD
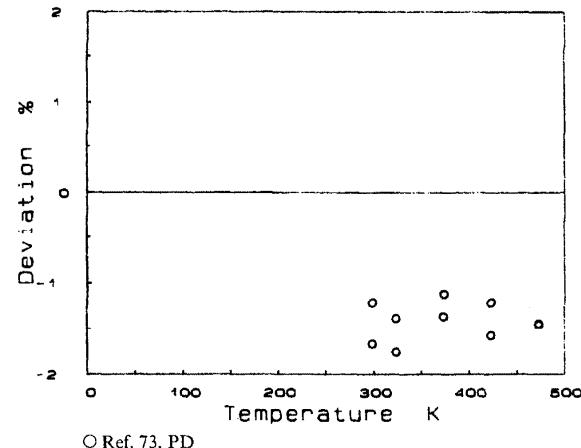
D42. Deviation plot for the viscosity of N₂O-Ne mixtures.
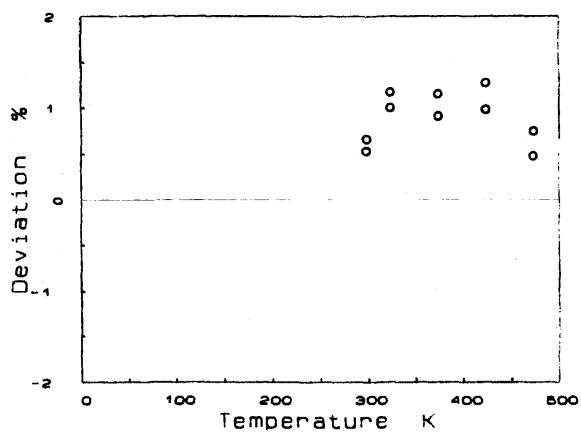
O Ref. 68, PD

D43. Deviation plot for the viscosity of N_2O-Ar mixtures.
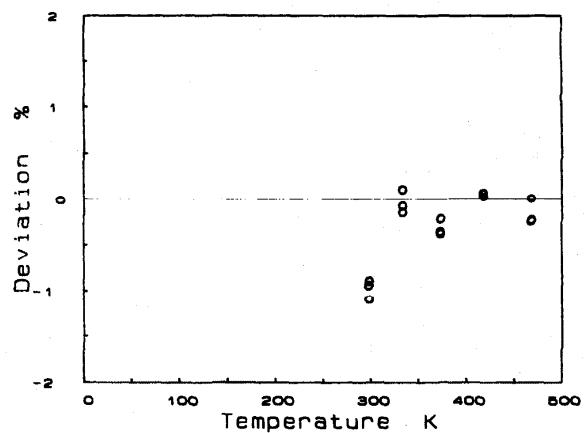
O Ref. 1, PD

D46. Deviation plot for the viscosity of CH_4-C_2H_6 mixtures.
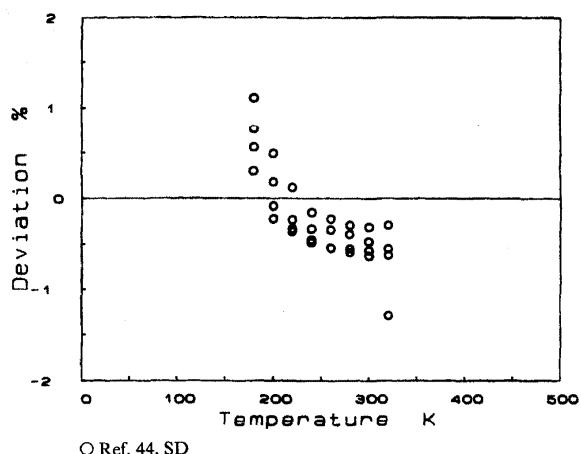
O Ref. 44, SD

D44. Deviation plot for the viscosity of CH_4-CF_4 mixtures.
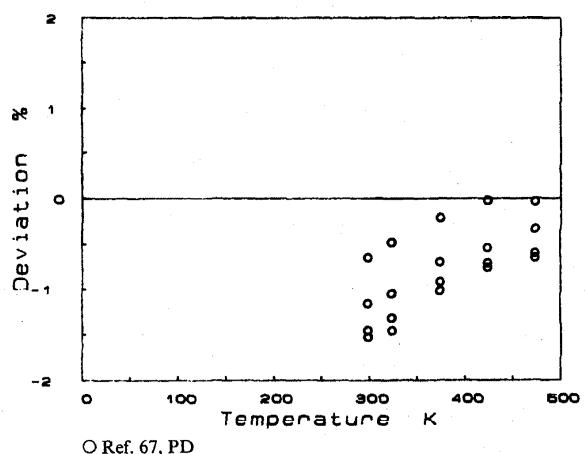
O Ref. 67, PD

D47. Deviation plot for the viscosity of CH_4-He mixtures.
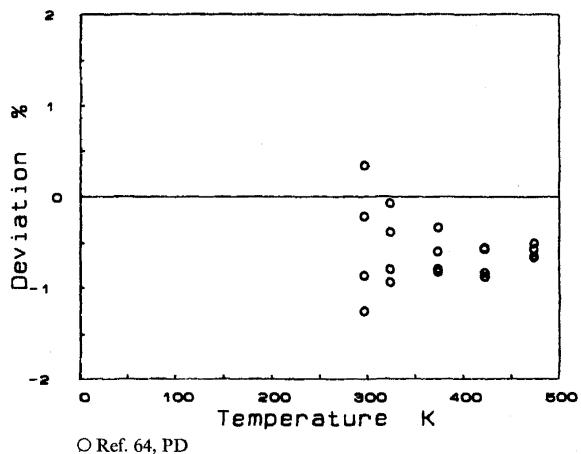
O Ref. 64, PD

D45. Deviation plot for the viscosity of CH_4-SF_6 mixtures.
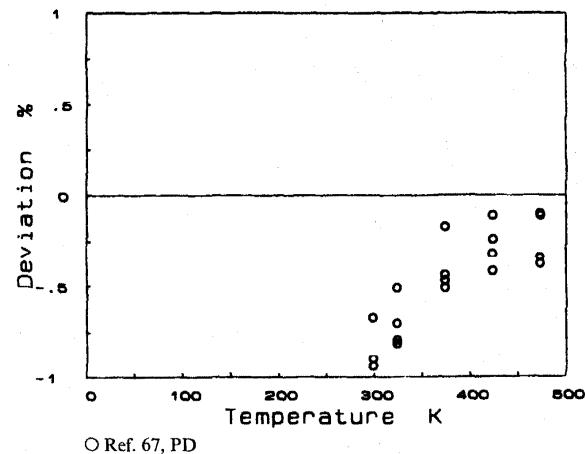
O Ref. 67, PD

D48. Deviation plot for the viscosity of CH_4-Ne mixtures.

○ Ref. 89, SD
□ Ref. 67, PD
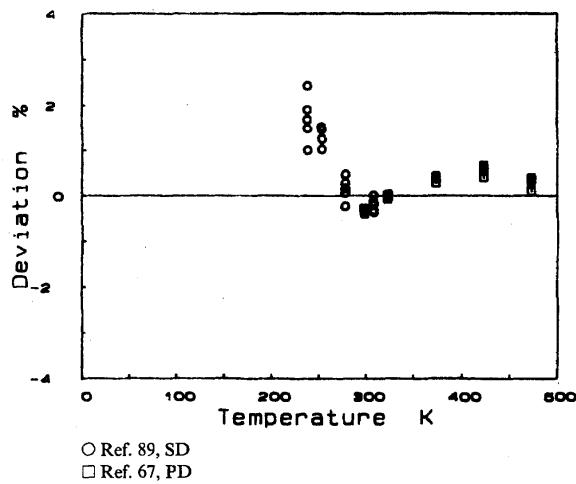
D49. Deviation plot for the viscosity of CH_4-Ar mixtures.

○ Ref. 2, PD
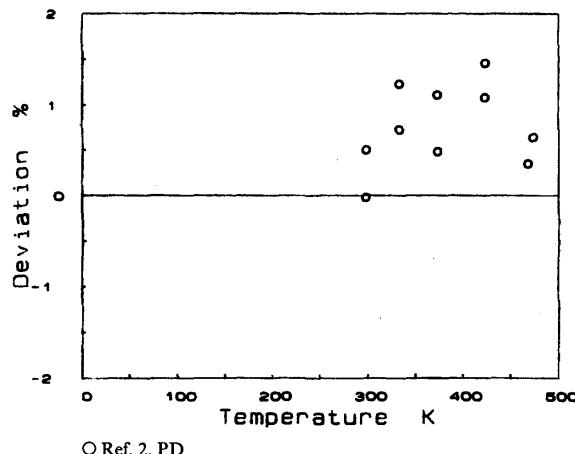
D52. Deviation plot for the viscosity of CF_4-C_2H_6 mixtures

○ Ref. 65, PD
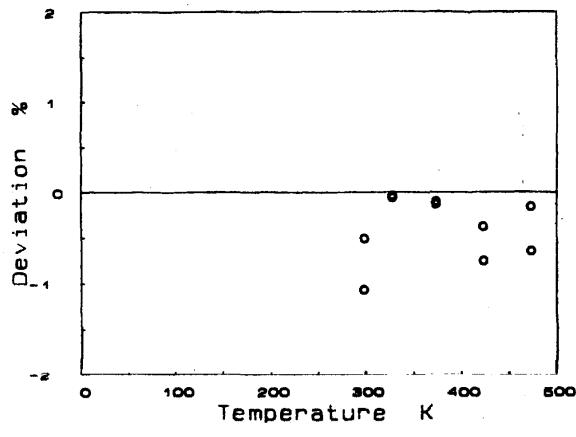
D50. Deviation plot for the viscosity of CH_4-Kr mixtures.

○ Ref. 64, PD
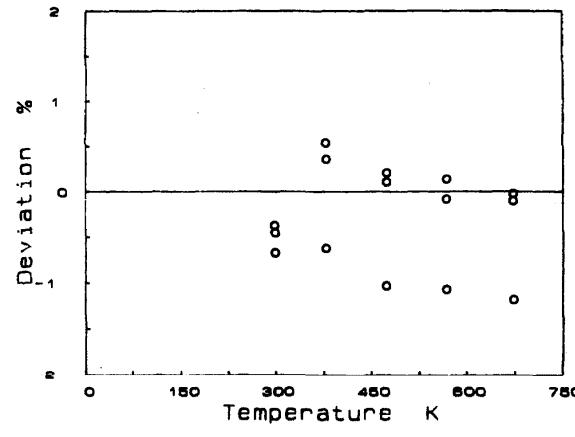
D53. Deviation plot for the viscosity of CF_4-He mixtures.

○ Ref. 64, PD
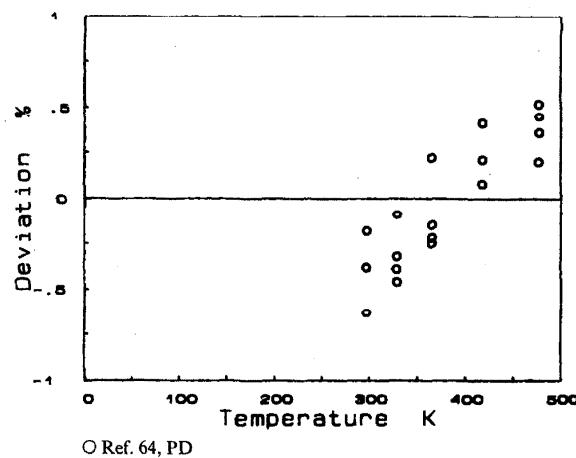
D51. Deviation plot for the viscosity of CF_4-SF_6 mixtures.

○ Ref. 64, PD
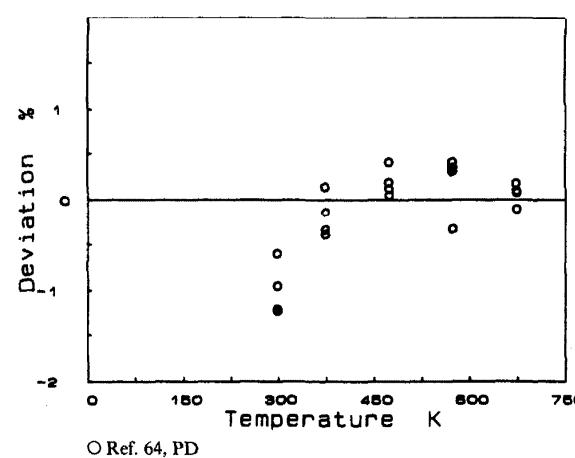
D54. Deviation plot for the viscosity of CF_4-Ne mixtures.

○ Ref. 64, PD
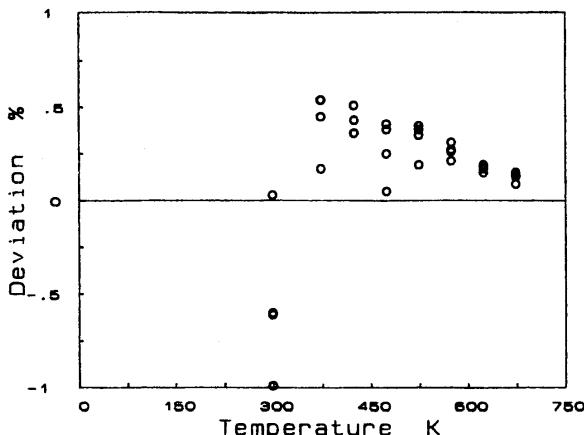
D55. Deviation plot for the viscosity of CF_4-Ar mixtures.

○ Ref. 64, PD
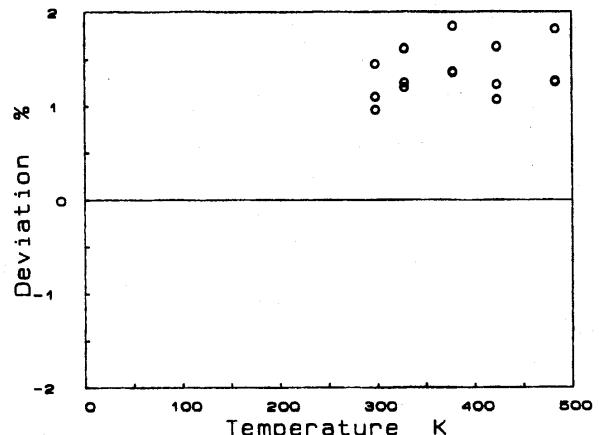
D58. Deviation plot for the viscosity of SF_6-He mixtures.

○ Ref. 65, PD
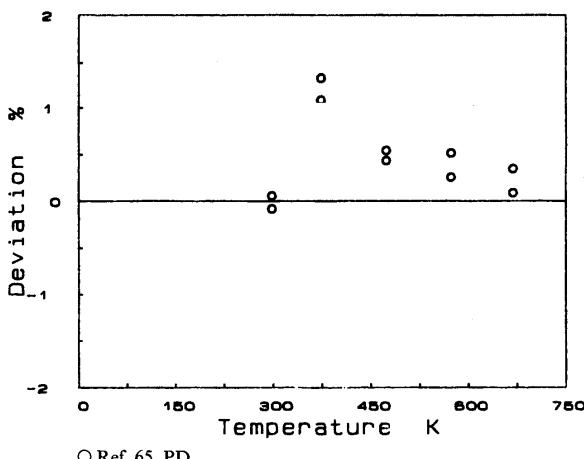
D56. Deviation plot for the viscosity of CF_4-Kr mixtures.

○ Ref. 64, PD
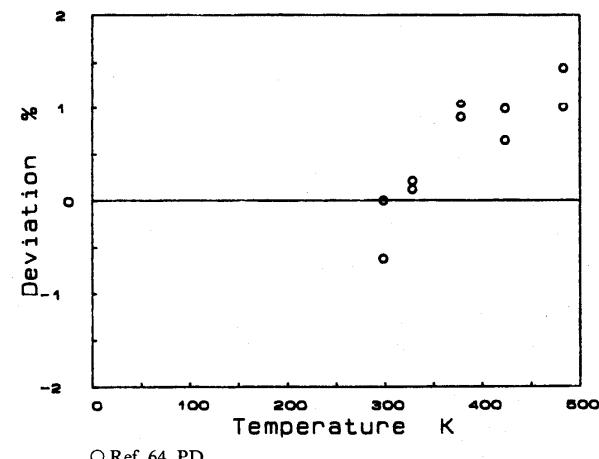
D59. Deviation plot for the viscosity of SF_6-Ne mixtures.

○ Ref. 2, PD
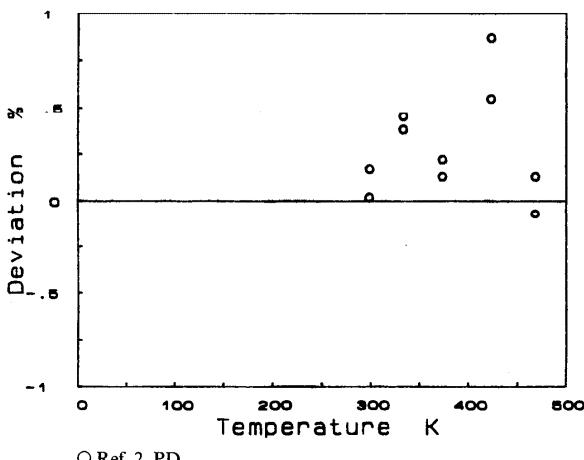
D57. Deviation plot for the viscosity of SF_6-C_2H_6 mixtures.

○ Ref. 64, PD
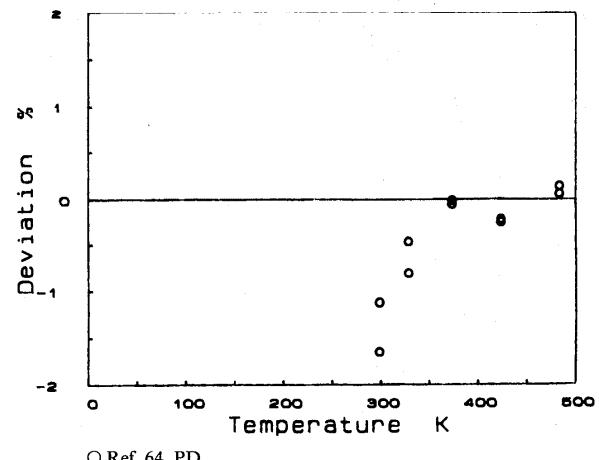
D60. Deviation plot for the viscosity of SF_6-Ar mixtures.

O Ref. 65, PD
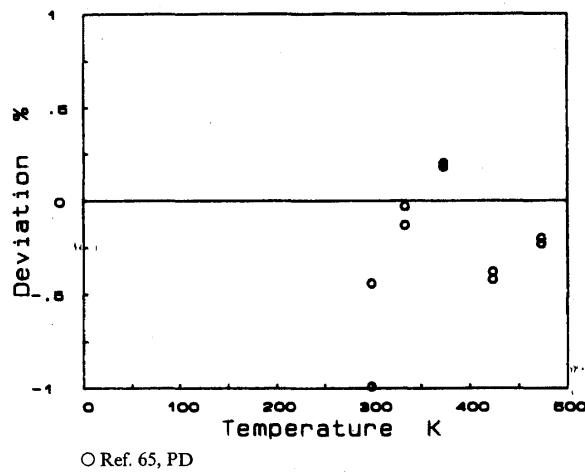
D61. Deviation plot for the viscosity of SF_6-Kr mixtures.

O Ref. 5, SD   ◇ Ref. 116, PD
□ Ref. 58, SD
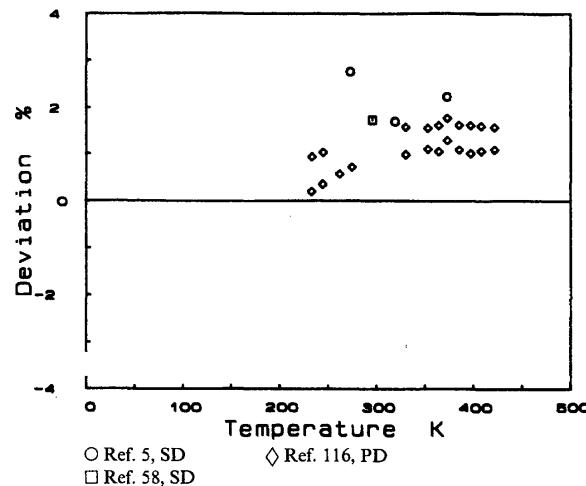
D64. Deviation plot for the diffusion coefficient of N_2-CO.

O Ref. 61, SD
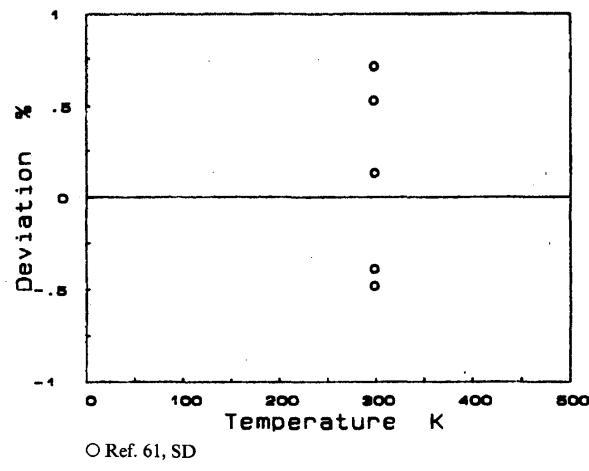
D62. Deviation plot for the viscosity of C_2H_4-Ar mixtures.

O Ref. 85, SD   △ Ref. 129, SD
□ Ref. 16, PD   X Ref. 97, SD
Y Ref. 124, SD   X̄ Ref. 90b, PD
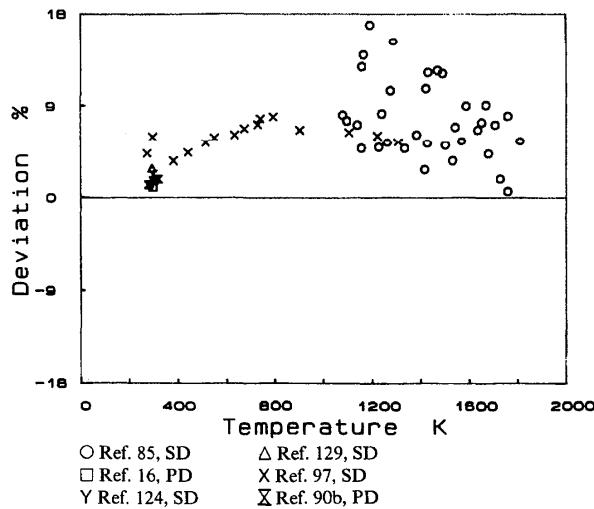
D65. Deviation plot for the diffusion coefficient of N_2-CO_2; first of two figures.


O Ref. 122, SD   Y Ref. 42, SD
□ Ref. 15, SD   △ Ref. 90b, PD

D63. Deviation plot for the diffusion coefficient of N_2-O_2.

O Ref. 23, SD   X Ref. 104, SD
□ Ref. 42, SD   * Ref. 15, SD
◇ Ref. 117, SD   ⊗ Ref. 37, SD
+ Ref. 59, SD   Y Ref. 125, SD
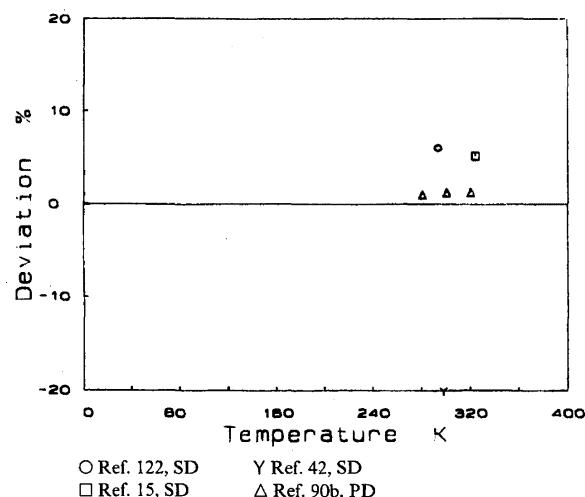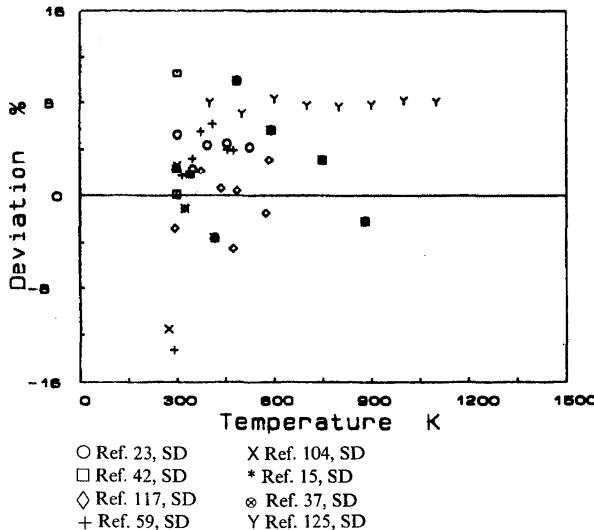
D66. Deviation plot for the diffusion coefficient of N_2-CO_2; second of two figures.
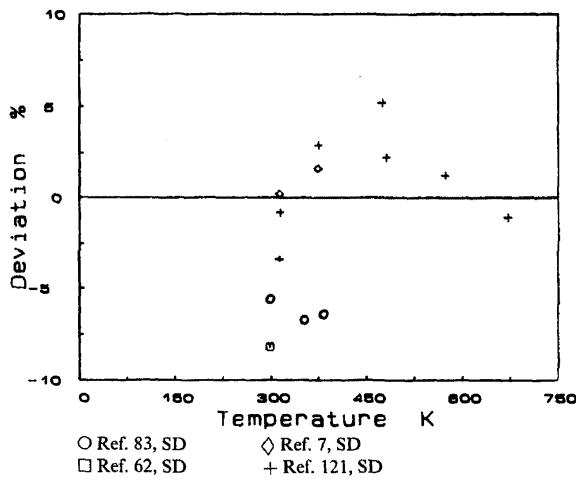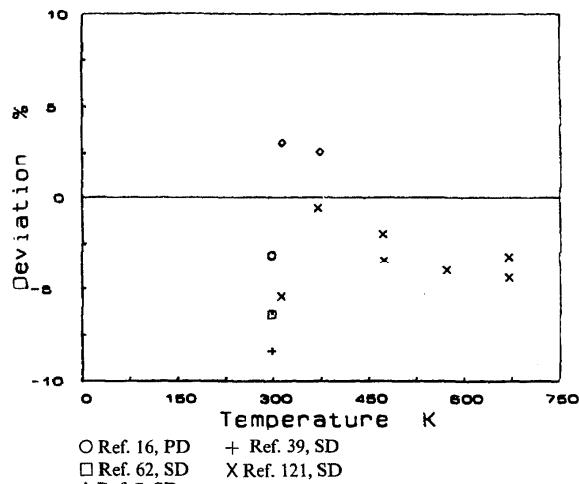
O Ref. 83, SD   ◊ Ref. 7, SD
□ Ref. 62, SD   + Ref. 121, SD

D67. Deviation plot for the diffusion coefficient of N_2-CH_4.

O Ref. 16, PD   + Ref. 39, SD
□ Ref. 62, SD   X Ref. 121, SD
◊ Ref. 7, SD

D70. Deviation plot for the diffusion coefficient of N_2-C_2H_6.

O Ref. 59, SD
□ Ref. 104, SD
Y Ref. 31, PD

D68. Deviation plot for the diffusion coefficient of N_2-SF_6.

O Ref. 129, SD   X Ref. 104, SD
□ Ref. 100, PD   * Ref. 87, SD
◊ Ref. 127, SD   ⊗ Ref. 37, SD
+ Ref. 23, SD
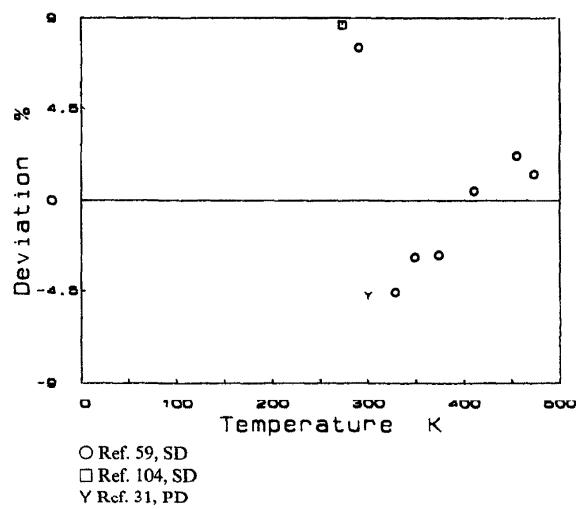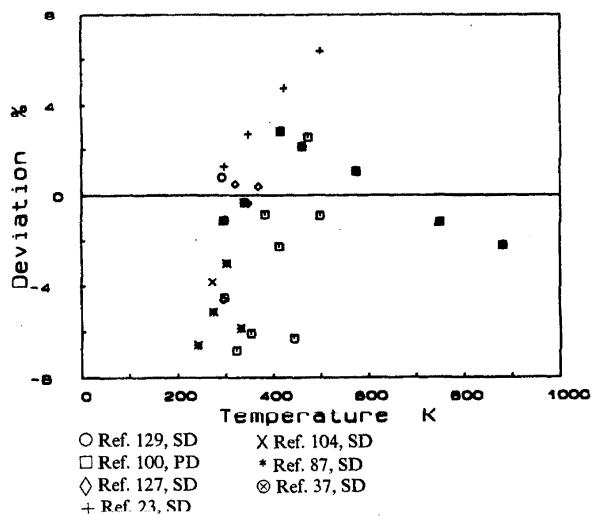
D71. Deviation plot for the diffusion coefficient of N_2-He; first of two figures.

O Ref. 16, PD
□ Ref. 41, SD

D69. Deviation plot for the diffusion coefficient of N_2-C_2H_4.

O Ref. 111, PD   △ Ref. 125, SD
□ Ref. 109, PD   X Ref. 120, SD
Y Ref. 124, SD
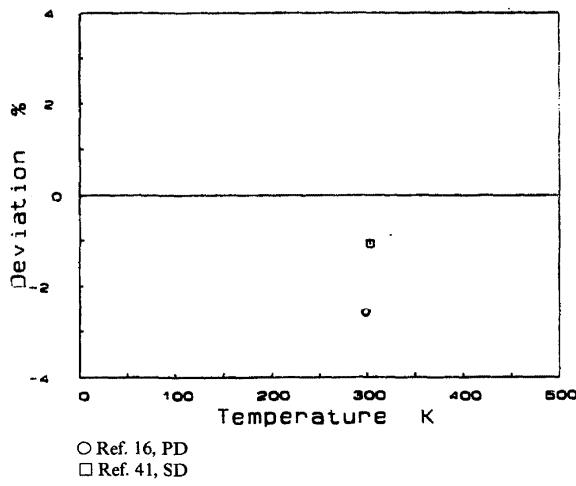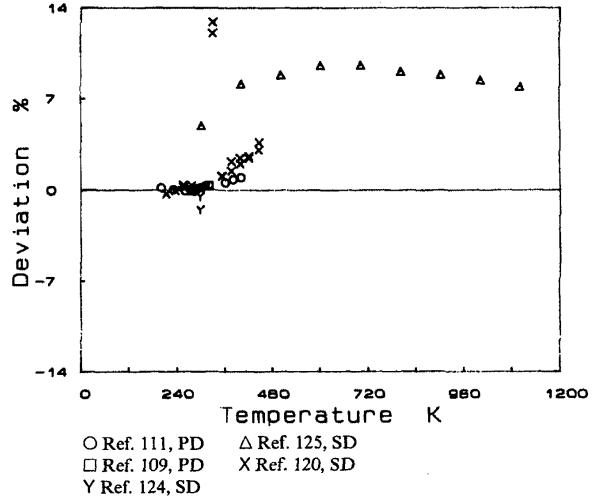
D72. Deviation plot for the diffusion coefficient of N_2-He; second of two figures.
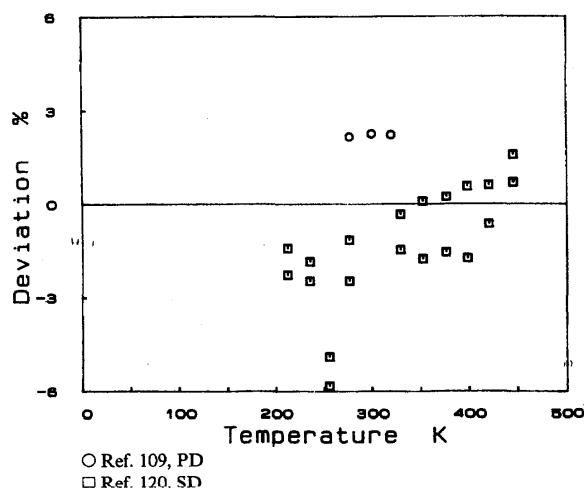
O Ref. 109, PD
□ Ref. 120, SD

D73. Deviation plot for the diffusion coefficient of N_2-Ne.
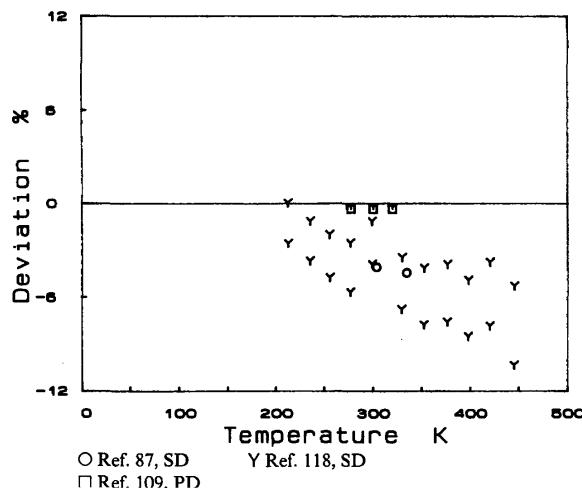
O Ref. 87, SD   Y Ref. 118, SD
□ Ref. 109, PD

D76. Deviation plot for the diffusion coefficient of N_2-Xe.

O Ref. 129, SD   △ Ref. 111, PD
□ Ref. 87, SD   X Ref. 118, SD
Y Ref. 109, PD

D74. Deviation plot for the diffusion coefficient of N_2-Ar.

O Ref. 126, SD

D77. Deviation plot for the diffusion coefficient of O_2-CO.

O Ref. 34, SD
□ Ref. 109, PD
Y Ref. 118, SD

D75. Deviation plot for the diffusion coefficient of N_2-Kr.

O Ref. 126, SD
□ Ref. 104, SD
Y Ref. 90b, PD

D78. Deviation plot for the diffusion coefficient of O_2-CO_2.

O Ref. 126, SD
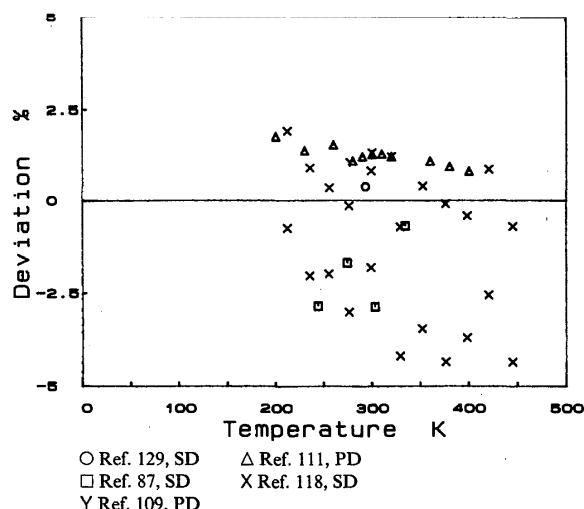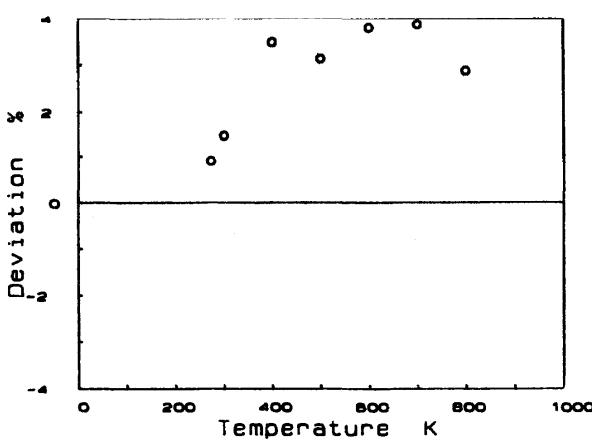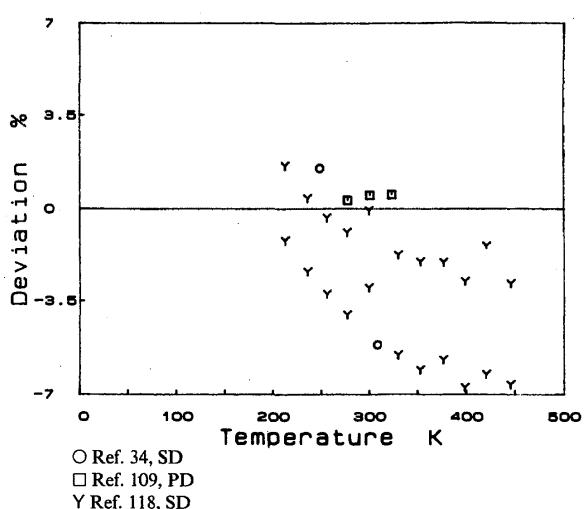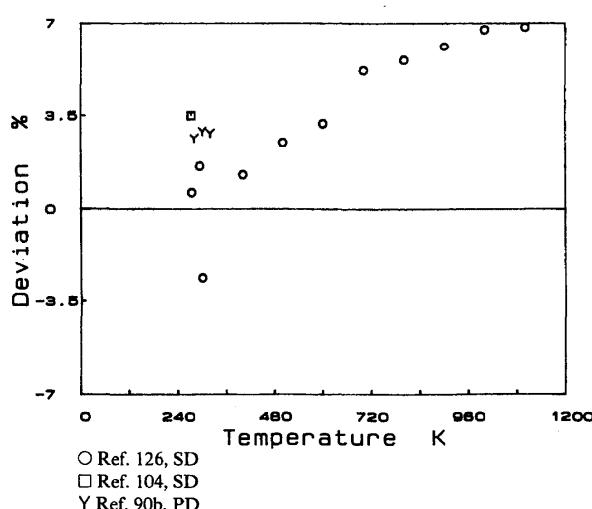
D79. Deviation plot for the diffusion coefficient of O_2-CH_4.

O Ref. 86, SD
□ Ref. 111, PD
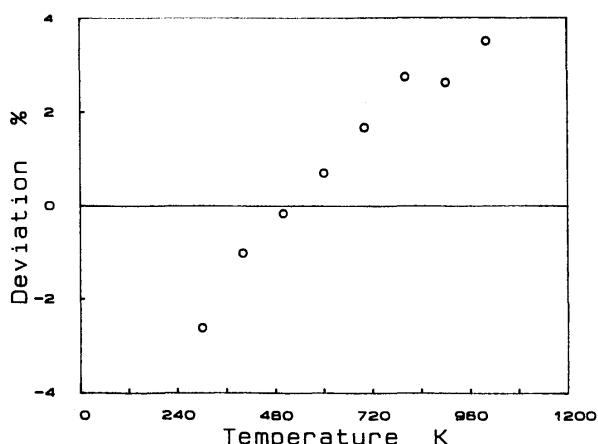
D82. Deviation plot for the diffusion coefficient of O_2-Ar.

O Ref. 60, SD
□ Ref. 104, SD
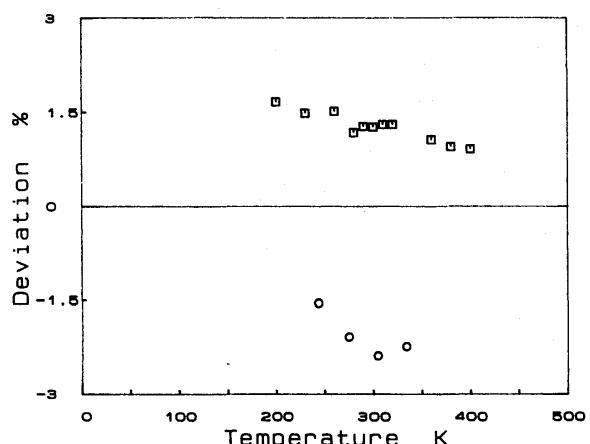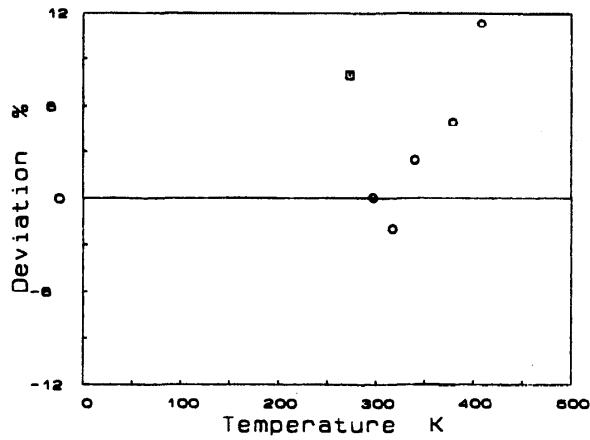
D80. Deviation plot for the diffusion coefficient of O_2-SF_6.

O Ref. 60, SD

D83. Deviation plot for the diffusion coefficient of O_2-Kr.

O Ref. 86, SD   X Ref. 13, PD
□ Ref. 42, SD   XRef. 113, PD
Y Ref. 100, SD   ◊ Ref. 111, PD
△ Ref. 127, SD
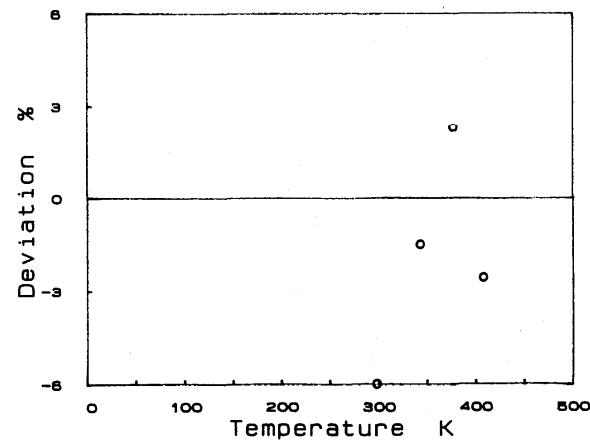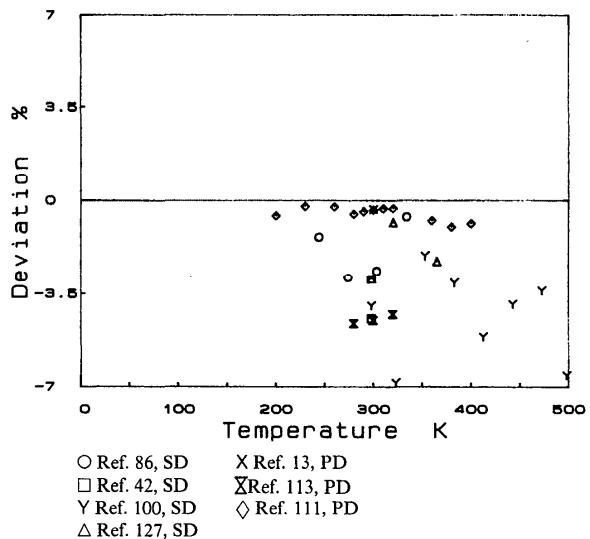
D81. Deviation plot for the diffusion coefficient of O_2-He.

O Ref. 86, SD
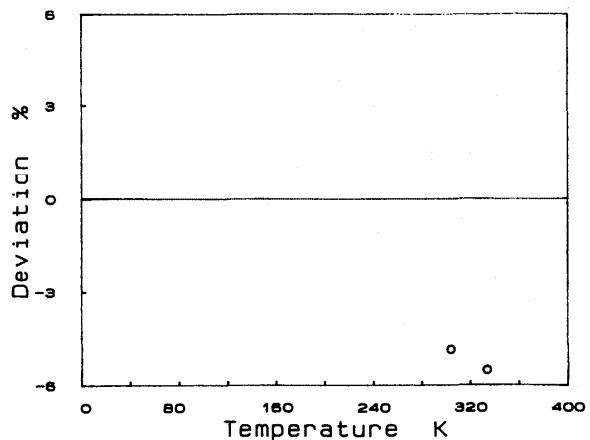
D84. Deviation plot for the diffusion coefficient of O_2-Xe.
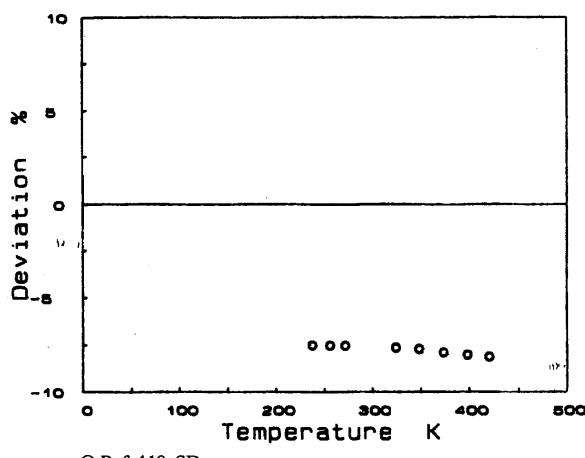
O Ref. 119, SD

D85. Deviation plot for the diffusion coefficient of NO-He.
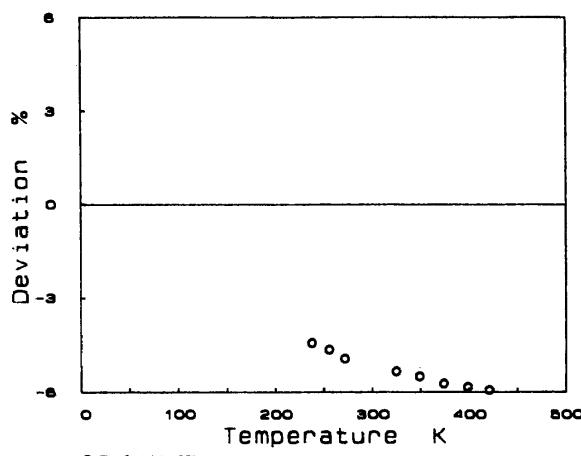
O Ref. 119, SD

D88. Deviation plot for the diffusion coefficient of NO-Kr.
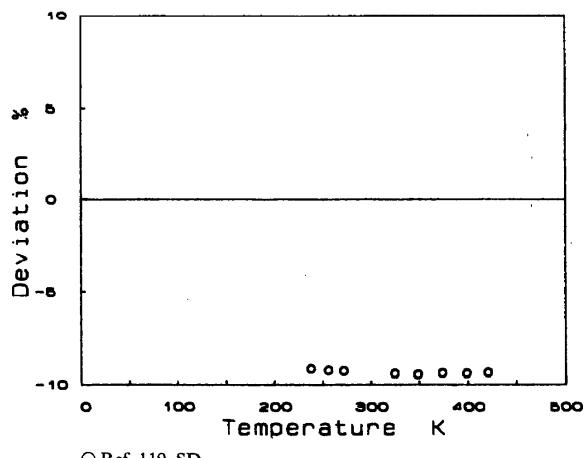
O Ref. 119, SD

D86. Deviation plot for the diffusion coefficient of NO-Ne.
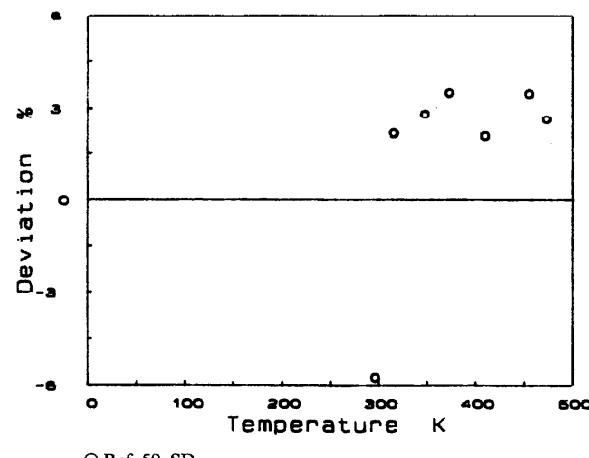
O Ref. 59, SD

D89. Deviation plot for the diffusion coefficient of CO-CO_2.
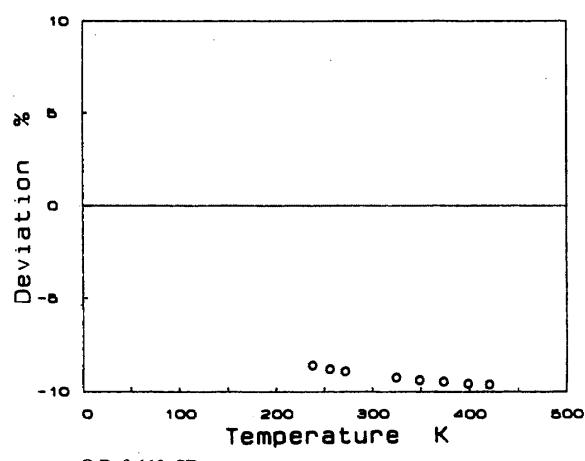
O Ref. 119, SD

D87. Deviation plot for the diffusion coefficient of NO-Ar.
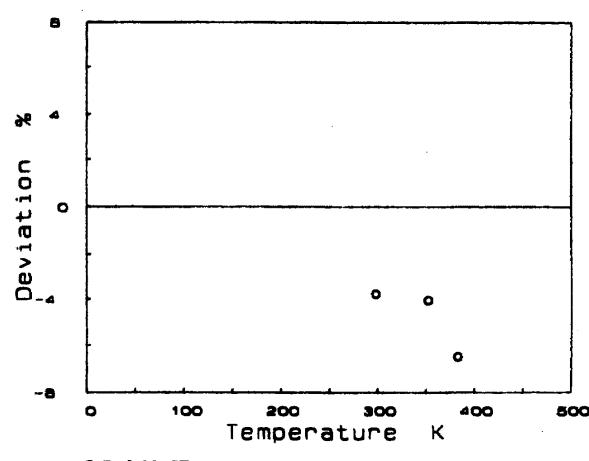
O Ref. 83, SD

D90. Deviation plot for the diffusion coefficient of CO-CH_4.

O Ref. 59, SD
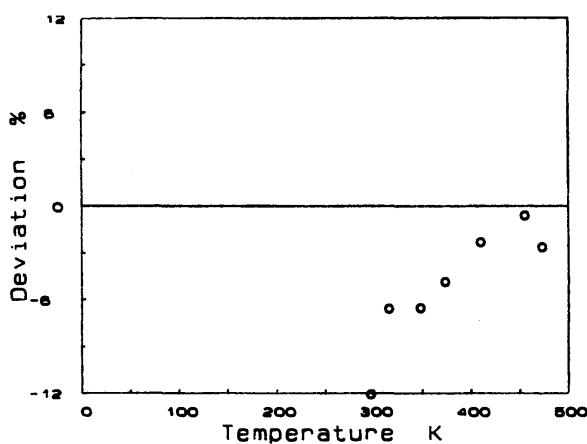
D91. Deviation plot for the diffusion coefficient of CO-SF$_6$.

O Ref. 58, SD
□ Ref. 113, PD
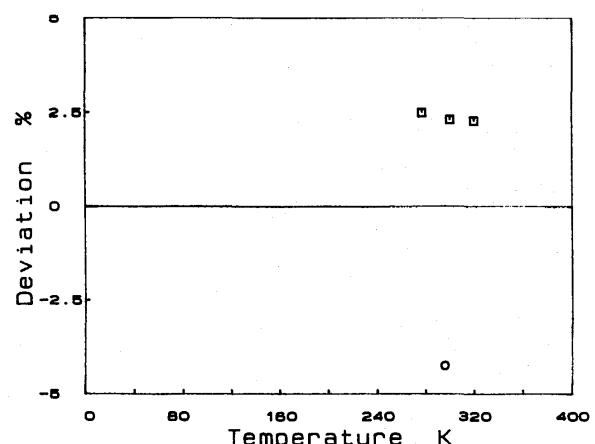
D94. Deviation plot for the diffusion coefficient of CO-Ar.

O Ref. 59, SD
□ Ref. 113, PD
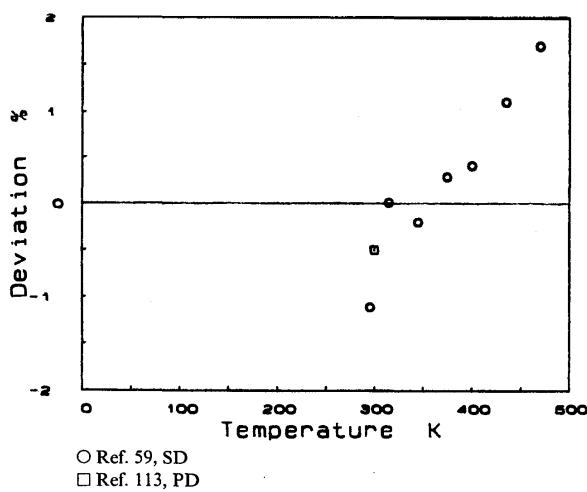
D92. Deviation plot for the diffusion coefficient of CO-He.

O Ref. 113, PD
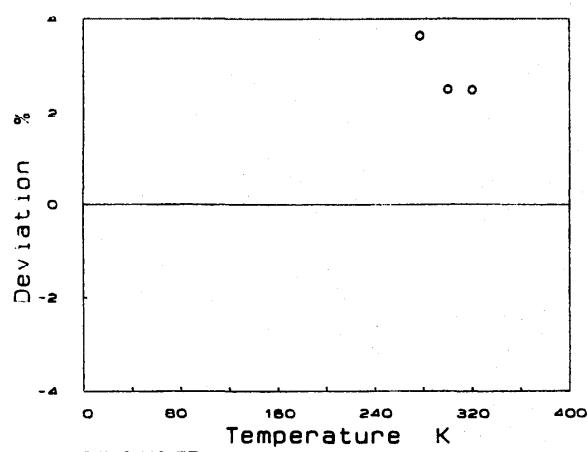
D95. Deviation plot for the diffusion coefficient of CO-Kr.

O Ref. 113, PD
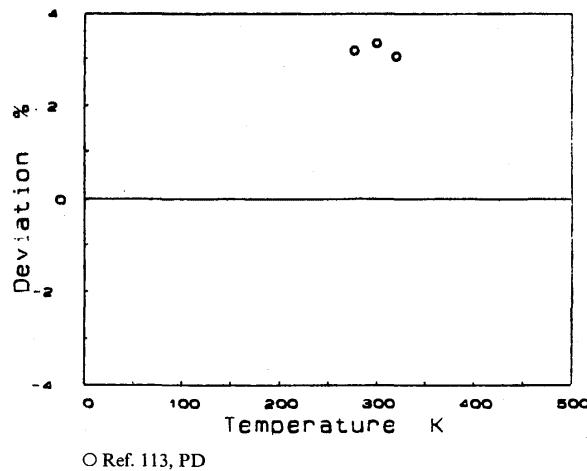
D93. Deviation plot for the diffusion coefficient of CO-Ne.

O Ref. 113, PD
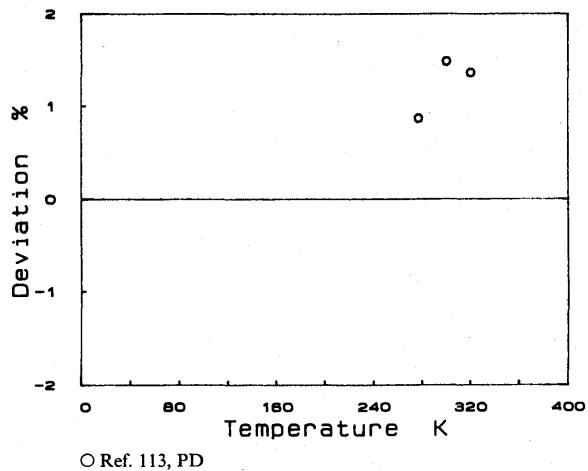
D96. Deviation plot for the diffusion coefficient of CO-Xe.

O Ref. 4, SD

D97. Deviation plot for the diffusion coefficient of CO_2-N_2O.

O Ref. 104, SD   △ Ref. 50, SD
⊓ Ref. 6, SD   X Ref. 111, PD
Y Ref. 56, SD
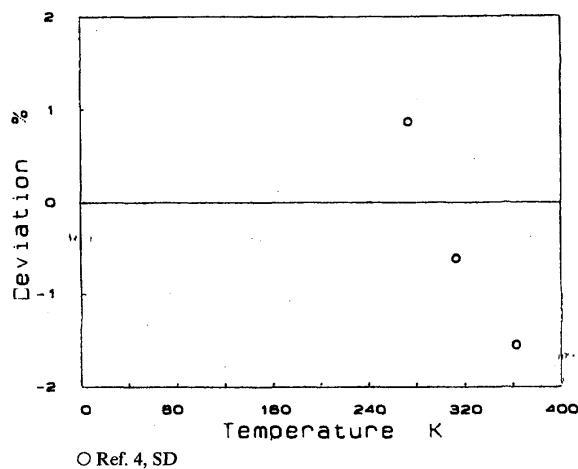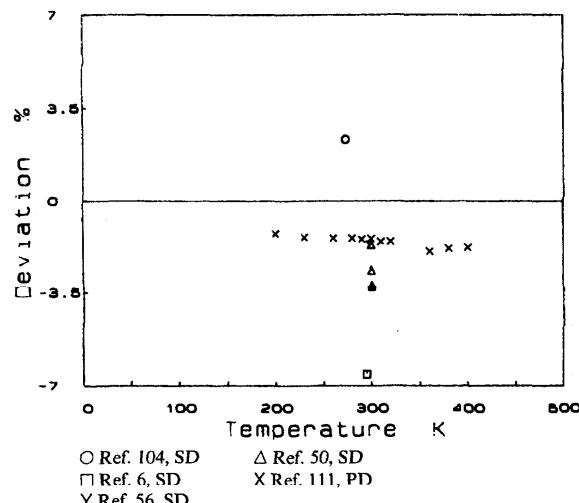
D100. Deviation plot for the diffusion coefficient of CO_2-He; first of two figures.

O Ref. 39, SD

D98. Deviation plot for the diffusion coefficient of CO_2-CH_4.

O Ref. 79, SD   Y Ref. 100, SD
□ Ref. 95, SD   △ Ref. 59, SD
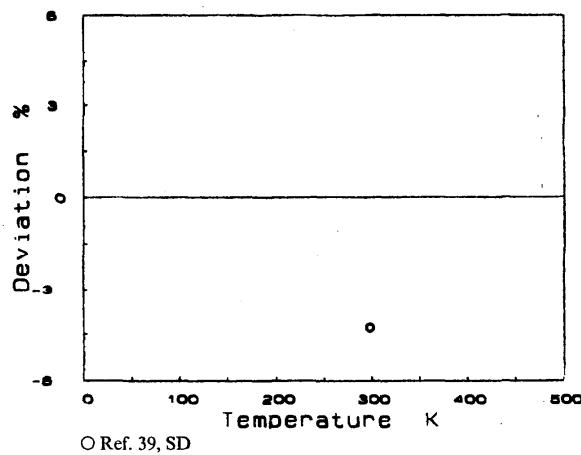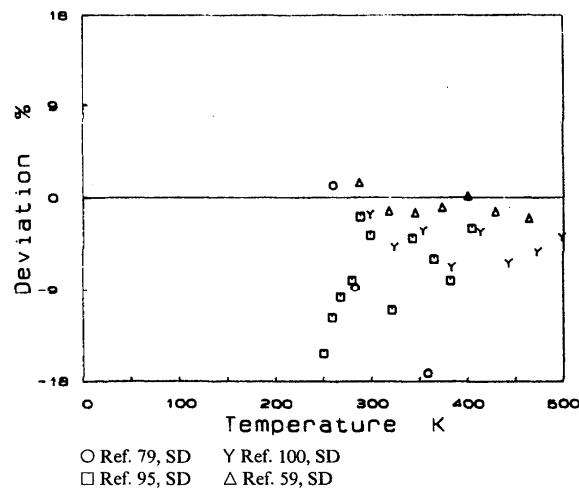
D101. Deviation plot for the diffusion coefficient of CO_2-He; second of two figures.
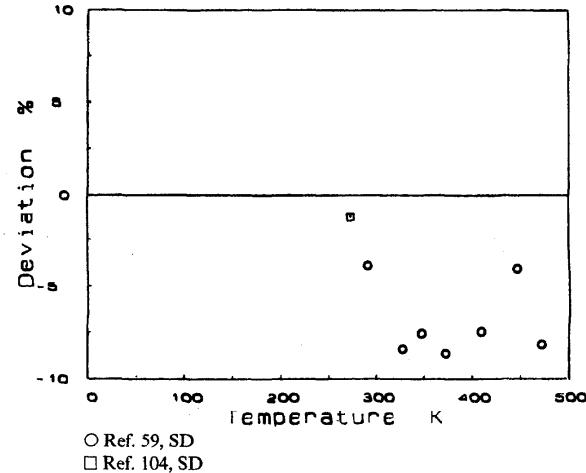
O Ref. 59, SD
□ Ref. 104, SD

D99. Deviation plot for the diffusion coefficient of CO_2-SF_6.

O Ref. 6, SD   Y Ref. 90a, PD
□ Ref. 128, SD

D102. Deviation plot for the diffusion coefficient of CO_2-Ne.

O Ref. 54, SD   △ Ref. 85, SD
□ Ref. 59, SD   X Ref. 90b, PD
Y Ref. 104, SD
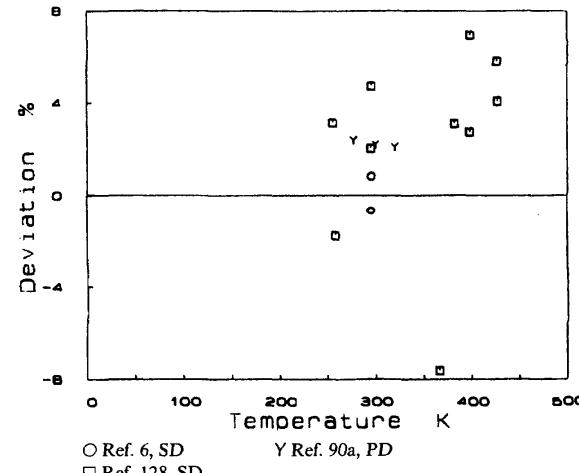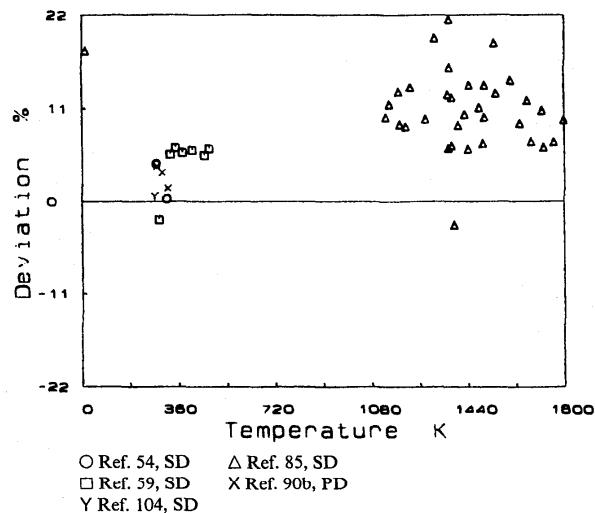
D103. Deviation plot for the diffusion coefficient of CO_2-Ar.

O Ref. 50, SD
□ Ref. 13, PD
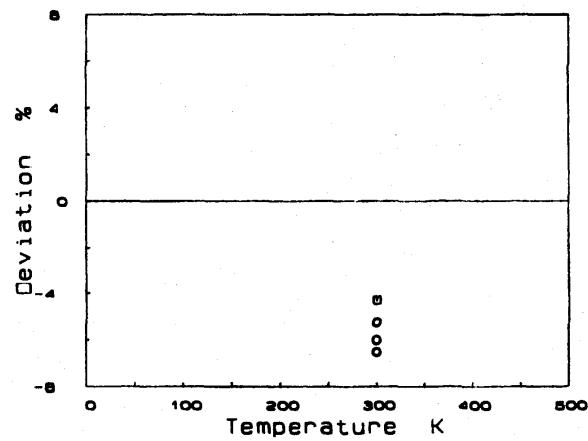
D106. Deviation plot for the diffusion coefficient of N_2O-He.

O Ref. 34, SD
□ Ref. 90a, PD

D104. Deviation plot for the diffusion coefficient of CO_2-Kr.

O Ref. 83, SD   Y Ref. 22, SD
□ Ref. 56, SD
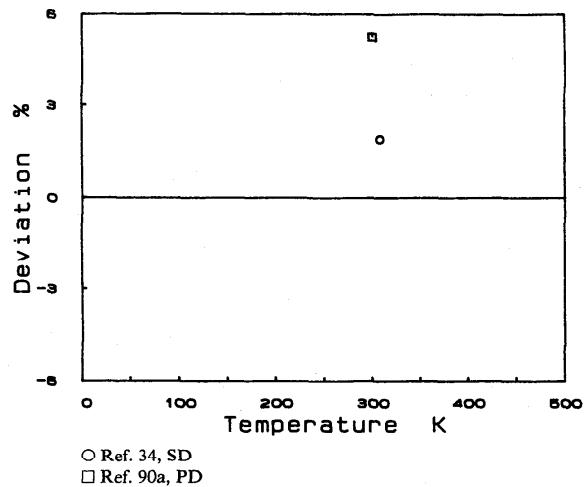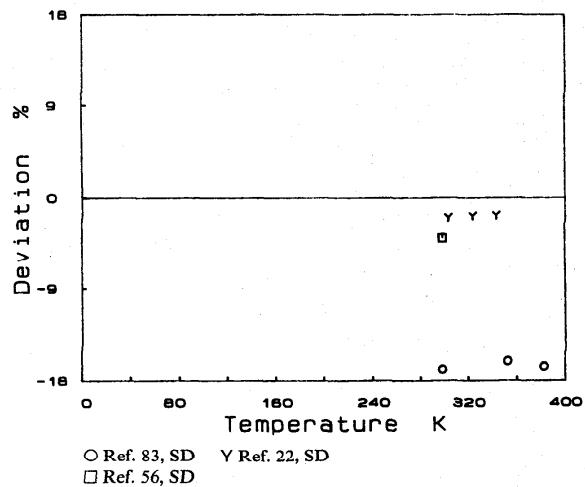
D107. Deviation plot for the diffusion coefficient of CH_4-CF_4.

O Ref. 90a, PD
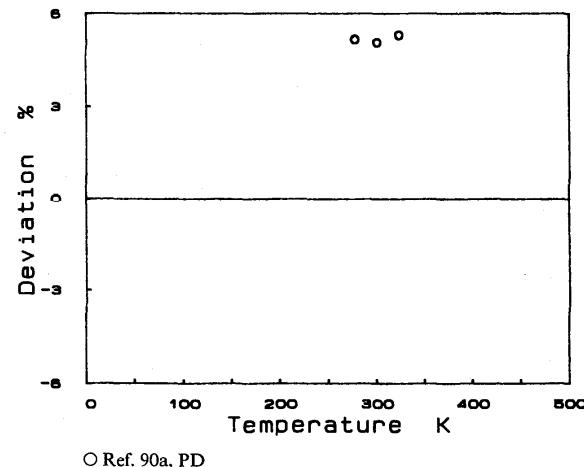
D105. Deviation plot for the diffusion coefficient of CO_2-Xe.
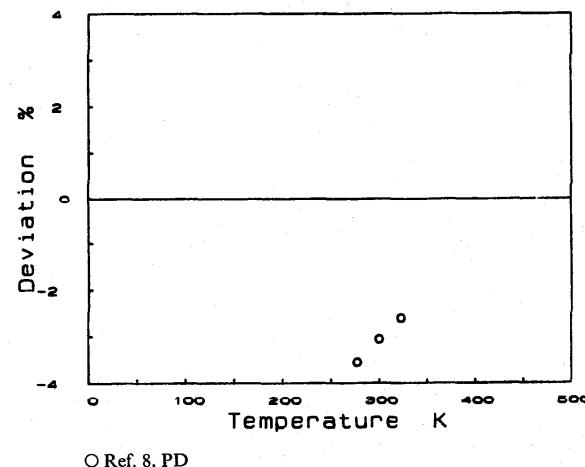
O Ref. 8, PD

D108. Deviation plot for the diffusion coefficient of CH_4-C_2H_6.

O Ref. 40, SD △ Ref. 13, PD
□ Ref. 7, SD   X Ref. 112, PD
Y Ref. 56, SD X̄ Ref. 32, PD

D109. Deviation plot for the diffusion coefficient of CH₄-He.

O Ref. 112, PD
□ Ref. 32, PD
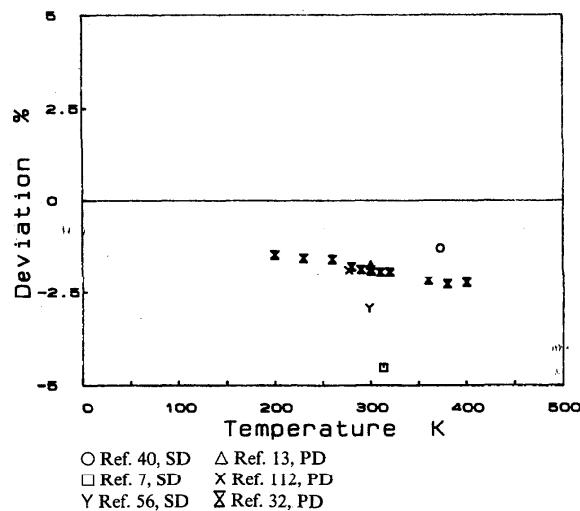
D112. Deviation plot for the diffusion coefficient of CH₄-Kr.

O Ref. 112, PD
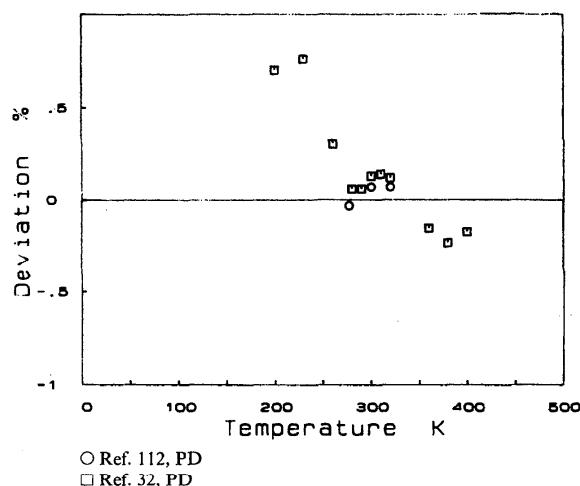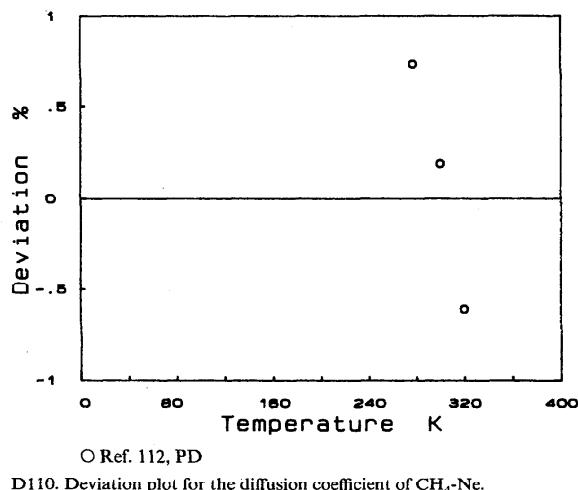
D110. Deviation plot for the diffusion coefficient of CH₄-Ne.

O Ref. 112, PD
□ Ref. 32, PD

D113. Deviation plot for the diffusion coefficient of CH₄-Xe.
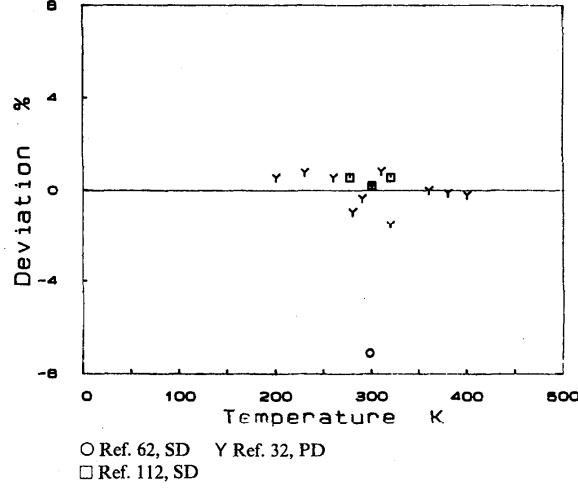
O Ref. 62, SD   Y Ref. 32, PD
□ Ref. 112, SD

D111. Deviation plot for the diffusion coefficient of CH₄-Ar.

O Ref. 13, PD

D114. Deviation plot for the diffusion coefficient of CF₄-He.

O Ref. 59, SD   Δ Ref. 50, SD
□ Ref. 104, SD   X Ref. 13, PD
Y Ref. 38, SD   X Ref. 111, PD
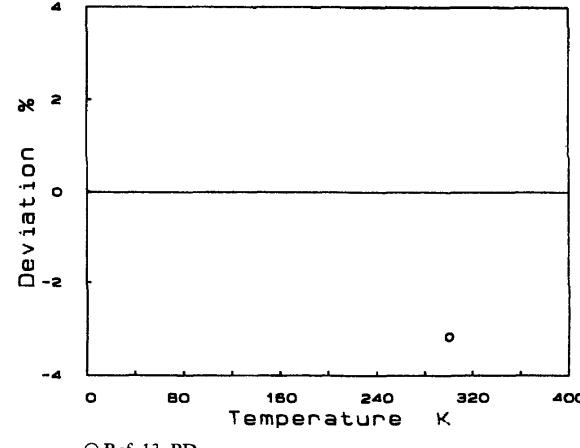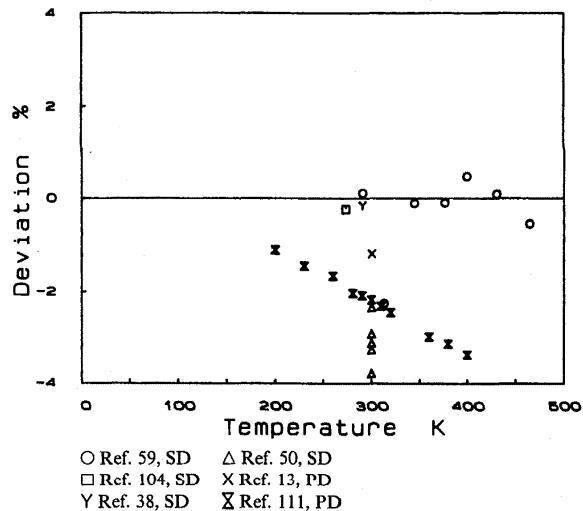
D115. Deviation plot for the diffusion coefficient of SF_6-He.

O Ref. 114, PD
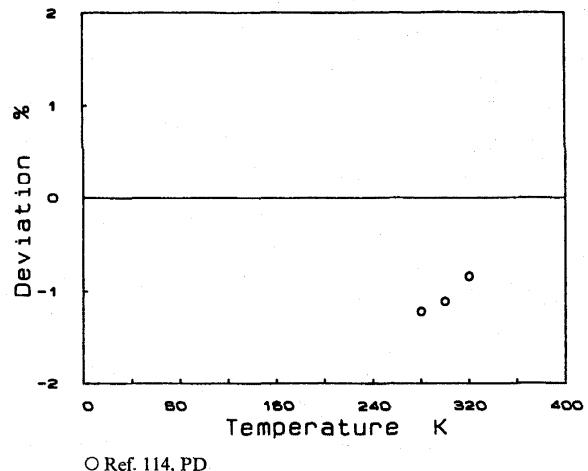
D118. Deviation plot for the diffusion coefficient of SF_6-Kr.

O Ref. 114, PD

D116. Deviation plot for the diffusion coefficient of SF_6-Ne.

O Ref. 114, PD

D119. Deviation plot for the diffusion coefficient of SF_6-Xe.

O Ref. 59, SD   Y Ref. 114, PD
□ Ref. 104, SD
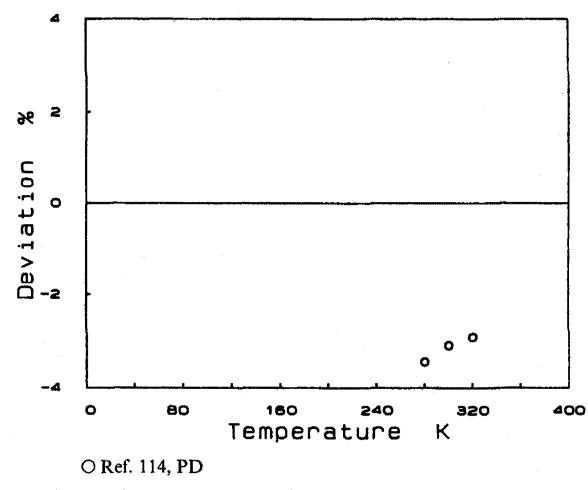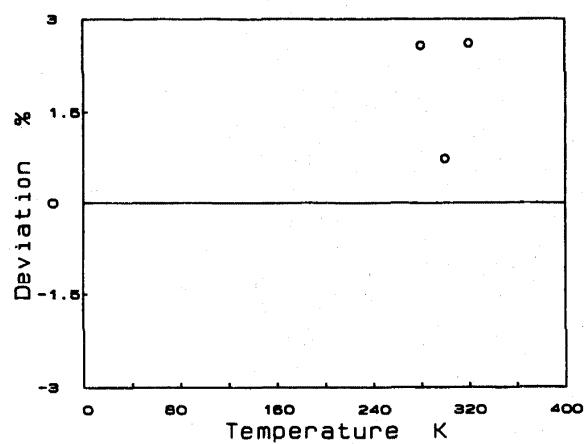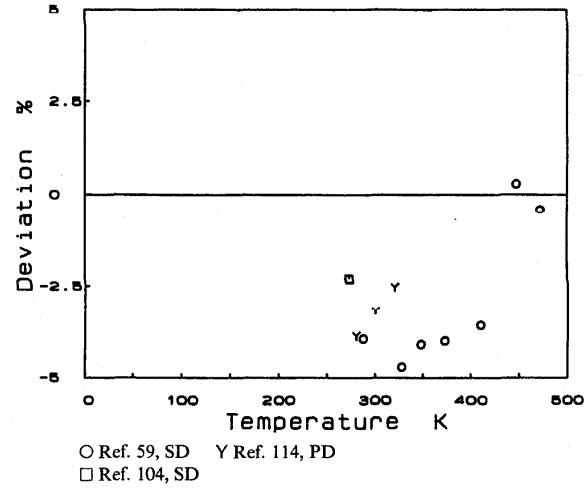
D117. Deviation plot for the diffusion coefficient of SF_6-Ar.

O Ref. 83, SD
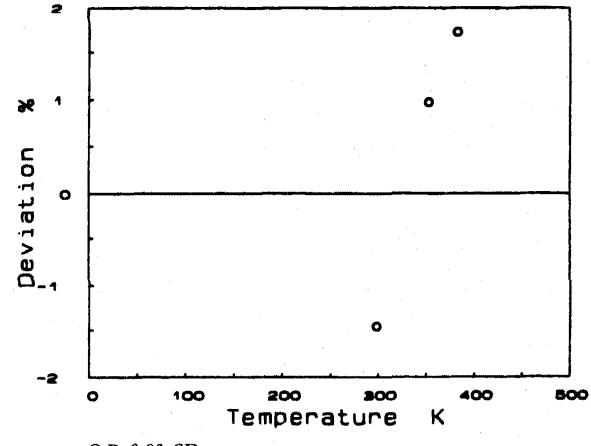
D120. Deviation plot for the diffusion coefficient of C_2H_4-C_2H_6.

O Ref. 34, SD

D121. Deviation plot for the diffusion coefficient of C_2H_4-Kr.

O Ref. 36, SD	Δ Ref. 24, SD	◇ Ref. 80b, PD
□ Ref. 43, PD	X Ref. 81, SD	
Y Ref. 88, PD	⊠ Ref. 46, SD	
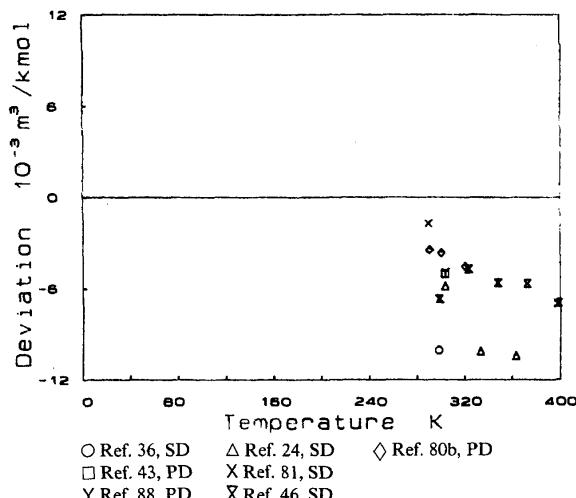
D124. Deviation plot for the interaction second virial coefficient of N_2-CO_2.

O Ref. 62, SD

D122. Deviation plot for the diffusion coefficient of C_2H_6-Ar.

| O Ref. 81, SD | Y Ref. 80b, PD |
| □ Ref. 91, PD | |

D125. Deviation plot for the interaction second virial coefficient of N_2-CH_4.

O Ref. 43, PD
□ Ref. 80b, PD
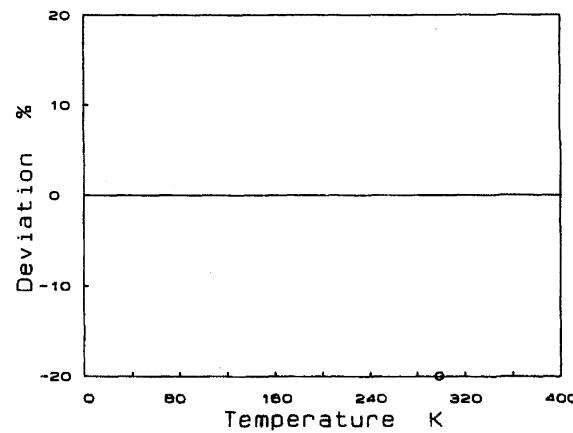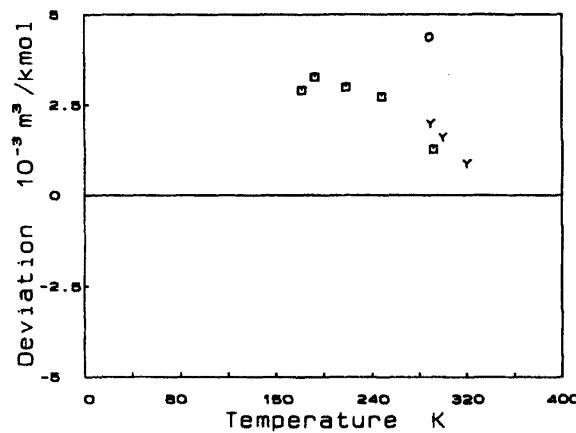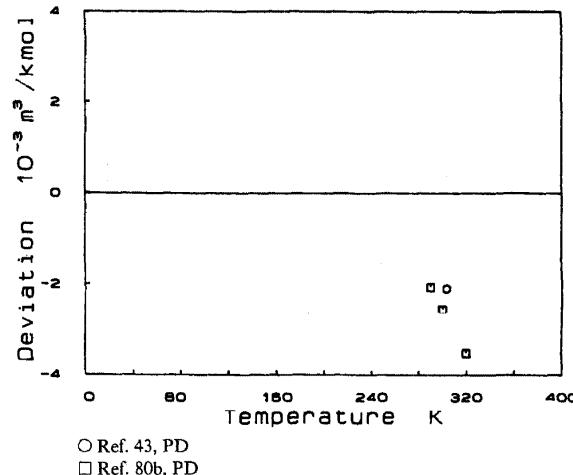
D123. Deviation plot for the interaction second virial coefficient of N_2-O_2.

O Ref. 33, PD
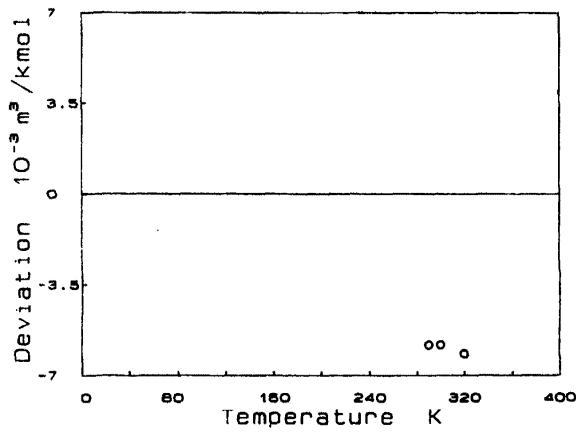
D126. Deviation plot for the interaction second virial coefficient of N_2-CF_4.
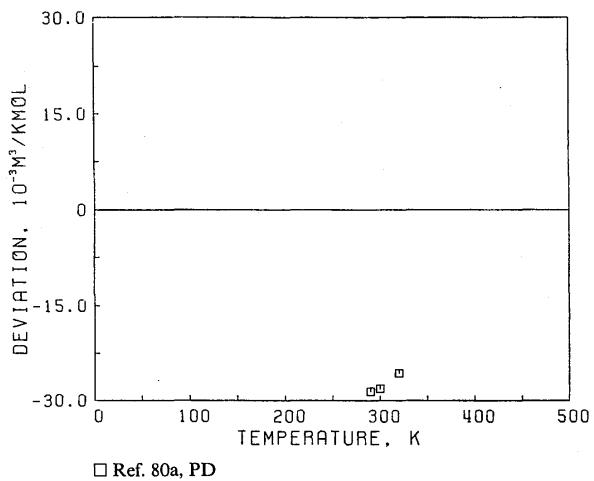
D127. Deviation plot for the interaction second virial coefficient of N_2-SF_6.
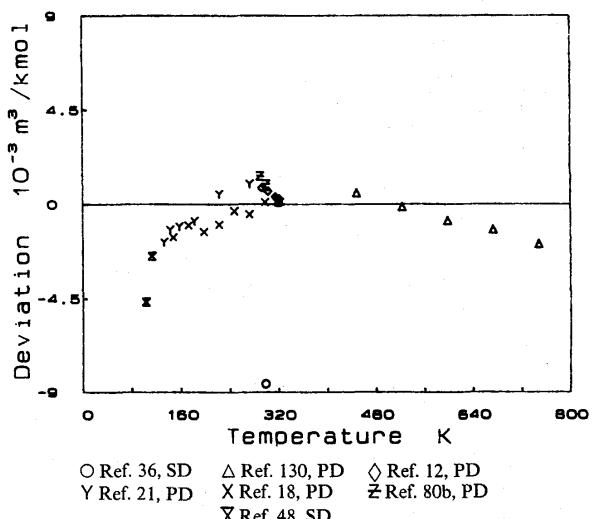
□ Ref. 36, SD

D128. Deviation plot for the interaction second virial coefficient of N_2-C_2H_4.

□ Ref. 20, SD
○ Ref. 81, SD

D129. Deviation plot for the interaction second virial coefficient of N_2-C_2H_6.

○ Ref. 36, SD	△ Ref. 130, PD	◇ Ref. 12, PD
Y Ref. 21, PD	X Ref. 18, PD	⊋ Ref. 80b, PD
	⟨ Ref. 48, SD	

D130. Deviation plot for the interaction second virial coefficient of N_2-He.

□ Ref. 18, PD
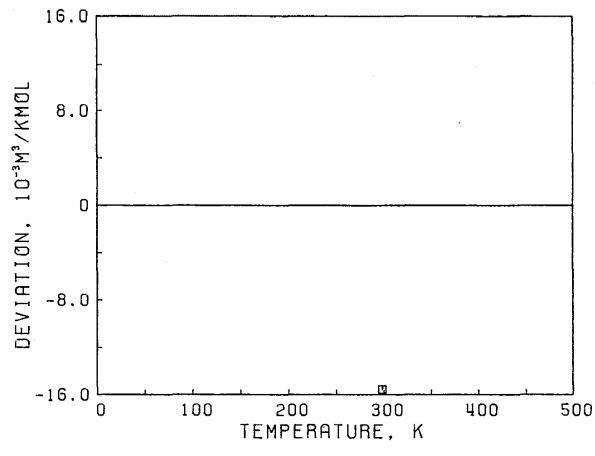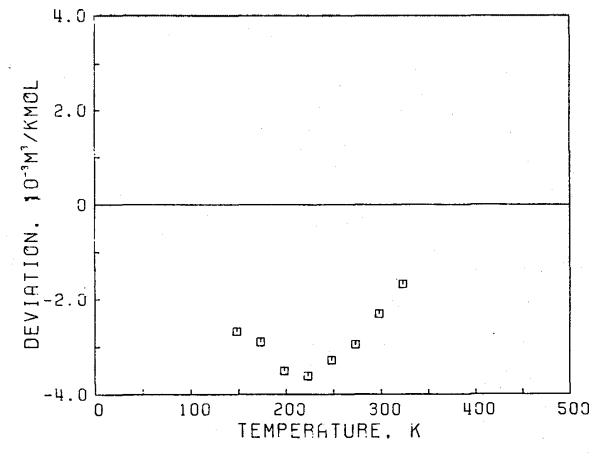
D131. Deviation plot for the interaction second virial coefficient of N_2-Ne.

| ○ Ref. 98, SD | △ Ref. 18, PD |
| □ Ref. 99, SD | X Ref. 80b, PD |
| Y Ref. 132, PD | ⟨ Ref. 33, PD |

D132. Deviation plot for the interaction second virial coefficient of N_2-Ar.

O Ref. 36, SD   Y Ref. 24, SD
⊔ Ref. 43, PD   △ Ref. 80b, PD
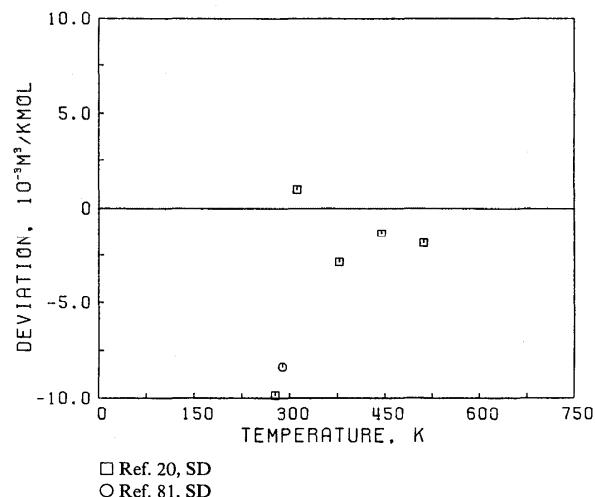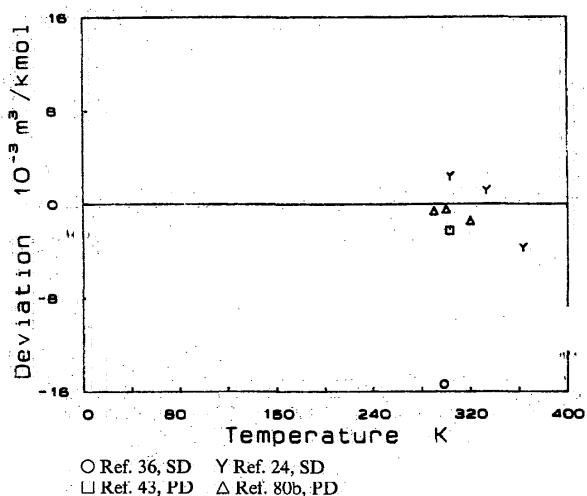
D133. Deviation plot for the interaction second virial coefficient of O_2-CO_2.

□ Ref. 80a, PD
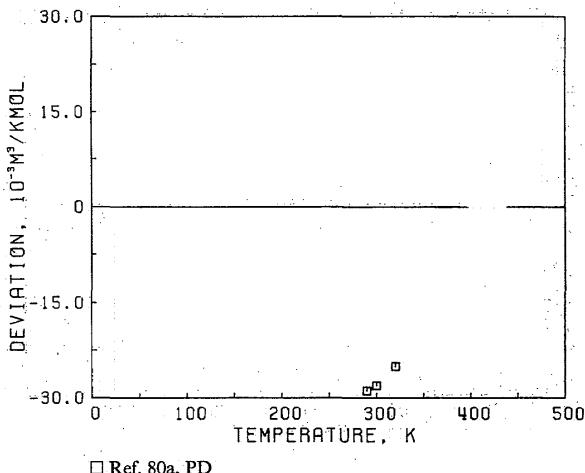
D136. Deviation plot for the interaction second virial coefficient of O_2-SF_6.

O Ref. 80b, PD
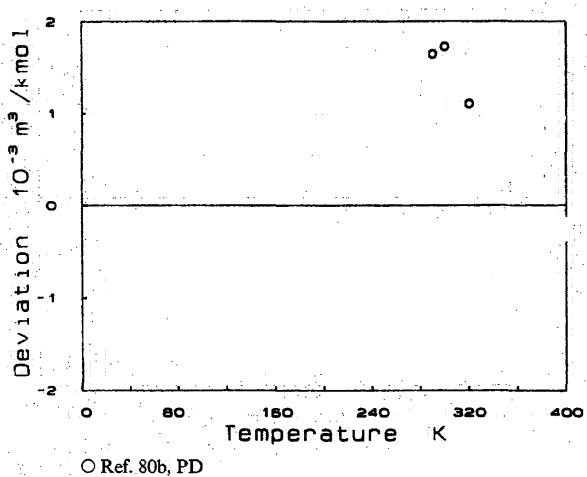
D134. Deviation plot for the interaction second virial coefficient of O_2-CH_4.


O Ref. 80b, PD
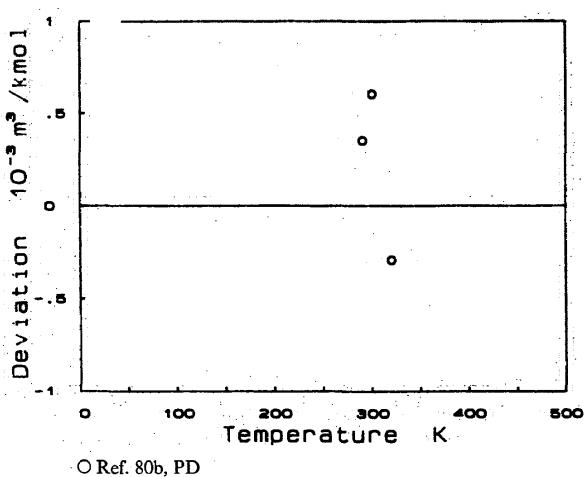
D137. Deviation plot for the interaction second virial coefficient of O_2-He.

O Ref. 33, PD
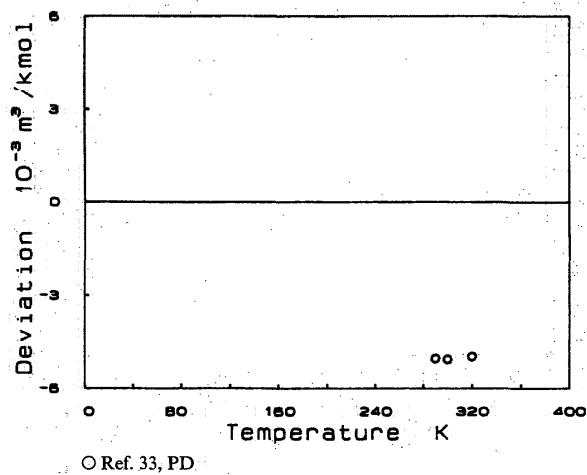
D135. Deviation plot for the interaction second virial coefficient of O_2-CF_4.

O Ref. 80b, PD
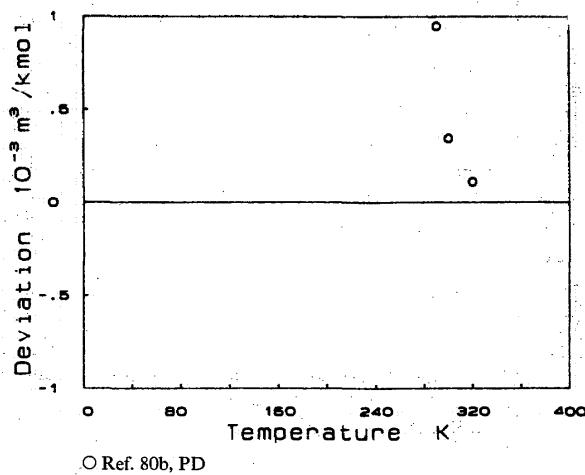
D138. Deviation plot for the interaction second virial coefficient of O_2-Ar.
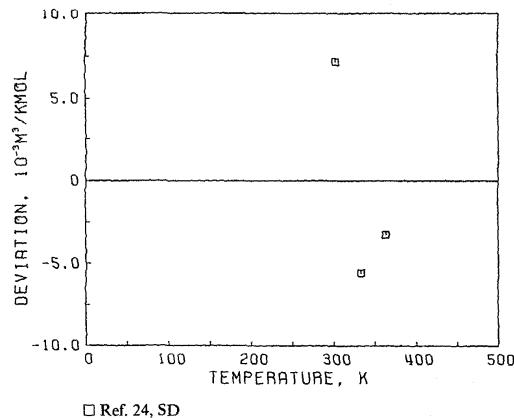
□ Ref. 24, SD

D139. Deviation plot for the interaction second virial coefficient of CO-CO$_2$.
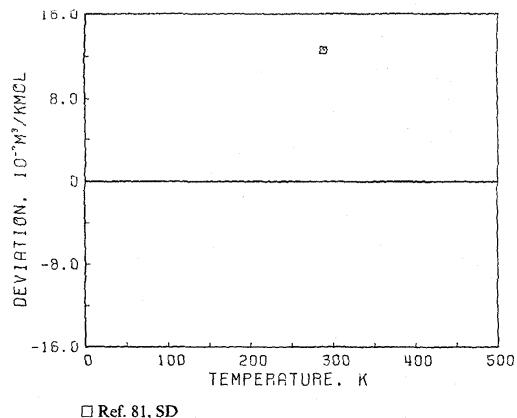
□ Ref. 81, SD

D142. Deviation plot for the interaction second virial coefficient of CO-C$_2$H$_4$.
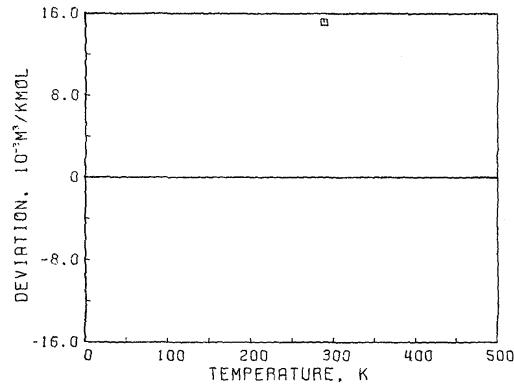
□ Ref. 81, SD

D140. Deviation plot for the interaction second virial coefficient of CO-CH$_4$.
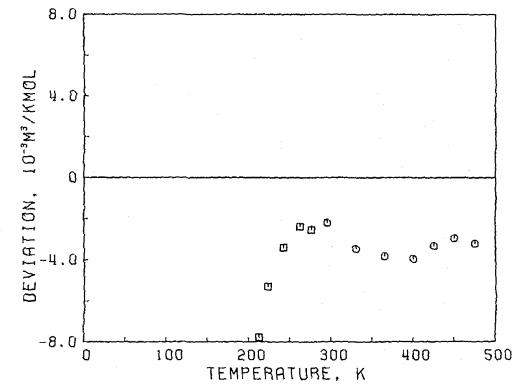
□ Ref. 98, SD
⊙ Ref. 99, SD

D143. Deviation plot for the interaction second virial coefficient of CO-Ar.
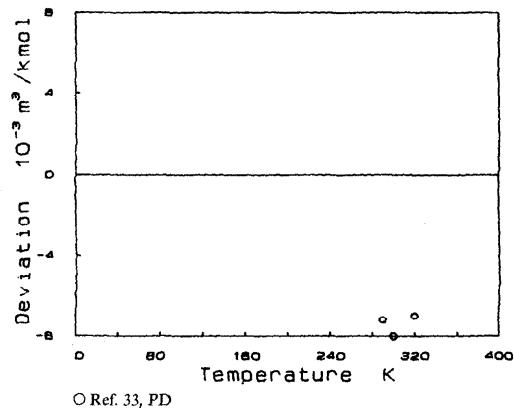
O Ref. 33, PD

D141. Deviation plot for the interaction second virial coefficient of CO-CF$_4$.
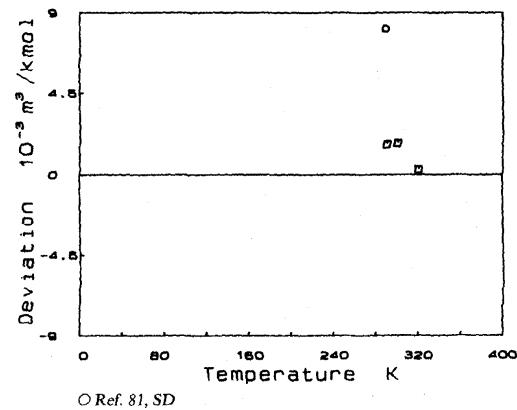
O *Ref. 81, SD*
□ Ref. 80b, PD

D144. Deviation plot for the interaction second virial coefficient of CO$_2$-CH$_4$.
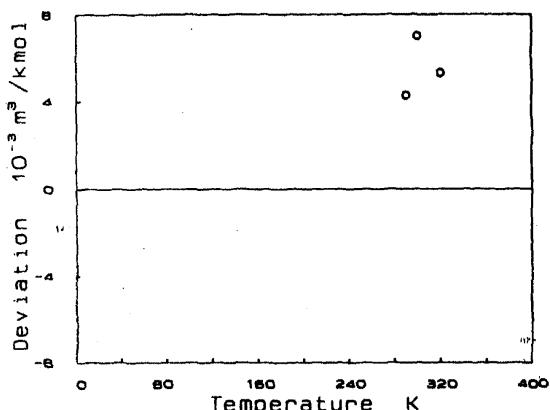
○ Ref. 33, PD

D145. Deviation plot for the interaction second virial coefficient of CO_2-CF_4.

□ Ref. 80a, PD

D146. Deviation plot for the interaction second virial coefficient of CO_2-SF_6.

□ Ref. 36, SD
○ Ref. 94, PD
△ Ref. 84, PD

D147. Deviation plot for the interaction second virial coefficient of CO_2-C_2H_4.
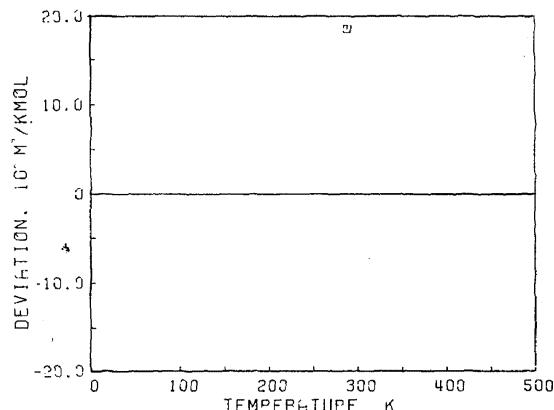
□ Ref. 81, SD

D148. Deviation plot for the interaction second virial coefficient of CO_2-C_2H_6.

○ Ref. 24, SD   △ Ref. 12, PD
□ Ref. 115, SD   X Ref. 80b, PD
Y Ref. 78, SD
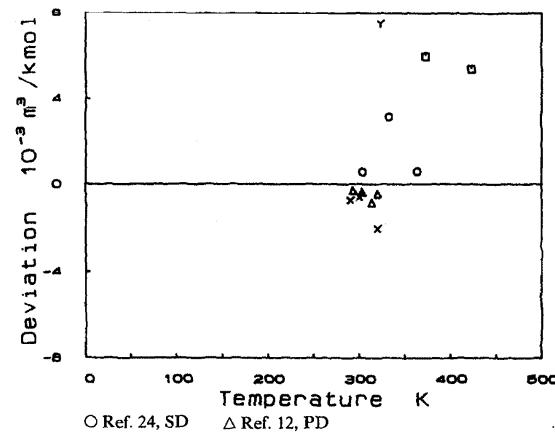
D149. Deviation plot for the interaction second virial coefficient of CO_2-He.

○ Ref. 24, SD   △ Ref. 98, SD
□ Ref. 77, SD   X Ref. 99, SD
Y Ref. 105, SD   ⊠ Ref. 80b PD
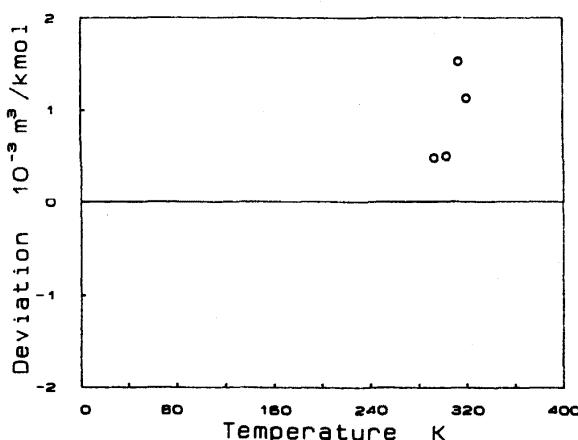
D150. Deviation plot for the interaction second virial coefficient of CO_2-Ar.

D151. Deviation plot for the interaction second virial coefficient of N₂O-He.

O Ref. 12, PD

O Ref. 30, PD Y Ref. 80b, PD
□ Ref. 26, PD

D152. Deviation plot for the interaction second virial coefficient of CH₄-CF₄.

□ Ref. 49, SD △ Ref. 80a, PD
O Ref. 14, SD
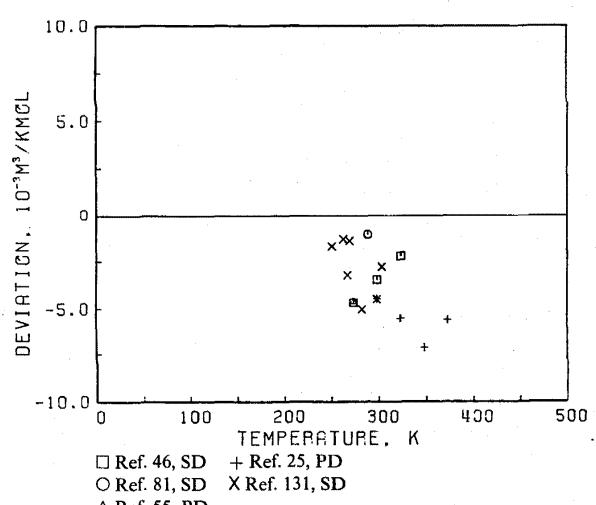
D153. Deviation plot for the interaction second virial coefficient of CH₄ SF₆.

□ Ref. 81, SD + Ref. 75, SD
O Ref. 82, SD X Ref. 84, PD
△ Ref. 76, SD

D154. Deviation plot for the interaction second virial coefficient of CH₄-C₂H₄.

□ Ref. 46, SD + Ref. 25, PD
O Ref. 81, SD X Ref. 131, SD
△ Ref. 55, PD

D155. Deviation plot for the interaction second virial coefficient of CH₄-C₂H₆.
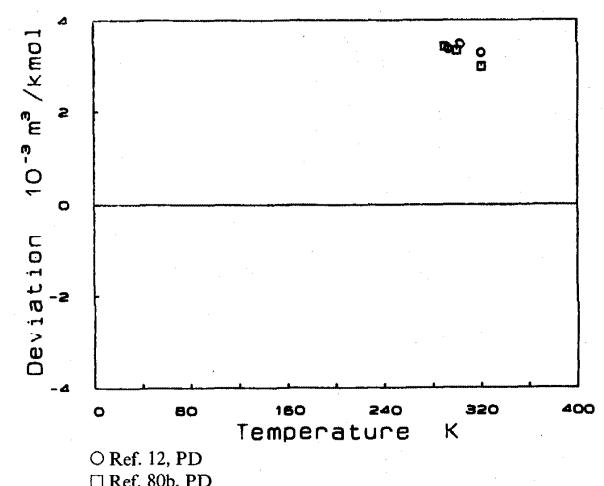
O Ref. 12, PD
□ Ref. 80b, PD

D156. Deviation plot for the interaction second virial coefficient of CH₄-He.
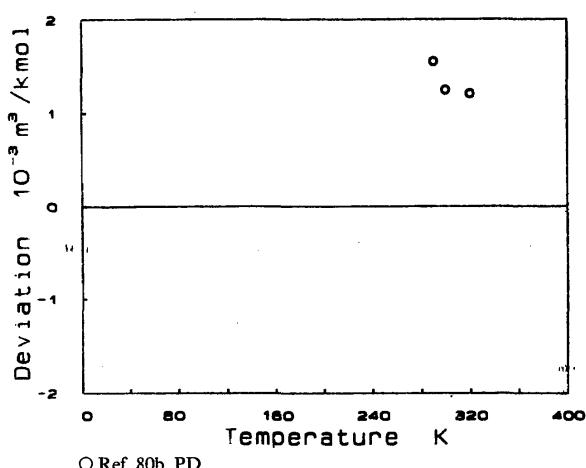
O Ref. 80b, PD

D157. Deviation plot for the interaction second virial coefficient of CH₄-Ne.

□ Ref. 36, PD   △ Ref. 80a, PD
O Ref. 101, PD
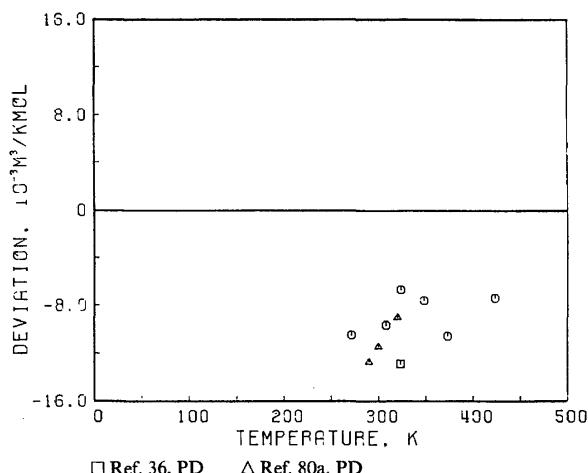
D160. Deviation plot for the interaction second virial coefficient of CF_4-SF_6.
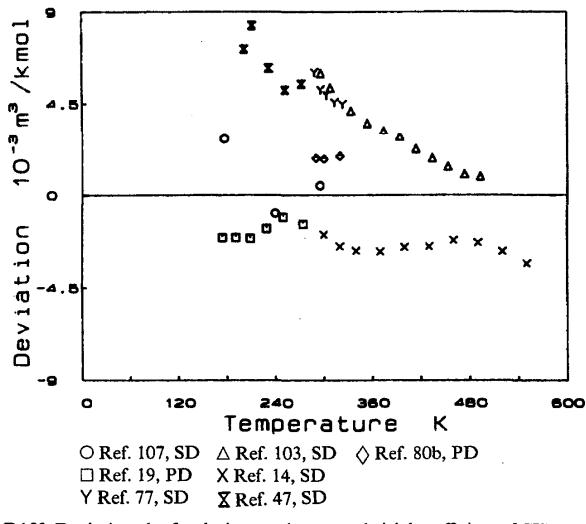
O Ref. 107, SD   △ Ref. 103, SD   ◇ Ref. 80b, PD
□ Ref. 19, PD   X Ref. 14, SD
Y Ref. 77, SD   X Ref. 47, SD

D158. Deviation plot for the interaction second virial coefficient of CH₄-Ar.
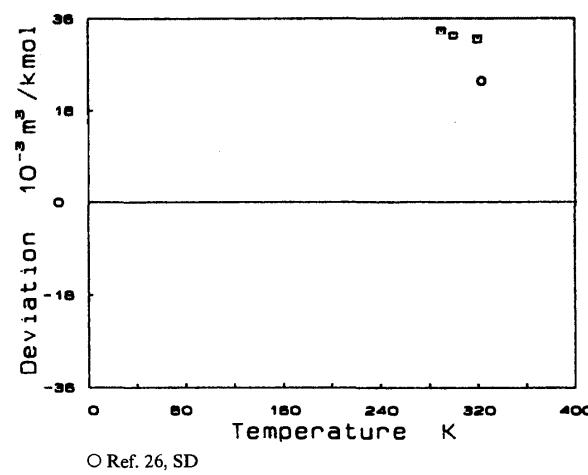
O Ref. 26, SD
□ Ref. 33, PD

D161. Deviation plot for the interaction second virial coefficient of CF_4-C_2H_6.

□ Ref. 19, PD
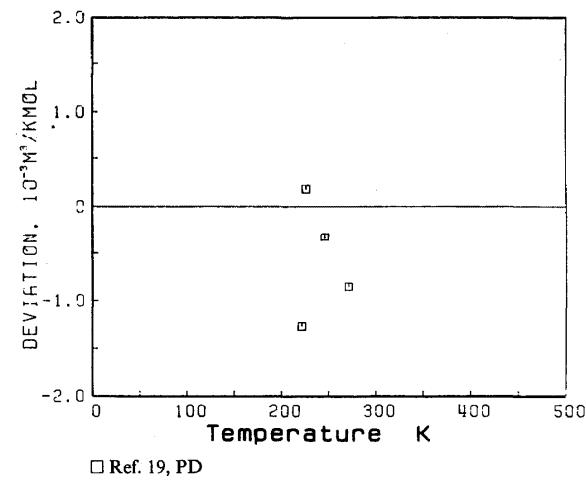
D159. Deviation plot for the interaction second virial coefficient of CH₄-Kr.

O Ref. 63, PD
□ Ref. 12, PD
Y Ref. 33, PD
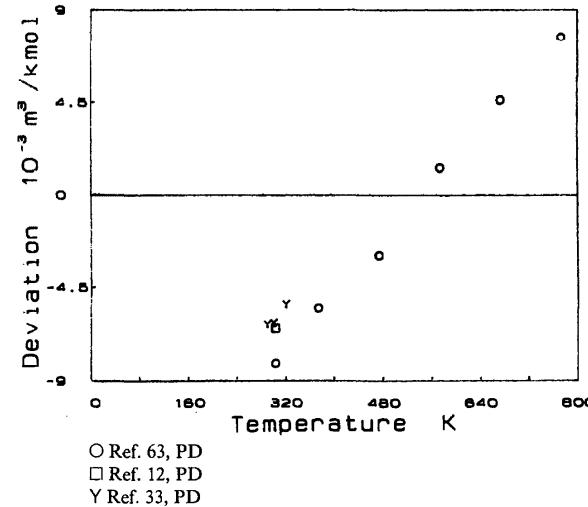
D162. Deviation plot for the interaction second virial coefficient of CF₄-He.

O Ref. 80b, PD
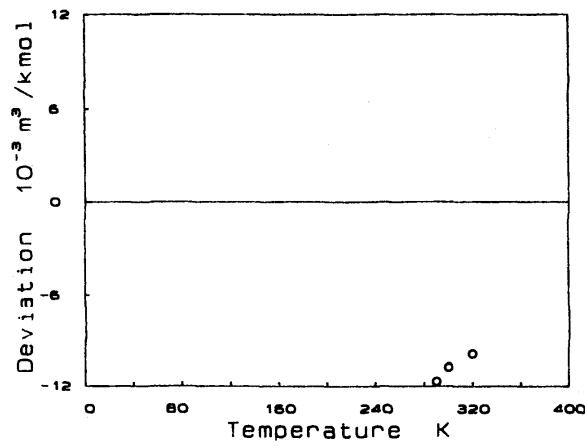
D163. Deviation plot for the interaction second virial coefficient of CF_4-Ne.

O Ref. 33, PD
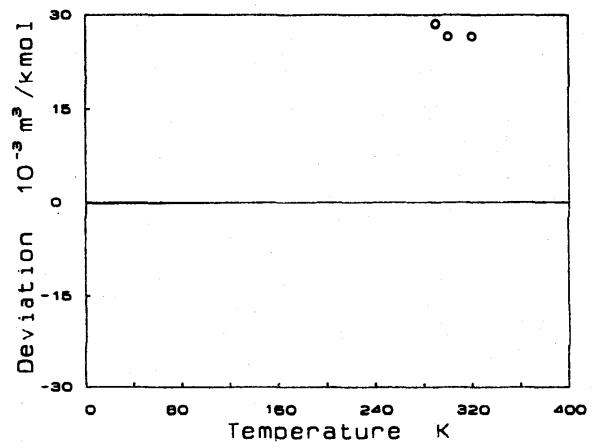
D166. Deviation plot for the interaction second virial coefficient of CF_4-Xe.

O Ref. 26, PD
□ Ref. 80b, PD
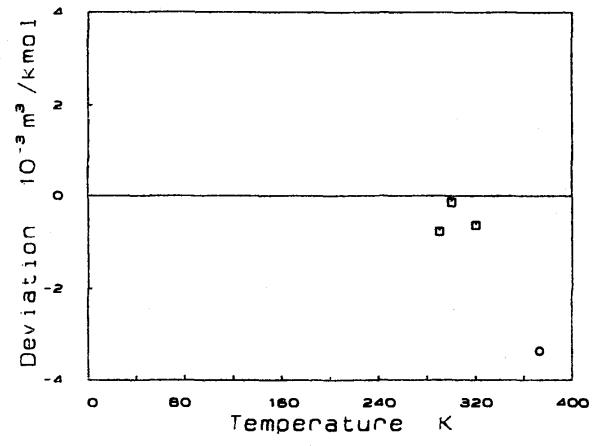
D164. Deviation plot for the interaction second virial coefficient of CF_4-Ar.

□ Ref. 12, PD
O Ref. 80a, PD
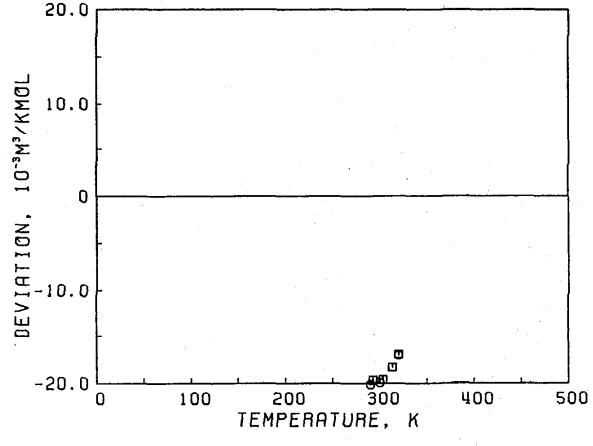
D167. Deviation plot for the interaction second virial coefficient of SF_6-He.

O Ref. 33, PD
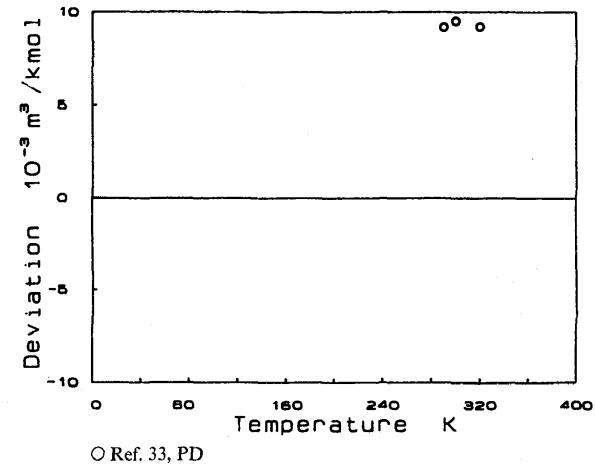
D165. Deviation plot for the interaction second virial coefficient of CF_4-Kr.
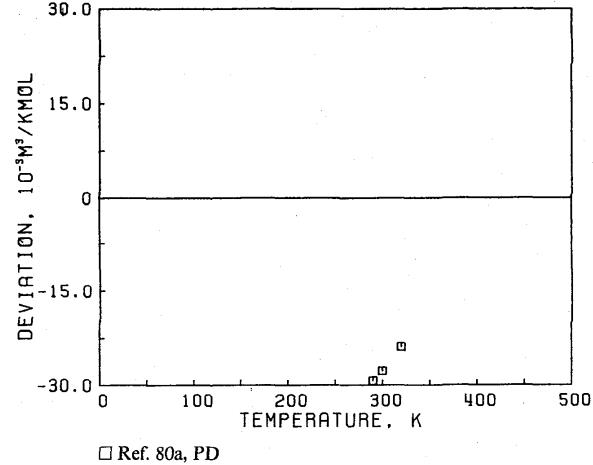
□ Ref. 80a, PD

D168. Deviation plot for the interaction second virial coefficient of SF_6-Ne.
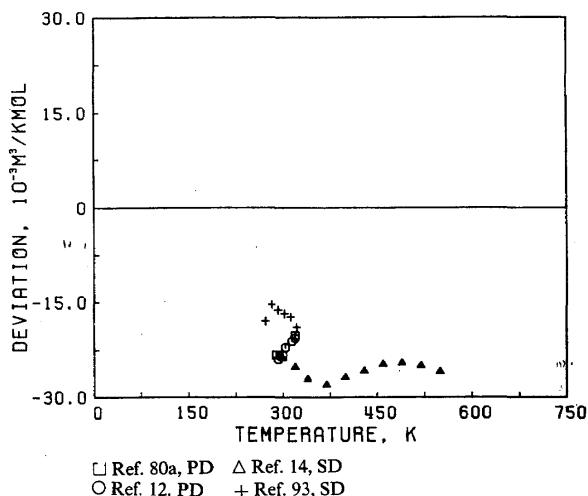
□ Ref. 80a, PD　△ Ref. 14, SD
○ Ref. 12, PD　+ Ref. 93, SD

D169. Deviation plot for the interaction second virial coefficient of SF_6-Ar.

□ Ref. 84, PD

D172. Deviation plot for the interaction second virial coefficient of C_2H_4-C_2H_6.


□ Ref. 80a, PD
○ Ref. 93, SD

D170. Deviation plot for the interaction second virial coefficient of SF_6-Kr.


□ Ref. 77, SD　△ Ref. 96, SD
○ Ref. 47, SD

D173. Deviation plot for the interaction second virial coefficient of C_2H_6-Ar.

□ Ref. 80a, PD
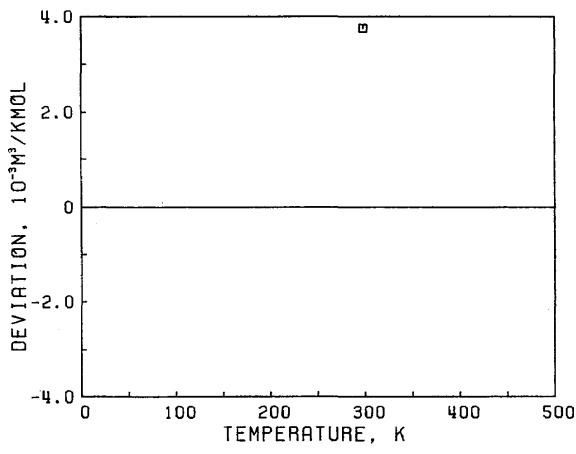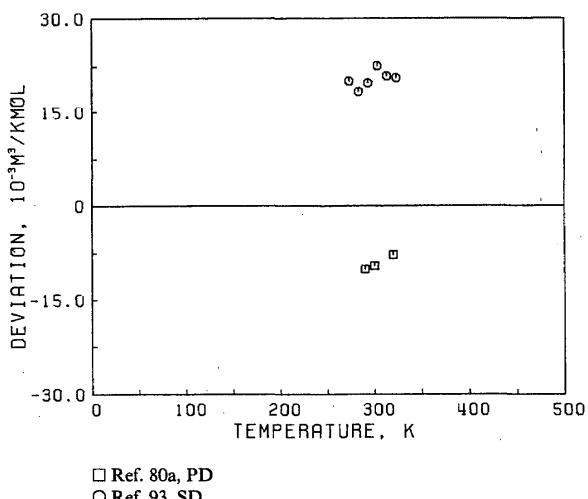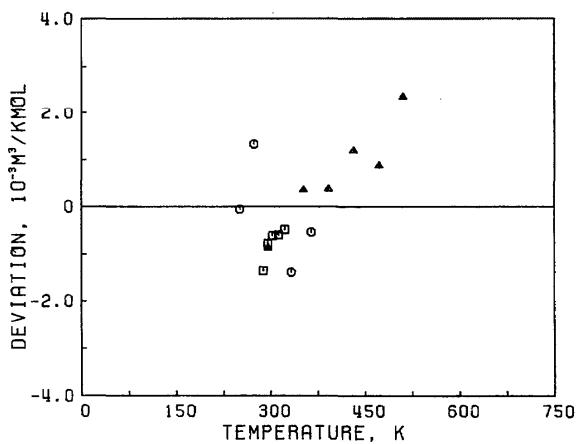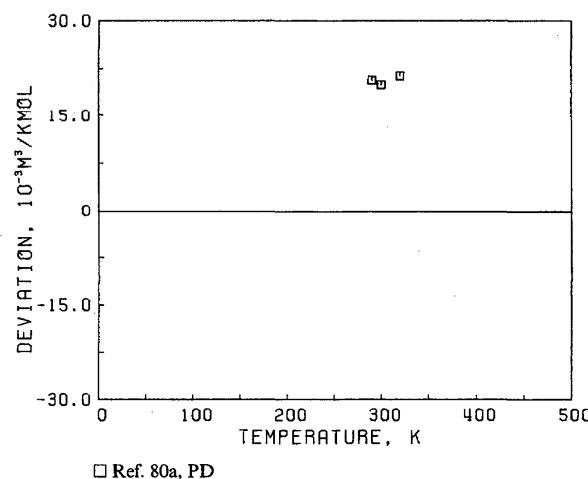
D171. Deviation plot for the interaction second virial coefficient of SF_6-Xe.

□ Ref. 122, SD
○ Ref. 123, SD
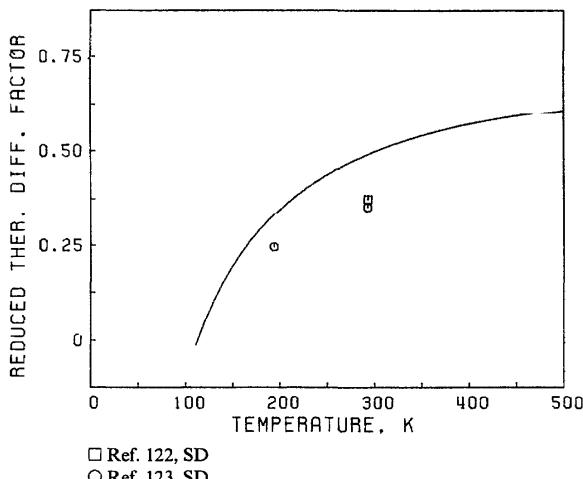
D174. Reduced thermal diffusion factor of N_2-O_2.

D175. Reduced thermal diffusion factor of N_2-CO_2.

□ Ref. 122, SD △ Ref. 9, SD
O Ref. 45, SD   + Ref. 123, SD
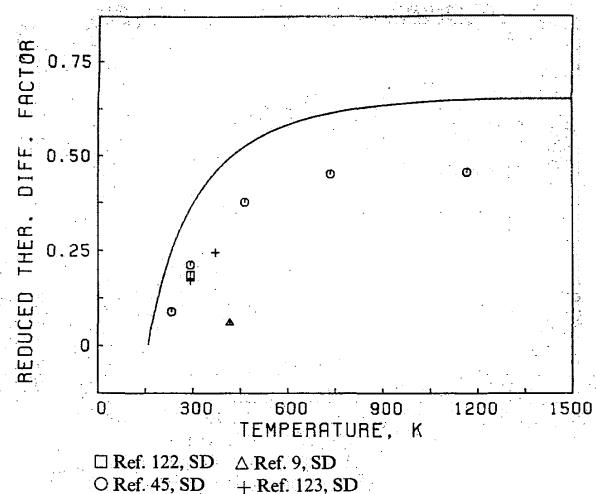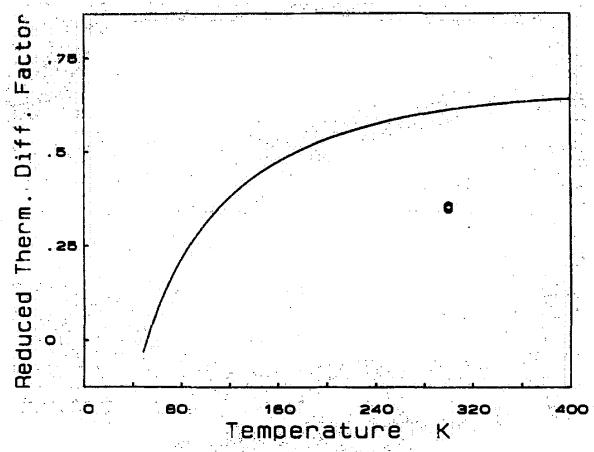
D178. Reduced thermal diffusion factor of N_2-Ne.

O Ref. 109, PD
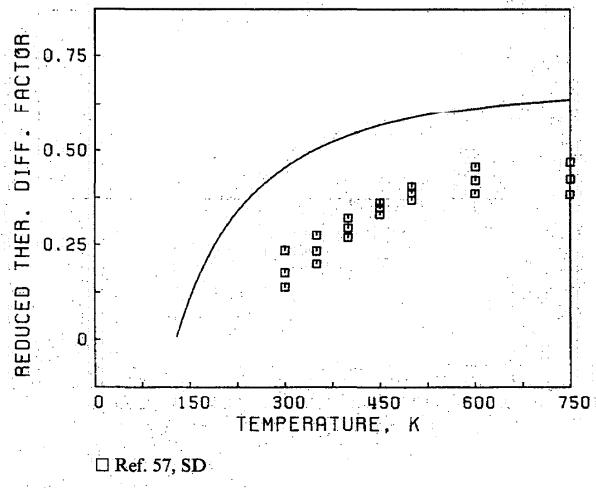
D176. Reduced thermal diffusion factor of N_2-CH_4.

□ Ref. 57, SD

D179. Reduced thermal diffusion factor of N_2-Ar.

O Ref. 122, SD   Y Ref. 11, SD
□ Ref. 45, SD   △ Ref. 109, PD
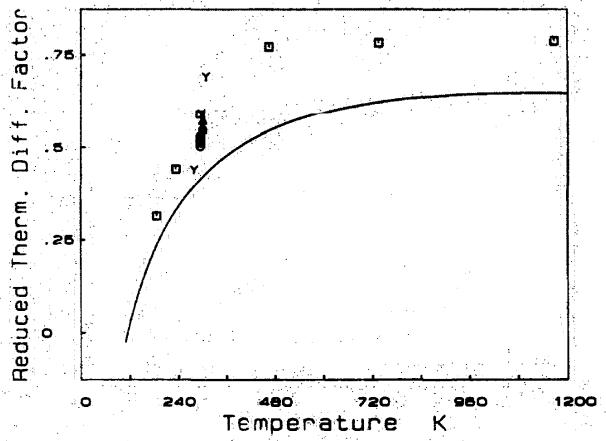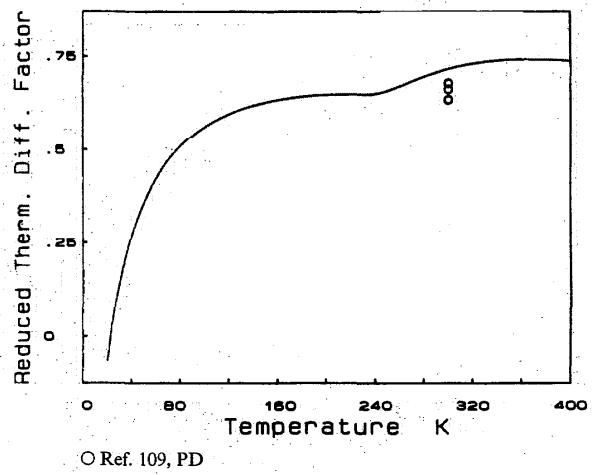

D177. Reduced thermal diffusion factor of N_2-He.

O Ref. 109, PD

D180. Reduced thermal diffusion factor of N_2-Kr.

O Ref. 45, SD
□ Ref. 109, PD

O Ref. 53, PD
□ Ref. 109, PD

D181. Reduced thermal diffusion factor of N_2-Xe.

O Ref. 122, SD   Y Ref. 45, SD
□ Ref. 123, SD   △ Ref. 111, PD
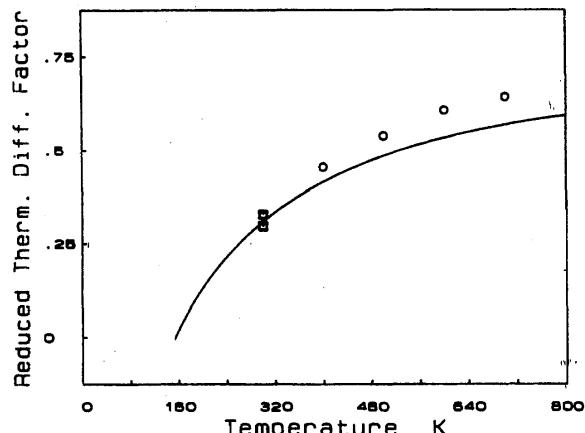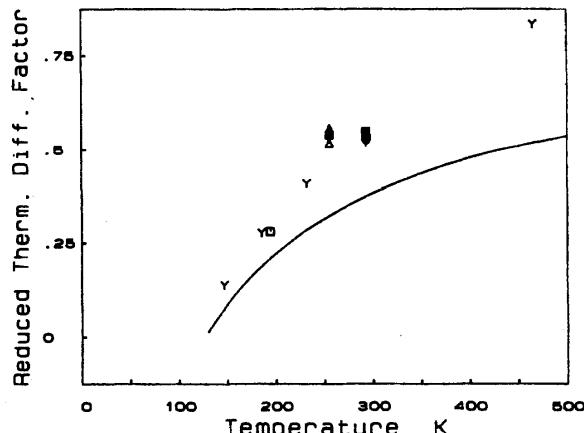
D184. Reduced thermal diffusion factor of O_2-Ar.


□ Ref. 122, SD
O Ref. 123, SD
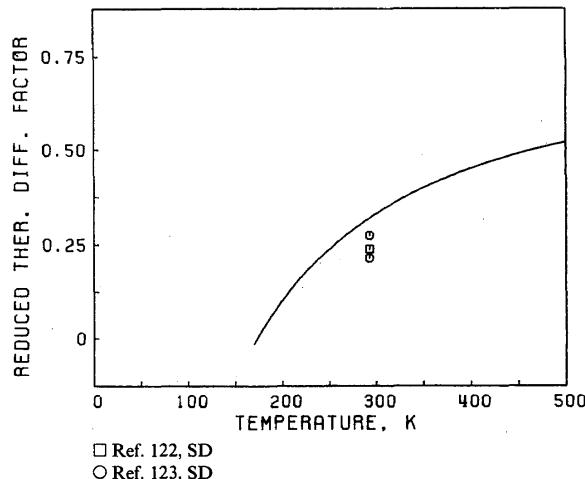
D182. Reduced thermal diffusion factor of O_2-CO_2.

O Ref. 113, PD
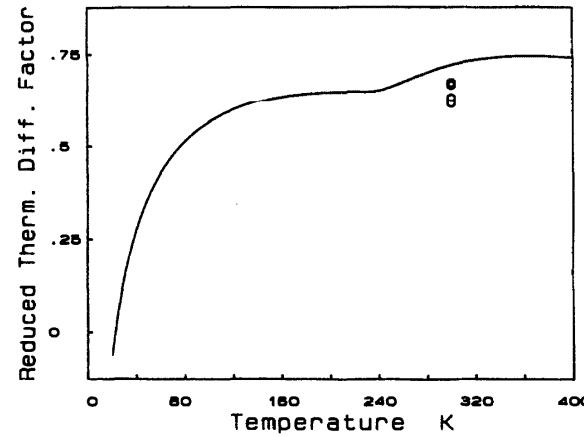
D185. Reduced thermal diffusion factor of CO-He.

O Ref. 113, PD
□ Ref. 111, PD
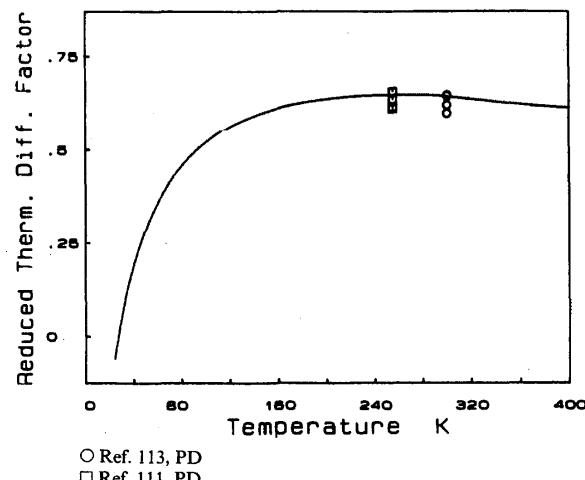
D183. Reduced thermal diffusion factor of O_2-He.

O Ref. 113, PD
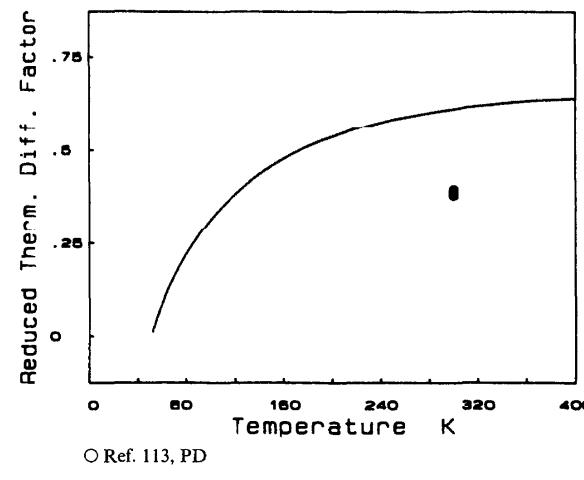
D186. Reduced thermal diffusion factor of CO-Ne.

O Ref. 113, PD

D187. Reduced thermal diffusion factor of CO-Ar.

□ Ref. 110, PD   △ Ref. 106, PD
O Ref. 10, SD
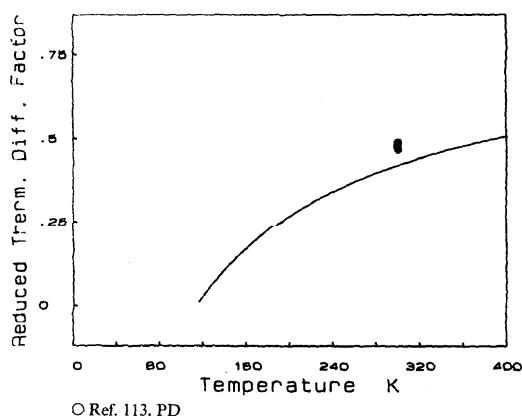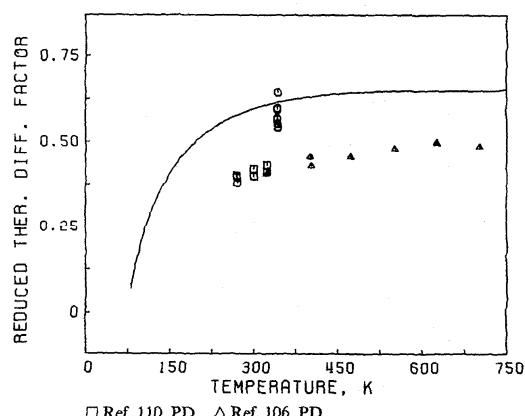
D190. Reduced thermal diffusion factor of CO_2-Ne.

□ Ref. 57, SD
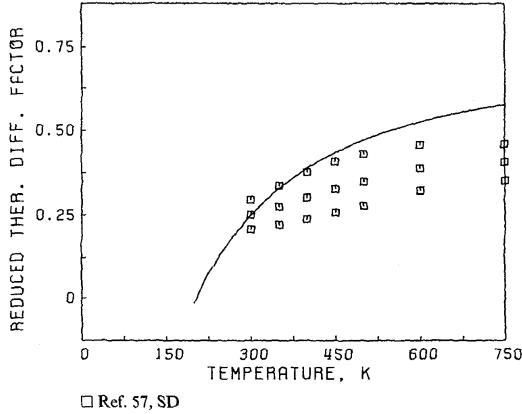
D188. Reduced thermal diffusion factor of CO_2-CH_4.

O Ref. 28, SD

D191. Reduced thermal diffusion factor of CO_2-Kr.

O Ref. 79, SD   Y Ref. 11, PD
□ Ref. 10, SD
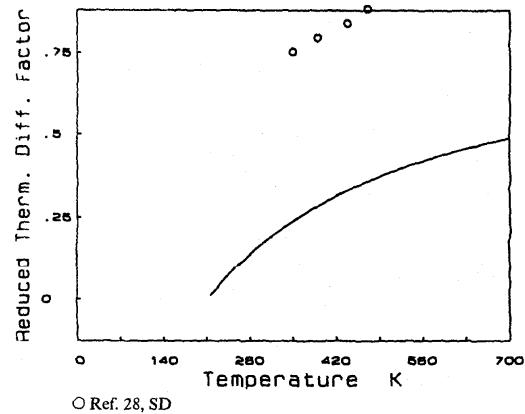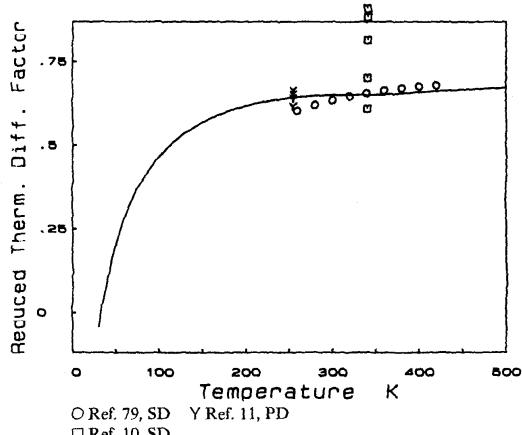
D189. Reduced thermal diffusion factor of CO_2-He.

O Ref. 28, SD
□ Ref. 10, SD
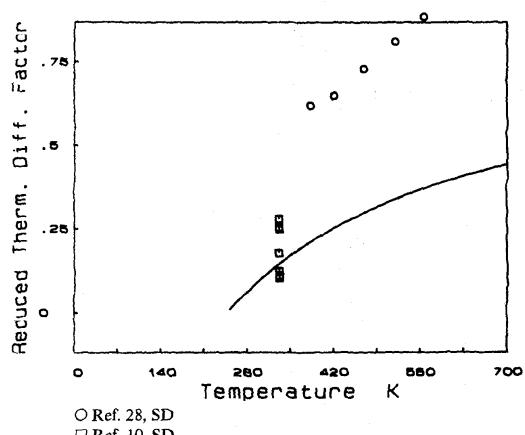
D192. Reduced thermal diffusion factor of CO_2-Xe.

O Ref. 27, SD

D193. Reduced thermal diffusion factor of N_2O-Ne.

O Ref. 3, SD   Y Ref. 112, PD
□ Ref. 92, SD   △ Ref. 32, PD
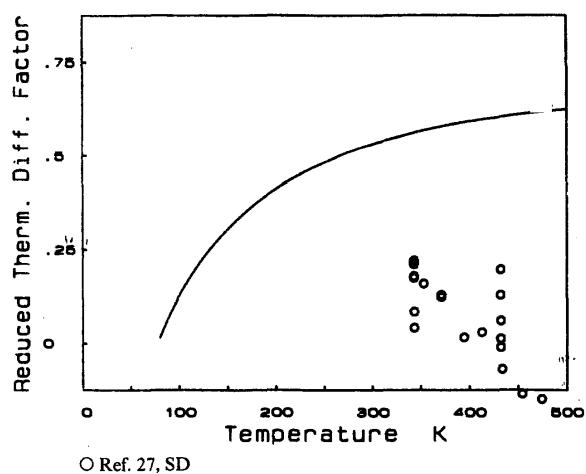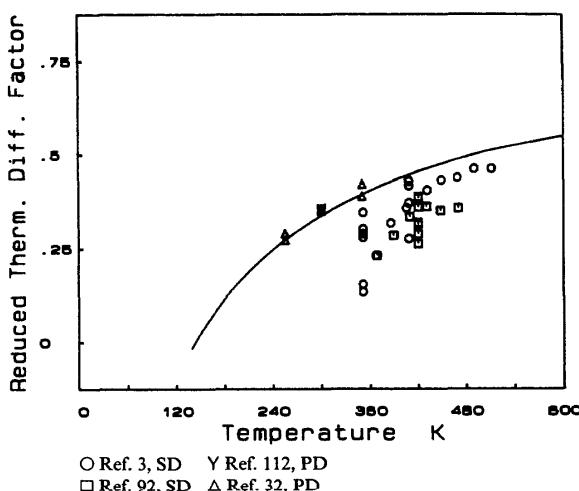
D196. Reduced thermal diffusion factor of CH_4-Ar.

O Ref. 27, SD

D194. Reduced thermal diffusion factor of N_2O-Kr.

O Ref. 92, SD   Y Ref. 32, PD
□ Ref. 112, PD
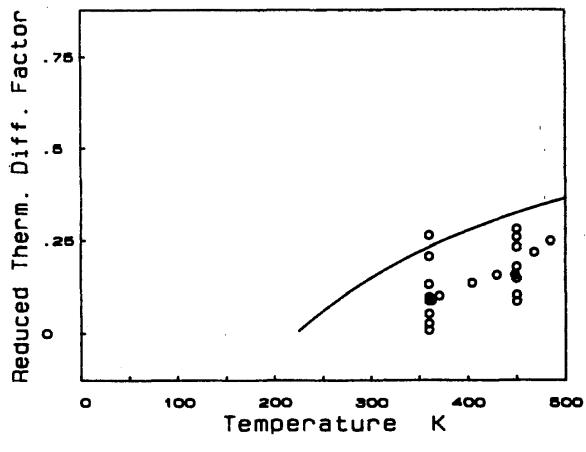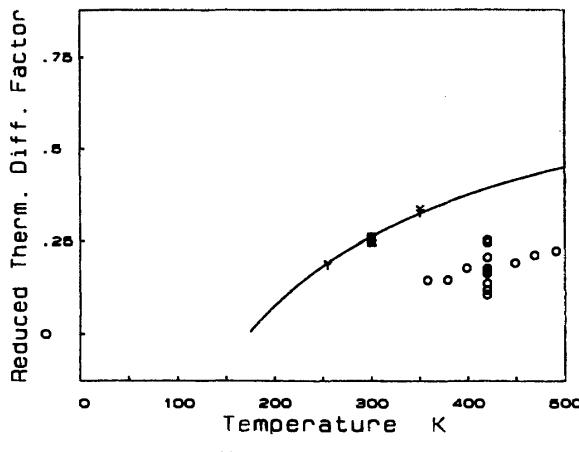
D197. Reduced thermal diffusion factor of CH_4-Kr.

O Ref. 112, PD

D195. Reduced thermal diffusion factor of CH_4-He.


O Ref. 92, SD   Y Ref. 32, PD
□ Ref. 112, PD
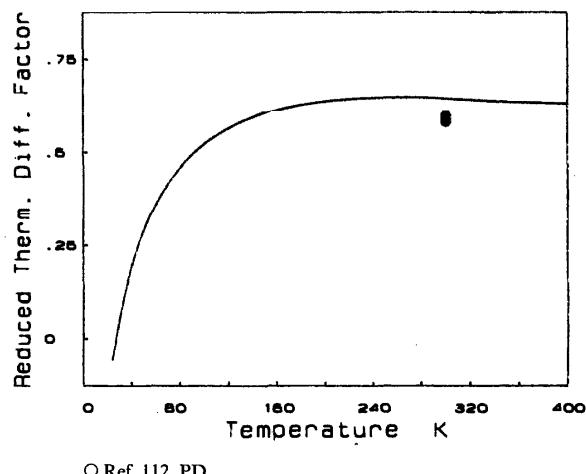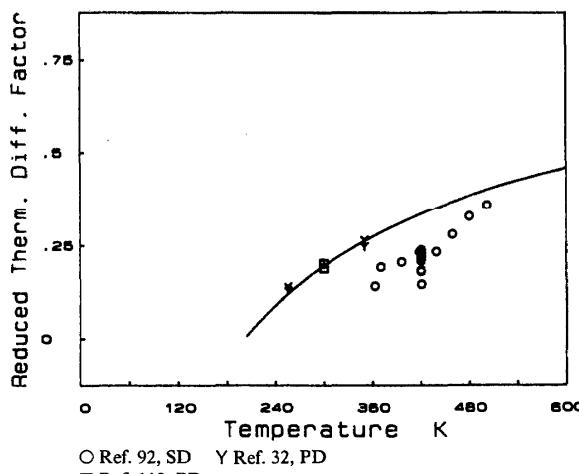
D198. Reduced thermal diffusion factor of CH_4-Xe.
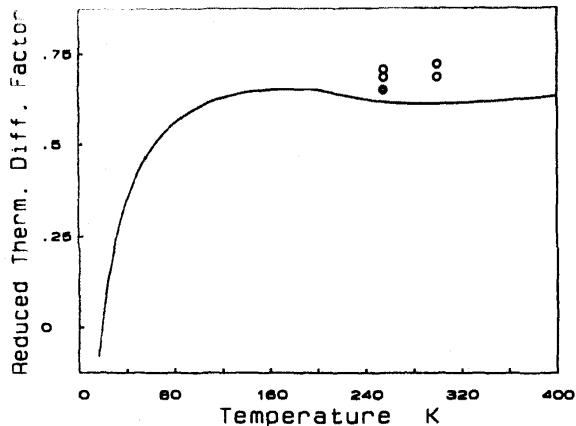
O Ref. 114, PD

D199. Reduced thermal diffusion factor of SF_6-He.
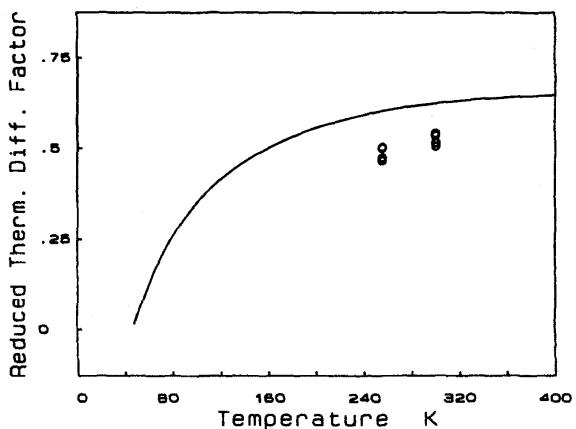
O Ref. 114, PD

D200. Reduced thermal diffusion factor of SF_6-Ne.
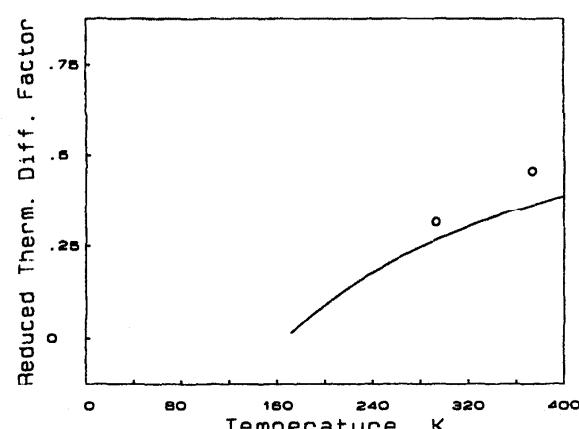
O Ref. 123, SD

D201. Reduced thermal diffusion factor of C_2H_4-Ar.

Appendix E: References For Deviation Plots

Some experimental data were considered redundant or superseded, and do not appear on the deviation and comparison plots or in the following list of references. Additional references for D_{12} can be found in the review by T. R. Marrero and E. A. Mason, J. Phys. Chem. Ref. Data **1**, 3 (1972). Additional references for B_{12} can be found in the compilation by J. H. Dymond and E. B. Smith (Ref. 35). Additional references for α_T can be found in the review by E. A. Mason, R. J. Munn, and F. J. Smith, Adv. At. Mol. Phys. **2**, 33 (1966).

References

[1]Y. Abe, J. Kestin, H. E. Khalifa, and W. A. Wakeham, Physica 93A, 155 (1978).
[2]Y. Abe, J. Kestin, H. E. Khalifa, and W. A. Wakeham, Ber. Bunsenges. Phys. Chem. 83, 271 (1979).
[3]S. Acharyya and A. K. Barua, J. Phys. Soc. Japan 31, 250 (1971).
[4]I. Amdur, J. W. Irvine, Jr., E. A. Mason, and J. Ross, J. Chem. Phys. 20, 463 (1952).
[5]I. Amdur and L. M. Shuler, J. Chem. Phys. 38, 1988 (1963).
[6]B. K. Annis, A. E. Humphreys, and E. A. Mason, Phys. Fluids 12, 78 (1969).
[7]K. Arai, S. Saito, and S. Maeda, Kagaku Kogaku 31, 25 (1967).
[8]P. S. Arora, H. L. Robjohns, T. N. Bell, and P. J. Dunlop, Aust. J. Chem. 33, 1993 (1980).
[9]R. E. Bastick, H. R. Heath, and T. L. Ibbs, Proc. R. Soc. London, Ser. A. 173, 543 (1939).
[10]A. K. Batabyal and A. K. Barua, J. Chem. Phys. 48, 2557 (1968).
[11]A. K. Batabyal, A. K. Ghosh, and A. K. Barua, J. Chem. Phys. 47, 448 (1967).
[12]T. N. Bell and P. J. Dunlop, Chem. Phys. Lett. 84, 99 (1981).
[13]T. N. Bell, I. R. Shankland, and P. J. Dunlop, Chem. Phys. Lett. 45, 445 (1977).
[14]J. Bellm, W. Reineke, K. Schäfer, and B. Schramm, Ber. Bunsenges. Phys. Chem. 78, 282 (1974).
[15]J. Bohemen and J. H. Purnell, J. Chem. Soc., 360 (1961).
[16]C. A. Boyd, N. Stein, V. Steingrimsson, and W. F. Rumpel, J. Chem. Phys. 19, 548 (1951).
[17]J. D. Breetveld, R. DiPippo, and J. Kestin, J. Chem. Phys. 45, 124 (1966).
[18]J. Brewer and G. W. Vaughn, J. Chem. Phys. 50, 2960 (1969).
[19]M. A. Byrne, M. R. Jones, and L. A. K. Staveley, Trans. Faraday Soc. 64, 1747 (1968).
[20]D. W. Calvin and T. M. Reed III, J. Chem. Phys. 54, 3733 (1971).
[21]F. B. Canfield, T. W. Leland, and R. Kobayashi, Adv. Cryogen. Eng. 8, 146 (1963).
[22]A. A. Clifford, E. Dickinson, G. P. Matthews, and E. B. Smith, J. Chem. Soc. Faraday Trans. I 72, 2917 (1976).
[23]J. Coates and A. A. Mian, Industrie Chimique Belge 32, 285 (1967).
[24]T. L. Cottrell, R. A. Hamilton, and R. P. Taubinger, Trans. Faraday Soc. 52, 1310 (1956).
[25]E. M. Dantzler, C. M. Knobler, and M. L. Windsor, J. Phys. Chem. 72, 676 (1968).
[26]E. M. Dantzler Siebert and C. M. Knobler, J. Phys. Chem. 75, 3863 (1971).
[27]K. K. Datta, P. Seal, and A. K. Barua, J. Phys. Soc. Japan 37, 1089 (1974).
[28]S. K. Deb, Indian J. Phys. 41, 719 (1967).
[29]R. DiPippo, J. Kestin, and K. Oguchi, J. Chem. Phys. 46, 4758 (1967).
[30]D. R. Douslin, R. H. Harrison, and R. T. Moore, J. Phys. Chem. 71, 3477 (1967).
[31]P. J. Dunlop [private communication to E. A. Mason (1988)].
[32]P. J. Dunlop and C. M. Bignell, Physica 145A, 584 (1987).
[33]P. J. Dunlop, C. M. Bignell, and H. L. Robjohns, Ber. Bunsenges. Phys. Chem. 90, 351 (1986).

[34]L. Durbin and R. Kobayashi, J. Chem. Phys. **37**, 1643 (1962).

[35]J. H. Dymond and E. B. Smith, *The Virial Coefficients of Pure Gases and Mixtures. A Critical Compilation.* (Clarendon, Oxford, 1980).

[36]A. E. Edwards and W. E. Roseveare, J. Am. Chem. Soc. **64**, 2816 (1942).

[37]C. S. Ellis and J. N. Holsen, Ind. Eng. Chem., Fundam. **8**, 787 (1969).

[38]E. B. Fedorov, A. B. Ivakin, and P. E. Suetin, Zh. Tekh. Fiz. **36**, 569 (1966) [Sov. Phys.-Tech. Phys. **11**. 424 (1966)].

[39]P. Fejes and L. Czárán, Acta Chim. Hungar. **29**, 171 (1961).

[40]E. N. Fuller and J. C. Giddings, J. Gas Chromatog. **3**, 222 (1965).

[41]E. N. Fuller, K. Ensley, and J. C. Giddings, J. Phys. Chem. **73**, 3679 (1969).

[42]J. C. Giddings and S. L. Seager, Ind. Eng. Chem., Fundam. **1**, 277 (1962).

[43]R. A. Gorski and J. G. Miller, J. Am. Chem. Soc. **75**, 550 (1953).

[44]D. W. Gough, G. P. Matthews, and E. B. Smith, J. Chem. Soc. Faraday Trans. I **72**, 645 (1976).

[45]K. E. Grew, F. A. Johnson, and W. E. J. Neal, Proc. R. Soc. London, Ser. A **224**, 513 (1954).

[46]R. D. Gunn (unpublished results); Ref. 35, pp. 369 (N_2-CO_2) and 318 (CH_4-C_2H_6).

[47]R. Hahn, K. Schäfer, and B. Schramm, Ber. Bunsenges. Phys. Chem. **78**, 287 (1974).

[48]K. R. Hall and F. B. Canfield, Physica **47**, 219 (1969).

[49]S. D. Hamann, J. A. Lambert, and R. B. Thomas, Aust. J. Chem. **8**, 149 (1955).

[50]K. R. Harris, T. N. Bell, and P. J. Dunlop, Canad. J. Phys. **50**, 1874 (1972).

[51]J. M. Hellemans, J. Kestin, and S. T. Ro, J. Chem. Phys. **57**, 4038 (1972).

[52]J. M. Hellemans, J. Kestin, and S. T. Ro, Physica **65**, 362 (1973).

[53]D. Heymann and J. Kistemaker, Physica **25**, 556 (1959).

[54]J. N. Holsen and M. R. Strunk, Ind. Eng. Chem., Fundam. **3**, 143 (1964).

[55]A. E. Hoover, I. Nagata, T. W. Leland, Jr., and R. Kobayashi, J. Chem. Phys. **48**, 2633 (1968).

[56]A. T.-C. Hu and R. Kobayashi, J. Chem. Eng. Data **15**, 328 (1970).

[57]A. E. Humphreys and P. Gray, Proc. R. Soc. London. Ser. A **322**, 89 (1971).

[58]B. A. Ivakin and P. E. Suetin, Zh. Tekh. Fiz. **33**, 1007 (1962) [Sov. Phys.-Tech. Phys. **8**, 748 (1964)].

[59]B. A. Ivakin and P. E. Suetin, Zh. Tekh. Fiz. **34**, 1115 (1964) [Sov. Phys.-Tech. Phys. **9**, 866 (1964)].

[60]B. A. Ivakin, P. E. Suetin, and V. P. Plesovskikh Zh. Tekh. Fiz. **37**, 1913 (1967) [Sov. Phys.-Tech. Phys. **12**, 1403 (1968)].

[61]W. M. Jackson, J. Phys. Chem. **60**, 789 (1956).

[62]T. Jacobs, L. Peeter, and J. Vermant, Bull. Soc. Chim. Belges **79**, 337 (1970).

[63]N. K. Kalfoglou and J. G. Miller, J. Phys. Chem. **71**, 1256 (1967).

[64]J. Kestin, H. E. Khalifa, S. T. Ro, and W. A. Wakeham, Physica **88A**, 242 (1977).

[65]J. Kestin, H. E. Khalifa, and W. A. Wakeham, J. Chem. Phys. **67**, 4254 (1977).

[66]J. Kestin, Y. Kobayashi, and R. T. Wood, Physica **32**, 1065 (1966).

[67]J. Kestin and S. T. Ro, Ber. Bunsenges. Phys. Chem. **78**, 20 (1974).

[68]J. Kestin and S. T. Ro, Ber. Bunsenges. Phys. Chem. **86**, 948 (1982),

[69]J. Kestin and S. T. Ro, Ber. Bunsenges. Phys. Chem. **87**, 600 (1983).

[70]J. Kestin, S. T. Ro, and W. A. Wakeham, J. Chem. Phys. **56**, 4036 (1972).

[71]J. Kestin, S. T. Ro, and W. A. Wakeham, J. Chem. Phys. **56**, 5837 (1972).

[72]J. Kestin, S. T. Ro, and W. A. Wakeham, Ber. Bunsenges. Phys. Chem. **86**, 753 (1982).

[73]J. Kestin and W. A. Wakeham, Ber. Bunsenges. Phys. Chem. **87**, 309 (1983).

[74]J. Kestin and J. Yata, J. Chem. Phys. **49**, 4780 (1968).

[75]J. W. Lee and G. Saville (1976), (unpublished results); Ref. 35, p. 317 (CH_4-C_2H_6).

[76]R. C. Lee and W. C. Edmister, AIChE J. **16**, 1047 (1970).

[77]R. N. Lichtenthaler and K. Schäfer, Ber. Bunsenges. Phys. Chem. **73**, 42 (1969).

[78]L. R. Linshits, I. B. Rodkina, and D. S. Tsiklis, Zh. Fiz. Khim. **49**, 2141 (1975) [Russ. J. Phys. Chem. **49**, 1258 (1975)].

[79]H. K. Lonsdale and E. A. Mason, J. Phys. Chem. **61**, 1544 (1957).

[80](a).M. L. Martin, R. D. Trengove, K. R. Harris, and P. J. Dunlop, Ber. Bunsenges. Phys. Chem. **86**, 626 (1982). (b)M. L. Martin, R. D. Trengove, K. R. Harris, and P. J. Dunlop, Aust. J. Chem. **35**, 1525 (1982).

[81]D. McA. Mason and B. E. Eakin, J. Chem. Eng. Data **6**, 499 (1961).

[82]H. G. McMath and W. C. Edmister, AIChE J. **15**, 370 (1969).

[83]C. R. Mueller and R. W. Cahill, J. Chem. Phys. **40**, 651 (1964).

[84]K. Ohgaki, T. Mizuhaya, and T. Katayama, J. Chem. Eng. Japan **14**, 71 (1981).

[85]T. A. Pakurar and J. R. Ferron, Ind. Eng. Chem., Fundam. **5**, 553 (1966).

[86]R. Paul and I. B. Srivastava, Indian J. Phys. **35**, 465 (1961).

[87]R. Paul and I. B. Srivastava, Indian J. Phys. **35**, 523 (1961).

[88]W. C. Pfefferle, Jr., J. A. Goff, and J. G. Miller, J. Chem. Phys. **23**, 509 (1955).

[89]A. B. Rakshit, C. R. Roy, and A. K. Barua, J. Chem. Phys. **59**, 3633 (1973).

[90](a) H. L. Robjohns and P. J. Dunlop, Ber. Bunsenges. Phys. Chem. **85**, 655 (1981). (b) H. L. Robjohns and P. J. Dunlop, Ber. Bunsenges. Phys. Chem. **88**, 1239 (1984).

[91]D. R. Roe and G. Saville (1972), (unpublished results); Ref. 35, p. 336 (N_2-CH_4).

[92]C. S. Roy, S. K. Bhattacharyya, and A. K. Pal, Indian J. Phys. **48**, 651 (1974).

[93]J. Santafe, J. S. Urieta, and C. G. Losa, Chem. Phys. **18**, 341 (1974).

[94]A. Sass, B. F. Dodge, and R. H. Bretton, J. Chem. Eng. Data **12**, 168 (1967).

[95]S. C. Saxena and E. A Mason, Mol. Phys. **2**, 379 (1959).

[96]K. Schäfer, B. Schramm, and J. S. U. Navarro, Z. Phys. Chem. **93**, 203 (1974).

[97]M. Schneider and K. Schäfer, Ber. Bunsenges. Phys. Chem. **73** 702 (1969).

[98]B. Schramm and R. Gerhmann (1979), (unpublished results); Ref. 35, pp. 294-5 (N_2-Ar).

[99]B. Schramm and H. Schmiedel (1979), (unpublished results); Ref. 35, p. 295 (N_2-Ar).

[100]S. L. Seager, L. R. Geertson, and J. C. Giddings, J. Chem. Eng. Data **8**, 168 (1963).

[101]P. M. Sigmund, I. H. Silberberg, and J. J. McKetta, J. Chem. Eng. Data **17**, 168 (1972).

[102]Y. Singh, A. Saran, and B. N. Srivastava, J. Phys. Soc. Japan **23**, 1110 (1967).

[103]K. Strein, R. N. Lichtenthaler, B. Schramm, and K. Schäfer, Ber. Bunsenges, Phys. Chem. **75**, 1308 (1971).

[104]P. E. Suetin, in *ORNL-TR-316 (1964),* Vol. 1, Translated by A. L. Monks for Oak Ridge National Laboratory from Teplo i Massoperenos, Izdatel'stvo Akademii Nauk BSSR, Minsk, pp. 188-190 (1962).

[105]H. Sutter and R. H. Cole, J. Chem. Phys. **52**, 140 (1970).

[106]W. L. Taylor and P. T. Pickett, Int. J. Thermophys. **7**, 837 (1986).

[107]G. Thomaes, R. Van Steenwinkel, and W. Stone, Mol. Phys. **5**, 301 (1962).

[108]M. Trautz and A. Melster, Ann. Phys. **7**, 409 (1930).

[109]R. D. Trengove and P. J. Dunlop, Physica **115A**, 339 (1982).

[110]R. D. Trengove and P. J. Dunlop, Chem. Phys. Lett. **94**, 118 (1983).

[111]R. D. Trengove, K. R. Harris, H. L. Robjohns, and P. J. Dunlop, Physica **131A**, 506 (1985); erratum **144A**, 254 (1987).

[112]R. D. Trengove, H. L. Robjohns, and P. J. Dunlop, Ber. Bunsenges. Phys. Chem. **86**, 951 (1982).

[113]R. D. Trengove, H. L. Robjohns, and P. J. Dunlop, Ber. Bunsenges. Phys. Chem. **88**, 450 (1984).

[114]R. D. Trengove, H. L. Robjohns, and P. J. Dunlop, Physica **128A**, 486 (1984).

[115]D. S. Tsiklis, L. R. Linshits, and I. B. Rodkina, Zh. Fiz. Khim. **48**, 1541 1544 (1974), [Russ. J. Phys. Chem. **48**, 906, 908 (1974)].

[116]H. F. Vugts, A. J. H. Boerboom, and J. Los, Physica **50**, 593 (1970).

[117]V. F. Vyshenskaya and N. D. Kosov, in *ORNL-TR-506 (1965),* Translated by A. L. Monks for Oak Ridge National Laboratory from Teplo- i Massoperenos, Pervoe Vsesoyuznoe Soveschante, Minsk, pp. 181-7 (1961).

[118]A. S. M. Wahby, Physica **145C**, 78 (1987).

[119]A. S. M. Wahby, A. J. H. Boerboom, and J. Los, Physica **75**, 573 (1974).

[120]A. S. M. Wahby and J. Los, Physica **145C**, 69 (1987).

[121]W. A. Wakeham and D. H. Slater, J. Phys. **B6**, 886 (1973).

[122]L. Waldmann, Z. Physik **124**, 2 (1947).

[123]L. Waldmann, Z. Naturforsch. **4a**, 105 (1949).

[124]R. E. Walker and A. A. Westenberg, J. Chem. Phys. **29**, 1139 (1958).

[125]R. E. Walker and A. A. Westenberg, J. Chem. Phys. **29**, 1147 (1958).

[126]R. E. Walker and A. A. Westenberg, J. Chem. Phys. **32**, 436 (1960).

[127]S. P. Wasik and K. E. McCulloh, J. Res. Natl. Bur. Stand. (U.S.) **73A**, 207 (1969).

[128]S. Weissman, S. C. Saxena, and E. A. Mason, Phys. Fluids **4**, 643 (1961).

[129]A. A. Westenberg and R. E. Walker, J. Chem. Phys. **26**, 1753 (1957).

[130]R. J. Witonsky and J. G. Miller, J. Am. Chem. Soc. **85**, 282 (1963).

[131]C. J. Wormald, E. J. Lewis, and D. J. Hutchings, J. Chem. Thermodyn. **11**, 1 (1979).

[132]P. Zandbergen and J. J. M. Beenakker, Physica **33**, 343 (1967).